ABSTRACT

STOUGHTON, HANNAH LINDSEY. Ion Exchange Formation via Sulfonated Bicomponent Fibers. (Under the direction of Dr. Shim and Dr. Pourdeyhimi).

For many years ion exchange resins were used to: remove heavy metals from water, recover materials from wastewater, and eliminate harmful gases from the air. While use of these resin beads dominates the ion exchange industry, the beads have limitations that should be considered when decisions are made to employ them. For instance, officials must balance the inherent zero sum surface area and porosity of the materials. This series of studies investigates the use of bicomponent nonwovens as a base substrate for producing high surface area ion exchange materials for the removal of heavy metal ions. Functionalized materials were produced in a two-step process: (1) PET/PE spunbond bicomponent fibers were fractured completely, producing the high surface area nonwoven to be used as the base ion exchange material, and (2) the conditions for functionalizing the PET fibers of the nonwoven webs were investigated where an epoxy containing monomer was grafted to the surface followed by sulfonation of the monomer. The functionalization reactions of the PET fibers were monitored based on: weight gain, FTIR, TOF-SIMS, and SEM. Ion exchange properties were evaluated using titration and copper ion removal capacity from test solutions. The relationship between web structure and removal efficiency of the metal ions was defined through a comparison of the bicomponent and homocomponent nonwovens for copper ion removal efficiency. The investigation revealed that utilizing the high surface area, fractured bicomponent nonwoven ion exchange materials with capacities comparable to commercially available ion exchange resins could be produced.

Ion Exchange Formation via Sulfonated Bicomponent Nonwovens

by
Hannah L. Stoughton

A dissertation submitted to the Graduate Faculty of
North Carolina State University
in partial fulfillment of the
requirements for the degree of
Doctor of Philosophy

Fiber and Polymer Science

Raleigh, North Carolina

2014

APPROVED BY:

_____	_____
Dr. Behnam Pourdeyhimi Committee Co-Chair	Dr. Eunkyoung Shim Committee Co-Chair
_____	_____
Dr. Benoit Maze	Dr. Orlando Rojas

DEDICATION

To my family. You guys rock.

BIOGRAPHY

Hannah Stoughton was born in Fredericksburg, Virginia. As a child of a military family she grew up all over the United States before coming to North Carolina State University for college. She received a Bachelor of Science degree in Textile Engineering from the College of Textiles in 2010. During her sophomore year she began undergraduate research with the Nonwovens Cooperative Research Center (NCRC). Upon graduation she joined NCRC for her graduate studies, receiving her Master of Science in Textile Engineering in 2013. She will be moving with her husband, Will, and dog, Roxy, to Minnesota to pursue a research career with 3M.

ACKNOWLEDGMENTS

I can't thank Dr. Shim enough for her incredible support on this project. I couldn't of asked for a better mentor and advisor and I appreciate all of her help along the way. Thank you to Dr. Pourdeyhimi for all of his guidance, in my research and in life. Thank you to Dr. Rust and Dr. Joines for helping me find a home at the College of Textiles and for not giving up on me. Also, the Nonwovens Institute and my Industrial Advisors for their financial support for this project.

I would like to thank all of the people who helped me with my research, especially Farah Hamouda for being a rock star student intern, Birgit Anderson, Judy Elson, Elaine Zhou, and Chuck Mooney. Thanks to Sherwood Wallace and Bruce Anderson for teaching me how to manage a lab and keeping life interesting. I would like to thank all of my friends and colleagues at the Institute and the College of Textiles for making my time at NCSU a wonderful experience.

Finally, I would like to thank my family for their relentless support throughout grad school. You all mean the world to me. Thank you to my parents for their love and support, for flying me out to visit while I was a student, and for always encouraging me to strive for the best. Thank you to Lauren for a fun first two years of grad school and all the lunch dates and to Lindsay for the long runs that kept me sane. Thank you to my brother, Michael, for helping me keep my perspective. And thank you especially to my husband, Will; this would not of been possible without you. Thank you for taking care of me and the little dog,

sacrificing to allow me to be a full time student, picking up all the slack at home and life, and dealing with the crazy.

TABLE OF CONTENTS

LIST OF TABLES

LIST OF FIGURES

Chapter 1

1 Introduction

An efficient, cost effective method for filtering water is a necessity for improving the quality of life of millions of people around the world. Ion exchange resins have been used for many years as an efficient method of removing heavy metals from water, recovering materials from waste water, and removing harmful gases from the air [1], [2], [3], [4]. Important parameters must be considered when using ion exchangers such as ion exchange capacity, operating resistance, and adsorption rate. Due to the relationship between operating resistance and size of the resins, there is a limitation to increase the surface area, which increases the ion exchange capacity of the resin. For this reason, ion exchange fibers are being considered as an alternative to the traditional ion exchange resin. Ion exchange fibers would provide a significant increase in surface area, greatly increasing the ion exchange capacity and the life of the filter.

Ion exchange materials are insoluble matrices containing positive or negatively charged ions. These ions are exchanged for equivalent quantities of ions with like charges when the solution containing the ion comes in contact with the structure[5]. Ion exchange resins are commonly used to remove heavy metals ions, such as arsenic, copper, lead, cadmium, mercury, and nickel, from waste water. These metals can enter the water systems through industrial run off, pipe corrosion, and fertilizer run off. Long term exposure to these heavy metals can cause circulatory and nervous system problems, and eventually lead to brain damage. Ion exchangers are most commonly used for softening of water in homes, a POE (point of entry) filter. These filters remove calcium and magnesium from water that enters the house. The ion exchange resins are in the form of spherical beads[6]. The resins are either applied to a porous substrate or placed in a column. As water flows through the resins, the heavy metals in solution are replaced with either sodium or hydrogen ions attached to the surface of the resin.

In the case of the water softener, the anion groups attached to the surface of the substrate attract the magnesium and calcium ions and an equal number of sodium ions are released into the water. This exchange continues to occur while water is pumped through the ion exchange bed until all of the possible sodium ions have been released. The filter is then considered to be exhausted and must be regenerated. This is done by a reverse ion exchange operation in which a highly concentrated sodium chloride solution replaces the calcium ions on the exchange resins with sodium ions [7].

Ion exchange materials are also used in the semiconductor industry where ultrapure water is necessary for production[8], [9], [10]. The uses of ion exchange materials are not limited to removal of ions from liquid. They are also used for separation in the food industry[11], [12], separation and recovery in biotechnology[13], and analysis of soil properties[2].

Ion exchange resins have proven to be very efficient in targeting and removing heavy metals from water. Although these resins are highly selective in deionizing heavy metals and also have a high packing density, they still have many disadvantages. In order for the ions to be removed, they must interact with the functional groups on the surface of the resin. Therefore, the pores must be small enough to ensure there is adequate interaction between the functional groups and the metal ions. A balance between the pore size and the pressure drop is necessary to maintain an efficient operating resistance. The high pressure necessary for resin operation can also destroy the structure of the beads[14].

For this reason, ion exchange fibers would be an ideal alternative to the traditional ion exchange resins. The use of ion exchange fibers will allow for an increase in surface area while maintaining a low operating resistance, therefore increasing the ion exchange capacity and ultimately increasing the life and efficiency of the filter. Some research has been done on ion exchange fibers but there is still a need to improve their stability and capacity, as well as find a low cost alternative to the expensive base materials currently used [15], [16], [17], [18].

Since the ion exchange capacity is dependent on the number of functional groups present, using materials with a high surface area result in high ion exchange capacities. The few

commercially available ion exchange fibers have large fiber diameters, 30 - 50 μm [17]. Therefore, one of the biggest limitations with the current ion exchange fibrous materials is the low surface area. The commercially available ion exchange fibers, such as FIBAN™ and Spomex®, are also expensive. Most of the FIBAN™ ion exchange fibers are styrene divinylbenzene grafted to polypropylene and Spomex® is a styrene functionalized polyethylene web. Using a low cost material as the ion exchange substrate, along with cost efficient functionalization methods would be a great improvement to the current fibrous materials.

1.1 Research Approach and Objectives

The main objective of this project is to produce an ion exchange nonwoven material with a high ion exchange capacity and low operating resistance, using cost effective functionalization methods and materials. The current state of ion exchange technology is focused on the use of ion exchange resins. These resins are limited by the pore size necessary to encourage interaction between the ions and the functional groups on the structure. High operation costs result from the high pressure necessary to force the water through the resin structure. To overcome this limitation a fibrous nonwoven material with adequate sorption properties will be used as the ion exchange substrate to allow for liquid flow through the structure.

A few ion exchange fiber materials are currently commercially available. They have not been able to replace the use of ion exchange resins in industry due to their low ion exchange capacity and high cost of production. A nonwoven material made from a low cost polymer and functionalized using cost effective methods would address this issue. The other limitation of the current ion exchange fibers is the low surface area due to the large fiber diameter. A nonwoven material composed of microfibers would greatly increase the surface area compared to the current ion exchange fibrous materials.

In the proposed study, bicomponent nonwoven materials will be used as the base substrate of the ion exchange nonwoven. The fibers in the nonwoven webs will be grafted

with an epoxy containing monomer and sulfonated to create strongly cationic exchange fibers. The fracturing conditions of the fibers as well as the grafting parameters will be optimized. The degree of sulfonation of the grafted copolymers will also be investigated. Finally, adsorption isotherm and the rate controlling mechanisms of the exchangers will be analyzed using sorption kinetics. Achieving stable ion exchange fibers will mark a significant advancement in filtration technology as well as the field of nonwoven textiles.

The nonwovens manufacturing process is a cost effective method of producing large volumes of material. The nonwovens will be made of polyethylene terephthalate (PET) and polyethylene (PE) bicomponent fibers. Both of these polymers are quite low cost, especially compared to the polymers making up the current commercially available ion exchange materials. The bicomponent technology will be used to produce the high surface area substrate. The PET component of the nonwoven will be targeted for functionalization. PET is known for its strength, chemical resistance, and low cost. Achieving a functionalized PET surface and tailoring its properties to a specific application would be a significant contribution to a variety of industries as well as the ion exchange industry.

Chapter 2 of this dissertation is a review of the literature. It discusses ion exchange technology, bicomponent nonwovens, and functionalization techniques.

Chapter 3 is an investigation into the effect of the number of segments of the bicomponent nonwoven on the web properties.

Chapter 4 discusses the challenges associated with using UV initiation as a method for grafting the GMA monomer to the PET fibers, such as the high production of homopolymer.

Chapter 5 investigates the conditions for grafting of the GMA monomer to the PET fibers via ceric salt initiation. A comparison of the homocomponent and bicomponent nonwoven is presented, concluding that high grafting percentages result from the high surface area material.

Chapter 6 discusses the functionalization of the grafted PET-g-GMA materials and investigates the extent of functionalization through titration.

Chapter 7 evaluates the ion exchange properties of the functionalized bicomponent and homocomponent nonwovens through copper ion removal experiments Equilibrium and kinetic studies are presented to investigate the maximum capacities and rate of removal of the materials.

Chapter 8 summarizes the conclusions of the previous chapters and discussing recommendations for the future.

Appendix 1 is an interaction plot of the factors of the grafting reactions.

1.2 References

[1] C. Gerente, V. Lee, K. Lee, and C. Lee, "Application of Chitosan for the Removal of Metals From Wastewaters by Adsorption—Mechanisms and Models Review," *Crit. Rev. Environ. Sci. Technol.*, vol. 37, no. 1, pp. 41–127, Jan. 2007.

[2] M. P. Jones, B. L. Webb, D. A. Cook, and V. D. Jolley, "Comparing Nutrient Availability in Low-Fertility Soils using Ion Exchange Resin Capsules," *Commun. Soil Sci. Plant Anal.*, vol. 43, no. 1–2, pp. 368–376, Jan. 2012.

[3] Y. Bai and B. Bartkiewicz, "Removal of Cadmium from Wastewater Using Ion Exchange Resin Amberjet 1200H Columns," *Pol. J. Environ. Stud.*, vol. 18, no. 6, pp. 1191–1195, 2009.

[4] K. Fujiwara, "Separation functional fibers by radiation induced graft polymerization and application," *Nucl. Instruments Methods Phys. Res. Sect. B Beam Interactions Mater. Atoms*, vol. 265, no. 1, pp. 150–155, Dec. 2007.

[5] F. G. Helfferich, *Ion exchange*. New York: Dover Publications, 1995.

[6] J. K. Edzwald, *Water quality & treatment: a handbook on drinking water [...] [...]*. New York [u.a.: McGraw-Hill, 2011.

[7] APEC, "Ion exchange principle for water softners," *Water Education*. [Online]. Available: http://www.freedrinkingwater.com/water-education2/46-ion-exchange-principle.htm. [Accessed: 02-Nov-2010].

[8] S. Honkanen, A. Tervonen, H. von Bagh, and M. Leppihalme, "Ion exchange process for fabrication of waveguide couplers for fiber optic sensor applications," *J. Appl. Phys.*, vol. 61, no. 1, p. 52, 1987.

[9] K. Fujiwara, "Separation functional fibers by radiation induced graft polymerization and application," *Nucl. Instruments Methods Phys. Res. Sect. B Beam Interactions Mater. Atoms*, vol. 265, no. 1, pp. 150–155, Dec. 2007.

[10] T. Hori, M. Hashino, A. Omori, T. Matsuda, K. Takasa, and K. Watanabe, "Synthesis of novel microfilters with ion-exchange capacity and its application to ultrapure water production systems," *J. Membr. Sci.*, vol. 132, no. 2, pp. 203–211, Sep. 1997.

[11] J. Kammerer, R. Carle, and D. R. Kammerer, "Adsorption and Ion Exchange: Basic Principles and Their Application in Food Processing," *J. Agric. Food Chem.*, vol. 59, no. 1, pp. 22–42, Jan. 2011.

[12] P. J. Muldoon and B. J. Liska, "Comparison of a Resin Ion-Exchange Method and a Liquid Ion-Exchange Method for Determination of Ionized Calcium in Skimmilk," *J. Dairy Sci.*, vol. 52, no. 4, pp. 460–464, Apr. 1969.

[13] S. Pande, M. Kshirsagar, and A. Chandewar, "Ion exchange resins Pharmaceutical applications and recent advancement," *Int. J. Adv. Pharm. Sci.*, vol. 4, no. 1, pp. 8–16, 2011.

[14] J. Economy, L. Dominguez, and C. L. Mangun, "Polymeric Ion-Exchange Fibers," *Ind. Eng. Chem. Res.*, vol. 41, no. 25, pp. 6436–6442, Dec. 2002.

[15] A. Zagorodni, *Ion exchange materials : properties and applications*. Amsterdam ;;London: Elsevier, 2007.

[16] V. S. Soldatov, A. A. Shunkevich, I. S. Elinson, J. Johann, and H. Iraushek, "Chemically active textile materials as efficient means for water purification," *Desalination*, vol. 124, no. 1–3, pp. 181–192, Nov. 1999.

[17] V. Soldatov, A. Shunkevich, and G. Sergeev, "Synthesis, structure and properties of new fibrous ion exchangers⋆," *React. Polym. Ion Exch. Sorbents*, vol. 7, no. 2–3, pp. 159–172, Jan. 1988.

[18] G. Medyak, A. Shunkevich, A. Polikarpov, and V. Soldatov, "Features of Preparation and Properties of FIBAN K-4 Fibrous Sorbents," *Russ. J. Appl. Chem.*, vol. 74, no. 10, pp. 1658–1663, Feb. 2001.

Chapter 2

2 Literature Review

2.1 Polyethylene Terephthalate

Polyester fibers were first developed by W.H. Carothers of DuPont in the 1930's. The work done by J.R. Whinfield, J.T. Dickson, W.K. Birtwhistle, and C.G. Ritchie advanced the previous developments of Carothers. DuPont later bought the rights to the technology and released the first commercial polyester fiber called Dacron [1]. Since its production, polyethylene terephthalate (PET) has become one of the most popular fibers and is used in a variety of applications. In 2002, PET production exceeded cotton fiber production[1]. Since then, PET has been one of the most readily available synthetic fibers. PET is a commodity fiber that fluctuates in price based on the demands of the market. As it is an abundantly available material, it is natural that more uses for the material are being sought out.

2.1.1 Material Properties

Polyethylene Terephthalate (PET) is a highly crystalline, stiff polymer with moderate polarity. The properties of PET polymers are found in Table 2.1.

Table 2.1. Properties of PET Polymer [1]

Property	Value
Melting Point	260°C
Glass Transition	85°C
Density	1.43 g/mol

PET is hydrophobic and does not contain any chemically reactive groups, as shown in Equation 2.1. This makes dyeing and water absorption very difficult [2]. It is necessary to modify the surface of the PET fibers to make them more reactive for these particular applications. This increases the versatility of the fibers and broadens the applications that PET can be useful.

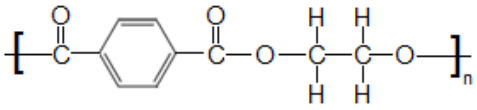

Figure 2.1. Structure of Polyethylene Terephthalate

Surface modification of PET is very difficult, as the chemical structure obstructs the production of radical sites or the attachment of grafting monomers. The amorphous, as well as the crystalline regions, of the PET structure form highly ordered regions making monomer diffusion very difficult [2]. The hydrogen bonding sites are located at the end of the molecule, not in the repeat unit, making chemical modification difficult [1]. Different surface modification techniques are available to bond functional groups to the structure using techniques just as redox reactions [2], [3], [4], [5], UV radiation [6], [7], [8], and melt state modification [9], [10].

2.2 Bicomponent Fibers

Bicomponent fibers are fibers composed of at least two polymers that are extruded into one single filament [11]. Bicomponent fibers have been used for many years as a way of producing nonwoven materials composed of fibers on the micro and nano scale.

Bicomponent fibers contain at least two polymers that share interface. Electrospinning has been the method for producing micro and nanofibers. However, electrospinning is a very slow, energy intensive process [12]. Though the splittable bicomponent technology was developed in the mid 1960's [13], Dupont Company made the first commercially available bicomponent fiber in the 1970's [14]. In the past 30 years, much research has been done in the area of bicomponent fibers, looking for ways to make cheaper and more efficient high surface area fibers.

When producing bicomponent fibers the selection of polymers is essential to produce fibers with proper adhesion and melt temperature properties. Extruding the two polymers through a spinneret of a particular configuration using a spunlaid process produces the bicomponent fiber webs. The bicomponent webs contain either soluble or splittable fibers. The soluble bicomponents, such as island-in-the-sea fibers, contain one component that is selectively removed by leaching with a solvent. Splittable fibers, such as segmented pie fibers, contain two polymers that are fractured by mechanical force, usually high powered water jets [15]. The resulting nonwoven fabric is then composed of high surface area micro and nano sized fibers making them ideal for a variety of applications such as air and water filters, adsorption materials, and medical textiles and can be used for many advanced applications [16].

2.2.1 Bicomponent Fiber Cross-Sections

Bicomponent fibers are unique in the variety of cross sectional fiber shapes that can be produced. Most cross sections have a particular purpose. For the purpose of making bicomponent microfiber webs, island in the sea, segmented pie, and tipped trilobal fibers are most commonly seen in the literature, **Figure 2.2**.

Figure 2.2. a) Island and the Sea b) Segmented Pie c) Tipped Trilobal [17].

The diameter of the resulting micro fibers after splitting is dependent on the number of islands or number of segments as well as the original diameter of the fiber. The more islands or segments present the smaller the resulting fibers. Island counts typically range from 3 to 108 in laboratory settings, 108 usually resulting in fiber diameters of .5 μm [18]. Similarly, the number of pie segments greatly affects the size of the resulting fibers. Due to the packing density of the segments, however, it is difficult to balance the mechanical properties with the increased number of segments. The pie segments can pack tightly together and therefore lose some of their individual mechanical strength under a load [12]. It is important to consider this decrease in mechanical strength when increasing the number of pie segments. It has been found that 24 segments is generally the max before the mechanical integrity of the fibers is threatened [18]. Fibers with 16 segments have been found to produce fibers with diameters ranging from 0.5 to 2 μm and do not lose their strength [19].

One of the most well known commercially available segmented pie nonwovens is Evolon® produced by Freudenberg Nonwovens. Evolon® is composed of polyester and nylon segments that are spunbond into a web and fractured using hydroentangling. The resulting microfiber materials are used as cleaning cloths, bedding, printing media, sound absorption, and as a synthetic leather [20].

2.2.2 Polymer Selection

Polymer selection is a key parameter in making bicomponent fibers. Since the two fibers are to be extruded from the same spinneret they must have similar melt and softening temperatures. The temperature of the spin pack will be based on the polymer with the higher melt temperature but will typically be at the bottom end of the polymer's softening range. Therefore the two polymers must have similar melt temperatures so as not to degrade the polymer with lower melt temperature[21].

The next parameter to be considered is the viscosity of the polymers. If the viscosities of the two polymers are very different, migration can occur and the definite interface that is required between the polymers can be compromised [13]. For the purpose of producing splittable fibers, a difference in crystallization rate is preferred to enhance the splittability of the fibers in the web. Two polymers that crystallize at different rates will maintain a distinct interface between their two surfaces. If the polymer structures are too similar, the polymers may be miscible and the resulting fibers will not spilt apart when fracturing. However, if the polymers repel each other, such as opposing polar polymers, they will not form a fiber and will likely destroy machinery. Therefore, the polarity, viscosity, rate of crystallinity, and melt temperature are important parameters to consider when choosing polymers for bicomponent spinning [21].

There are known polymer combinations that are ideal for bicomponent spinning based on these parameters. Such combinations include polyolefin-polyamide, polyolefin-polyester, and polyamide-polyester [13].

2.2.3 Fiber Extrusion

The fibers are extruded through a spinneret of that configuration in a spunlaid process, typically spunbond. There are some reports of meltblown bicomponent fibers [16], [22] but the cross section is typically limited to side-by-side configurations. In the spunbond process, Figure 2.3, the polymers are extruded through the spin pack in their configuration and elongated with cool air. This cool air pointed longitudinally down the length of the fiber quenches the polymer and causes crystallization. The fibers are drawn with a vacuum as they

gather on the moving belt below [23]. The spunbond webs can then be bonded using hydroentangling, a process that will also fracture the bicomponent fibers. Spunbond fibers are typically 10-80 μm in diameter and after splitting are as small as .3 μm [12].

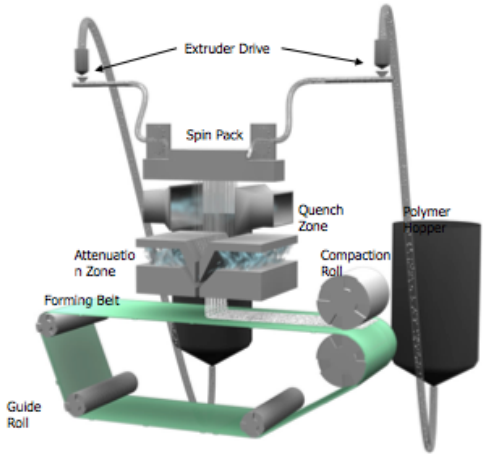

Figure 2.3. Schematic of a spunbond machine[11]

The meltblown process varies in that it uses hot air along the length of the extruded polymer rather than cool air. This prevents quenching from occurring and allows the molten polymer to be drawn out further before it is gathered on the collecting belt. This prevents quenching from occurring and allows the molten polymer to be drawn out further before it is gathered on the collecting belt. This produces small diameter fibers, typically 2-10 microns[18], which in turn would produce even smaller diameter fibers after the bicomponents are split, typically <1 – 2 microns[22]. Meltblowing is a self bonding process meaning that when the molten polymer fibers are collected on the belt, they bond to each other. However, the fibrous mats are still very weak and require another form of bonding[13]. For these reasons, spunbond processing is typically the method used to produce splittable bicomponent fibers.

2.2.4 Methods of Fiber Separation

The bicomponent fibers are fractured using mechanical force such as water energy, carding, twisting, or drawing [15]. Hydroentangling, , is the most commonly used mechanism to fracture bicomponent fibers [12]. Hydroentangling uses fine, high powered water jets that entangle the fibers to entangle the fibers to form a strong fibrous mat as well as split the two polymers of the bicomponent fiber. The resultant fabric is composed of two fiber types of micro and nano scale. Rather than using harsh chemicals or adhesives to bind the fibers of the mat, the hydroentangling simply uses water that is filtered, recycled, and reused in the process.

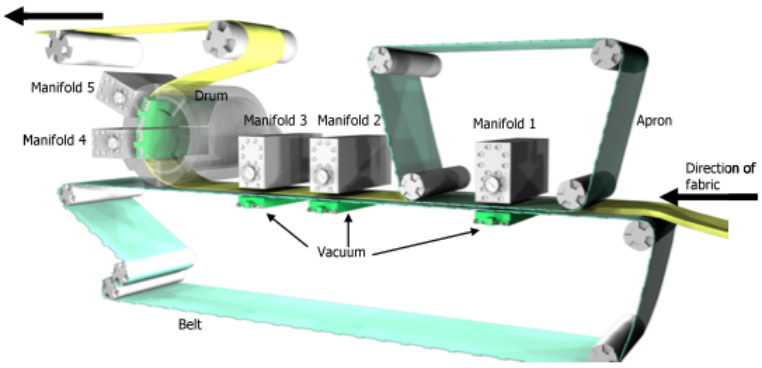

Figure 2.4. Schematic of the NCRC hydroentangling machine [27]

However, it is well known that hydroentangling is inefficient in the consistency of the degree of fracture of the bicomponent fibers through the cross section of the material. The high powered jets of the hydroentangling break up the fibers on the surface but are typically unable to split the fibers in the center of the web [18]. This was confirmed by Shim et al. [24]. It was found that the Mathis JFO Jet Dyeing machine was able to achieve close to 90%

splitting through the cross section of the fabric as shown in **Figure 2.5**. This was a vast improvement to the 50% in the center of the hydroentangled fabric samples. In the hydroentangled samples, high fracture occurred where the water jets interacted with the surface, while low fracture occurred in the areas between the jets. This phenomenon creates areas known as jet streaks where peaks and valleys are observed across the surface of the fabric.

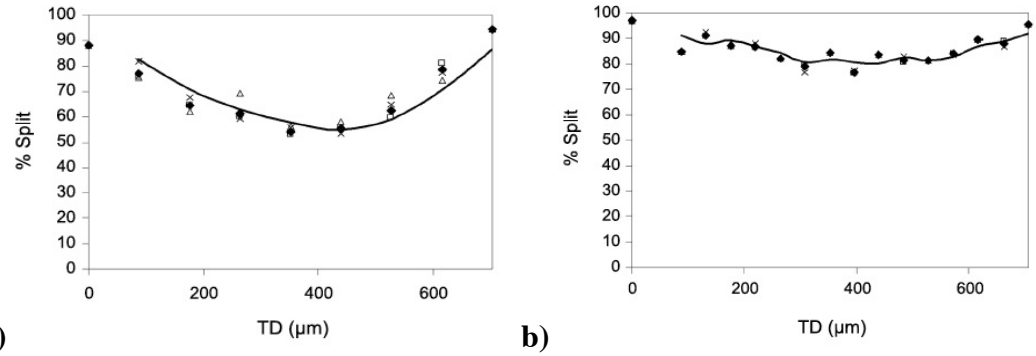

Figure 2.5. Percent of fractured fibers of a) hydroentangled and b) treated by jet dyeing machine

Shim et al. [24] also investigated the orientation of the fibers in the MD, CD, and TD directions of the jet dyed fabrics. They found that the orientation of the fibers was not significantly changed after washing in the jet dyeing machine, but that full fracture occurred.

2.2.5 Surface Area

The surface area of the fibers is dependent on the number of segments in each fiber, the number of segments split, and the size of the original fiber. The relationship between size of the fiber, number of segments, and surface area per unit volume can be easily calculated Equation 2.1.

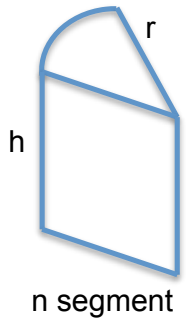

$$\frac{SA}{V} = \frac{2}{r} + \frac{2n}{\pi r} \qquad \textbf{(2.1)}$$

Specific surface area and fiber diameter have a linear inverse relationship; as the fiber diameter decreases, the surface area increases. Typical spunbond fibers range in diameter from 10 - 80 μm, while meltblown fibers range from 2 - 7 μm[25], and electrospun fibers are < 1 μm[12]. Based on these fiber diameters, the specific surface area of commercial fibers can be estimated as:

Spunbond Fibers - 0.05 - 0.4 μm^{-1} (about 0.06 ~ 0.3 m^2/g for PET fibers)
Meltspun Fibers - 0.57 to 2 μm^{-1} (about 0.4 ~ 1.4 m^2/g for PET fibers)
Electrospun Fibers - > 4 μm^{-1} (> 2.9 m^2/g for PET fibers)

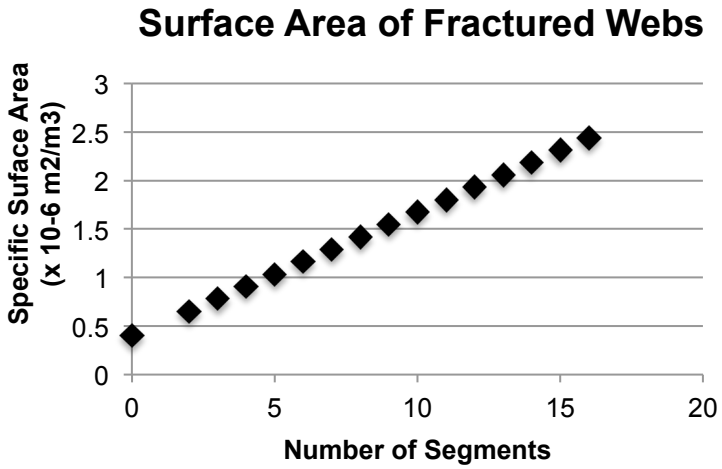

Figure 2.6. Surface area of bicomponent webs with increasing number of segments, Assuming a radius of 5 microns

The increase in the surface area with increasing number of segments in each fiber is seen in . For a fiber with a radius of 5 μm and 16 segments that has 100% splitting has a specific surface area of 2.44 μm^{-1}. This is even larger than the surface area of typical meltblown fibers. Therefore, it is important to achieve as close to 100% splitting as possible to ensure that the maximum surface area is available.

The ion exchange capacity is dependent on the number of functional groups on the surface of the fibers. Therefore, by maximizing the fracturing of the bicomponent fibers, the surface area available for functionalization is greatly increased.

2.3 Ion Exchange

Ion exchange resins were first developed in 1935 in the British Chemical Research Laboratory as a product of the condensation reaction between phenol and formaldehyde. Several ion exchange resins were produced thereafter and in 1939 the first commercial deionization system was installed [26]. Ion exchange resins are composed of a crosslinked

polymer matrix, typically in the form of a porous bead, with functional groups attached to the surface [27]. Advancements were made to these resins and they continued to be the state of the technology until recently.

2.3.1 Fundamentals of Ion Exchange

Ion exchange is the replacement of ions of a given charge by equivalent quantities of ions with the same change[28]. In order for this process to take place, there must be an interaction between ions in a solution and ions fixed to a solid[29]. The solid material contains fixed functional groups of a given charge with counter ions of the opposing charge attached to each functional group. When ions of the same charge as the counter ions come in contact with the material, the counter ions are exchanged for the ions in solution, assuming the electrostatic force of these ions is stronger than the counter ions. The exchange of positively charged ions is known as *cation* exchange, while the exchange of negatively charged ions is call *anion* exchange[28]. For example, a typical cation exchange reactions is seen in Equation

$$NaX + KCl(aq) \rightleftharpoons ClX + NaCl(aq) \qquad \textbf{(2.2)}$$

where X is the ion exchange structure and potassium chloride and sodium chloride are in aqueous (*aq*).

Ion exchange materials are categorized based on the charge of ions that take place in the exchange; cationic exchangers or anionic exchangers. Cation-exchange materials can be strongly acidic, containing sulfonic acid functional groups ($-SO_3H$) or weakly acidic, containing carboxylic functional groups (-COOH). Strong acid cations can dissociate in both alkaline and acidic solutions, making them very versatile in the solutions in which they can be used. Weak acid cation exchangers can be easily regenerated, but have a lower ion exchange capacity than the strong cation exchangers. Therefore, strong acid cation exchangers are the most widely used in industry [27].

Strong base anion exchange materials contain quaternary ammonium groups ($-NR_3OH$). Like strong acid cation exchangers, strong base anion exchangers are highly ionized and can be used in solutions over a wide range of pH. Weak base anion exchangers most commonly

contain tertiary amine groups, $-N(CH_3)_2$, but can also contain primary and secondary amines as well. Weak base anion exchangers are used for the removal of strong acids but are not capable of splitting neutral salts. Amphoteric ion exchange materials can also be developed, which contain both weak acid and weak base functional groups. These exchangers are capable of targeting both positively and negatively charged ions in solution [30].

These materials are typically in the form of resins, also referred to as beads. The resins are hydrophobic insoluble polymer matrices with a high degree of crosslinking, Figure 2.7. Functional groups are attached to the resin surface throughout the porous, three-dimensional structure. The size of the pores, as well as the overall size of the bead, is determined by the degree of crosslinking of the polymer matrix [28].

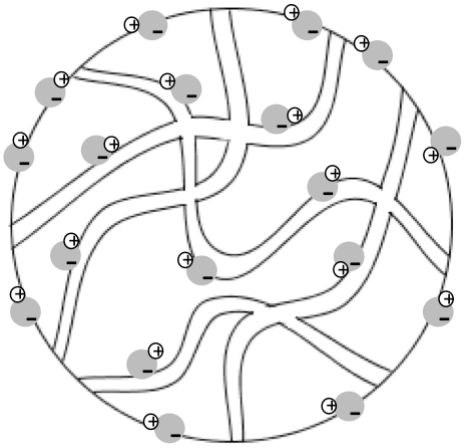

Represents the fixed anion functional group on the polymer chain

Represents the positive counter ion

Represents the polymer chain

Figure 2.7. Schematic of Ion Exchange REsin

The areas between the polymer chains are able to swell with the adsorption of a solvent and the counter ions are able to move throughout this region. The resin's ability to swell is limited by the degree of crosslinking, therefore limiting the mobility of the counter ions and the diffusion of the solvent[28].

2.3.2 Commercial Ion Exchange Resins

The ion exchange capacity of resins is dependent on the chemical and physical structure of the resin, as well as the experimental conditions. The degree of crosslinking is the most important factor as it determines the pore size and surface area, which in turn determines the number of functional groups available. The grafting and crosslinking of the monomers improves the physical durability of the resin and increases the surface area available for the attachment of the fixed functional groups. The degree of crosslinking controls the pore size distribution which must be small enough to insure interaction between the ions in solution and the counter ions. However, decreasing the pore size also reduces the resin's ability to swell. Limiting the swelling of the resin reduces the mobility of the counter ions and the diffusion of the ion containing solution throughout the structure. Smaller pore sizes lead to higher pressure drops and more energy for operation. Therefore, a balance between the degree of crosslinking (the pore size) and the operating resistance is necessary for efficient usage [28], [29], [31]

As previously mentioned, strong base cation exchangers containing sulfonic acid groups are the most widely used ion exchange resins. Most commercial ion exchange resins are spherical beads of styrene and divinylbenzene (DVB) copolymers. These resins are very mechanically and chemically stable and will accept many different functional groups [32], but are most often sulfonated to attach $-SO_3$ groups for cation exchange [30]. The resins are a result of suspension polymerization between styrene and DVB monomers. The degree of crosslinking is determined by the amount of DVB, in mole percents, added to the polymerization. Typical resins contain 8-12% DVB, while some resins can range from 0.25-25% depending on the application[28]. High DVB contents result in structurally sound resins

but are not able to swell. The surface area of these resins is about 33-35 m^2/g [33]. The process and the production of similar resins is well known and can be found extensively in the literature [27], [34], [35], [36].

The resins used for water filtration purposes are typically between 20-50 mesh size (297-840 μm) [27]. It is found that this diameter range results in resins with a relatively low pressure drop in a packed bed operation, allows for expansion of the resins, and provides adequate surface area while allowing for a high flow rate [29]. The characteristics of some of the commercially available ion exchange resins used for heavy metal removal are found in Table 2.2.

Table 2.2. Properties of Commercially Available Ion Exchange Resins

Name	**Company**	**Polymer Matrix**	**Functionality**	**IE Capacity (meq/g)**
Amberlyst™ 36Wet [33]	Rohm & Haas	Styrene DVB	Strong Acid Cation ($-SO_3H$)	5.4
Dowex™ Marathon™ MSC	Dow Chemical	Styrene DVB	Strong Acid Cation ($-SO_3H$)	2.1
Amberlite™ IRC76 [37]	Rohm & Haas	Styrene DVB	Weak Acid Cation (-COOH)	3.9
Lewatit® S8227 [38]	LanXess	Acrylate	Weak Acid Cation (-COOH)	5.5
Amberjet™ 4200 Cl [39]	Rohm & Haas	Styrene DVB	Strong Base Anion ($-N^+(CH_3)_3$)	1.9
Dowex™ Marathon™ 550A [38]	Dow Chemical	Styrene DVB	Strong Base Anion ($-N^+(CH_3)_3$)	1.7

In a study by Bai and Bartkiewicz [40], the removal of cadmium from waste water was investigated using a strongly cationic exchange resin column, AMBERJET™ 1200 H, commercially available from Dow Chemical [41]. The AMBERJET™ 1200 H resin is a styrene divinylbenzene copolymer matrix with sulfonate functional groups, in the hydrogen form. The gel type resin was tested in both bath and column operations. According to The Dow Chemical, the column in the hydrogen form has a capacity of ≥ 1.8 eq/L. In this study, it was found that the column had an average ion exchange capacity of 3.0 meq/g, making it a rather efficient resin when used in the pH range of 4-7.

In a similar study by Pehlivan and Altun [42], a Dowex 50W ion exchange resin was used to investigate the removal of copper, zinc, nickel, cadmium and lead metal ions. Dowex 50W is a gel styrene divinylbenzene microporous resin with sulfonic acid functional groups, a strongly cationic exchange resin, with an ion exchange capacity of 4.8 meq/g. The study found that by adjusting parameters such as pH, temperature, contact time and adsorbate amount, Dowex 50W ion exchange resin had 4.1, 4.6, 4.7, 4.8, and 4.7 meq/g dry resin for Pb^{2+}, Cu^{2+}, Zn^{2+}, Cd^{2+}, and Ni^{2+}, respectively.

The balance between the surface area and the operating resistance is the major drawback to using traditional ion exchange resins. With a need to increase the surface area and therefore the ion exchange capacity, while maintaining a low operating resistance, ion exchange fibers are being considered a reasonable alternative.

2.3.3 Ion Exchange Fibers

The earliest investigation of using fibrous media to remove ions from solution were performed by Economy et al. [43], [44] in the 1970's and focused on developing activated carbon coated glass fibers. Econonmy's group continued to work with activated carbon coated glass fibers and had great success in removing BTEX (benzene, toluene, ethylbenzene, and xylene) to below EPA standards[45]. However, activated carbon fibers are very expensive, about $100 per pound[46]. Dominguez[44] later developed divinylbenzene coated glass fiber ion exchange materials. Although these materials proved to successfully

remove lead and mercury from water, glass fibers are still an expensive substrate to be used for ion exchange. Other niche ion exchange fibers have been reported in the literature, such as nanoparticle impregnated fibers[47].

Other efforts have been made to produce cost efficient ion exchange fibers by functionalizing grafted copolymers on a base polymer. This has been done both in the melt state[10], [48] and directly on the base polymer[46], [49], [50], [51], [52]. Typical base polymers include polypropylene (PP)[49], [52], [53], [54], polyethylene terephthalate (PET) [3], [55], [56], [57], polyacrilonitrile (PAN) [58], polystyrene (PS) [59], and cellulose[60], [61], [62], [63], [64]. These fibers are grafted with a monomer, typically glycidyl methacrylate (GMA) [50], [65], styrene divinylbenzene (DVB) [52], [53], and acrylic acid (AA) [49], [54], [66]. There are several ways in which this grafting process can be performed including Co^{60}-γ-ray irradiation [67], electron beam irradiation [68], UV light radiation [69], [70], [71], [72], [73], and chemical initiation[74], [75], [76], [77], [78]. After grafting the monomer, the copolymers are given a functionality, typically by sulfonation [50], [52], [79] or amination [49], [52] to attach either cation or anion functional groups, respectively.

A series of commercially available ion exchange fibers were produced at the Institute of Physical Organic Chemistry as part of the National Academy of Sciences of Belarus in Minsk, Belarus under the trademark “Fiban”. These materials are produced by grafting styrene and DVB copolymers on polypropylene needlepunched nonwovens. FIBAN K-4 is used primarily for the filtration of heavy metals, such as lead, zinc, and cadmium from drinking water as well as ammines and aerosols from the air. It has a half ion transfer time of 2-10 seconds, compared to 30-200 seconds for industrial ion exchange resins [80]. Literature on the production of FIBAN K-4 in the melt form using gamma radiation can be found [53], [81] and information on its sorption of heavy metals are readily available, Figure 2.8.

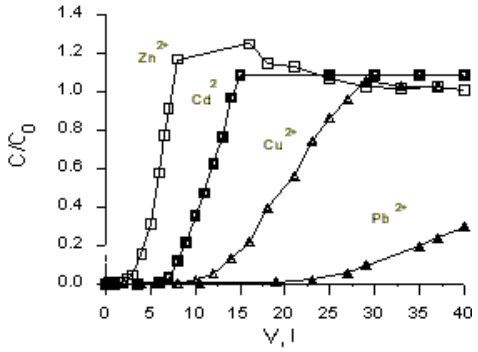

Figure 2.8. Sorption properties of FIBAN K-4 and removal of heavy and transition metal from a solution of Me2+ with 4 meq/g Ca2+ at pH=6, 9.5 cm/min flow rate, 3 cm filtering bed, .6 g of cation exchanger (C0 - Me2+ concentration in the initial solution equal 0. [52]

Similarly, FIBAN K-1 is a strong acid cation exchange resin also prepared by the polymerization of styrene and divinylbenzene to polypropylene nonwovens using radiation grafting. The styrene groups are then functionalized with sulfonic acid groups. The ion exchange capacity of the fibers is 3.0 meq/g and they have a diameter of 49 μm. The materials are used for the removal of organic substances, such as dyes and anitibiotics, the softening of water, as well as the purification of air[52].

Spomex® ion exchange fibers, produced by Johnson Matthey, is another line of IE materials that provide a wide range of functionalities used for metal removal. The base fibers are polyethylene strong acid cation exchange fibers. The strong acid cation exchange fibers contains a sulfonated styrene functionality and has a capacity of 3.2 meq/g, while the weak acid cation exchange fibers contains an acrylic acid functionality and has a capacity of 8.0 meq/g. Spomex® 107 contains both the strong and weak acid functionalities, making it selective for ions over a broader range, with a capacity of 8.0 meq/g. The ion exchange capacity of the strong acid exchange fiber is [82].

These commercial ion exchange fibers have all proven to be better alternatives to the traditional ion exchange resins. However, there is still a need to reduce the cost of the base

polymer fibers and find more cost efficient methods of functionalization. Successfully modifying the surface of an affordable base fiber, such as PET, would have a significant impact on the functional fiber industry.

2.3.4 Evaluation of Ion Exchange Properties

Batch reactors are ideal for laboratory experiments because of their small size and ease of use. The batch reactor allows for analysis of ion exchange properties by adding the adsorbent, the heavy metal in solution, to the sorbent, the nonwoven substrate [83]. The various parameters such as ion concentration, solution pH and temperature, and agitating speed will be varied to develop an understanding of their effect on the ion exchange materials.

Adsorption isotherms are used to describe the adsorption of the heavy metals on the surface of the substrate as it relates to the amount of heavy metals ions in a solution at a given temperature. Though there are several different adsorption isotherms, it is likely that the Freundlich and Langmuir will be ideal for the purpose of this research. The Freundlich isotherm, Equation (**2.3**), assumes the adsorption site energy distribution is decaying exponentially. It describes multilayer and non-ideal sorption on heterogeneous surfaces as follows:

$$q_e = K_f C_e^{1/n} \qquad \textbf{(2.3)}$$

The logarithmic form of Equation (**2.3**):

$$\ln q_e = \frac{1}{n} C_e + \ln K_f \qquad \textbf{(2.4)}$$

where q_e is the amount of copper removed per unit mass of sample (mg/g), K_f is the Freundlich constant related to the adsorption capacity, n is the Freundlich constant related to the adsorption intensity, and C_e is the concentration of the solution at equilibrium. The natural log plot of $\ln q_e$ versus $\ln K_f$ is plotted for the bicomponent and homocomponent nonwovens and used to calculate the Freundlich isotherm constants.

The Langmuir isotherm is commonly used to describe ion exchange capacities because it is able to predict a constant, single layer sorption capacity at high concentrations, C_e. It is described as follows:

$$q_e = \frac{q_m K_L C_e}{1 + K_L C_e} \quad \textbf{(2.5)}$$

Equation (2.5) can be expressed in its linear form as:

$$\frac{C_e}{q_e} = \frac{1}{q_m K_L} + \frac{C_e}{q_m} \quad \textbf{(2.6)}$$

where q_e, is the amount of adsorbed ions per unit mass (mg/g), C_e is the concentration of metal ions in solution at equilibrium (mg/L), q_m is the Langmuir constant describing the maximum number of metal ions per unit mass that can be removed after complete coverage (mg/g), and K_L is the Langmuir constant describing the energy of adsorption of the metal ions (L/mg). The plot of specific adsorption (C_e/q_e) versus the equilibrium concentration (C_e) is used to calculate q_m and K_L.

Sorption kinetics use the experimental sorption data to describe the rate controlling step of sorption of the heavy metal ions on the nonwoven substrate. The pseudo first and second order equations are used to provide theoretical and experimental understanding on the behavior of ion exchange fibers.

The pseudo first order equation is defined as:

$$\frac{dq_t}{dt} = k_1(q_e - q_t) \quad \textbf{(2.7)}$$

Equation (2.7) can be integrated based on the boundary conditions $t=0$ to $t=t$ and $q_t=0$ and $q_t=q_t$, to have the integrate form:

$$\ln(q_e - q_t) = \ln q_e - k_1 t \quad \textbf{(2.8)}$$

where q_t is the amount of copper adsorbed per unit of material (mg/g) at time t, k_1 is the pseudo first order rate constant (L/min) and t is the contact time.

The pseudo second order equation, describing the adsorption of heavy metals on a substrate, is as follows:

$$\frac{dq_t}{dt} = k_2(q_e - q_t)^2 \qquad \textbf{(2.9)}$$

Equation (2.9) can be integrated to the linear form on the boundary conditions $t=0$ to $t=t$ and $q_t=0$ and $q_t=q_t$ and expressed as:

$$\frac{t}{q_t} = \frac{1}{h} + \frac{1}{q_e}t \qquad \textbf{(2.10)}$$

The initial adsorption rate, h (mg/g□min) as t→0 is defined as:

$$h = k_2 q_e^2 \qquad \textbf{(2.11)}$$

where k_t is the pseudo second order rate constant (g/mg□min) and q_e is the theoretical maximum absorption (mg/g). A regression plot of t/q_t against t give the value of q_e as the slope and h as the intercept. The pseudo second order equation has been the most widely used equation for describing the sorption of heavy metals from waste water [84]. Experiments are typically carried out to identify system parameters such as initial concentration of ions, sorbent size, solution temperature, agitation speed, and solution pH. These parameters are important in determining appropriate order reaction and diffusion mass transfer. Determining the best fitting sorption isotherm and rate controlling step is essential to designing an optimal ion exchange system with maximum ion exchange capacity.

The removal of copper ions using ion exchange materials has been extensively studied [85], [86], [87], [88], [89]. This metal has a +2 charge, making the study of the kinetics more straightforward than many of the heavy metals with higher charges. This is an easy material to work with and the industrial importance is also of great significance. In a study by Lee, et al. [90], nonwoven polypropylene materials were functionalized with sulfonate containing functional groups and their ability of removal copper ions from water

was evaluated. The authors found that with grafting percentages ranging from 70-220% ion exchange capacities ranged from 0-2.16 meq/g, slightly lower than the total ion exchange capacity, 3.5-5.5 meq/g, determined through titration.

In a study by Hsien, et al.[89], mixed media membranes containing both chitosan and Amberjet weakly acidic ion exchange resins embedded in an ethylene vinyl alcohol polymer matrix were produced to remove copper ions from solution. The kinetics of the materials were evaluated at copper ion concentrations from 5-1500 mg/L of Cu^{2+} and pH 4-6. The maximum copper absorption occurred at 1,000 mg/L where the pH also increased at the greatest rate during the experiment, indicating that hydronium ion concentration was decreasing and hydronium ions were competing for functional group sites. The adsorption data fit the Langmuir and Freundlich models well. The sorption data was also evaluated based on first order, second order, and intra-particle diffusion equation models to find the rate controlling parameter. It was found that the data fit the second order kinetic model the best indicating that the rate controlling step for this material is likely chemical adsorption. This behavior is confirmed in some similar studies, [91], [92], [93].

2.4 Surface Grafting

Surface grafting techniques are often performed on polymers to control the physical and chemical properties of the polymer. These techniques modify the chemistry of the surface of the fiber, while maintaining the bulk properties of the material, such as the strength or elasticity[94]. Surface modification can be used to improve the wearability, wettability, biocompatibility, dyeability, adhesion, as well as physical strength of polymers [95], [96], [97], [98], [99].

Surface modification of polymers can be performed by physical or chemical initiation. Physical techniques include irradiation, chemical modification, flame treatment, ozone treatment, glow discharge, and corona discharge. Monomers are chosen based on their compatibility with the grafting technique and the base polymer, as well as the intended application. Typical grafting monomers used in radical polymerization include methacrylic

acids, acrylics, and styrene as well as the various forms of these monomers [100]. These monomers are then manipulated by attaching functional groups, typically either by sulfonation to attach negative sulfonic acid groups or amination to attach positive amine groups [28].

2.4.1 Physical Surface Modification

2.4.1.1 Plasma Treatment

Glow discharge, flame treatment, and corona discharge are all types of plasma treatments to be used in surface modification. While each type of plasma treatment has its own advantages and disadvantages, generally plasma treatment is less penetrating than other modification techniques. Therefore, plasma treatment is highly effective in targeting the modification of the surface of the polymers rather than affecting the bulk properties of the polymer [101]. Although plasma treatments result in a fairly uniform modification, the need for a vacuum makes operation costly and it is difficult to control the exact amount of functional groups that are attached to the surface [102].

Plasma is a gas that contains charged or neutral particles, which can be electrons, positive or negative ions, radicals, atoms, or other molecules. The radicals and ions are formed when atoms in the gas impact one another. Some of these free radicals will diffuse onto the surface of the polymers [103][112][113][109][109][103][102]. In the presence of an electric field, the particles move, gain kinetic energy, and increase the temperature of the plasma [103]. The temperature is therefore dependent on the species present and the intensity of the electric charge [102]. Free radicals are also formed on the surface through adsorption of the UV radiation that is formed in the plasma and electron-ion recombination [103].

2.4.1.2 Glow Discharge

Plasma treatment performed at low electron temperatures, 1 to 10 eV, and a relatively low pressure are considered glow discharge plasma. The electron density is typically between 10^{9} to 10^{12} cm^{-3} and the degree of ionization can vary anywhere between 10^{-6} to 0.3 [102]. The glow discharge is created by sending an electric current through a gas at low pressure,

typically hydrogen, helium, argon, or nitrogen [101], between two electrodes. The bombardment of positive ions and incident radiation causes secondary electrons to be released from the surface of the cathode. These secondary electrons increase to high degrees of energy as they pass through the electric field, which ionizes the gas atoms. In a study by Hsieh and Wu [99], argon glow discharge was used to improve the hydrophilicity of PET films. Acrylic acid was grafted onto the surface of the PET polymers in the presence of the argon glow discharge under 0.5 Torr of pressure with a radio frequency of 13.56 MHz to generate the glow discharge. Hseih and Wu were able to reduce the contact angle of the film from 73.1º ± .1º to between 33.7º to 41.0º with the grafting of acrylic acid monomers on the surface of the polymers. Glow discharge is not often used for the modification of polymer surfaces and the mechanisms of the process are still not well understood [102].

2.4.1.3 Corona Discharge

Corona discharge is often used for the modification of polyolefins to improve their printability and adhesion properties. The set up, , is simply a large capacitor consisting of a grounded metal roll, an electrode, and a high frequency, high voltage generator. The grounded roll and the electrode are the plates of the electrode, while the insulating material on the metal roll and the air are the dielectric. Corona is created when an electric charge is applied to the electrode and causing ionization of the air between the electrode and the metal roll. This creates a plasma in the air gap called the corona discharge.

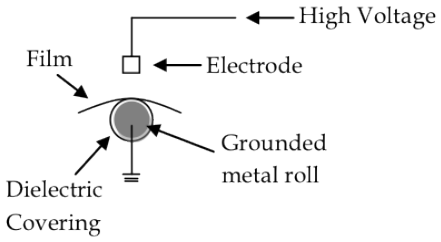

Figure 2.9. Corona Discharge

When the polymer comes in contact with the plasma discharge, the electrons, ions, photons, and excited neutrons found in the plasma react with the polymer surface. This generates free radicals on the surface which quickly react with the monomers present.

The use of plasma discharge, known as a "grafting from" technique often results in non-covalently bonded grafts. These coatings can be removed from the substrate and do not have strong physical properties. Because of the high energy involved with these techniques, the bulk properties of the substrate are more prone to deterioration, especially when micro-fibers are chosen as the base material rather than films[94].

2.4.1.4 Irradiation

Radiation grafting employs an energy source to induce grafting between the substrate and the monomer, typically in the presence of a solvent. Radiation grafting is split up into two main categories, ionization and photografting, based on the intensity of the source. Ionization radiation includes electron beam radiation, γ radiation, and X-rays. The study of these techniques is known as radiation chemistry. Grafting done by UV and visible light is photografting; the study of which is photochemistry. The primary difference between photografting and ionization radiation is the high amounts of energy that are used in ionization radiation compared to photografting, Figure 2.10. Ionization radiation produces a large amount of excited and ionized molecules and its high intensity makes it very difficult to be selective [102].

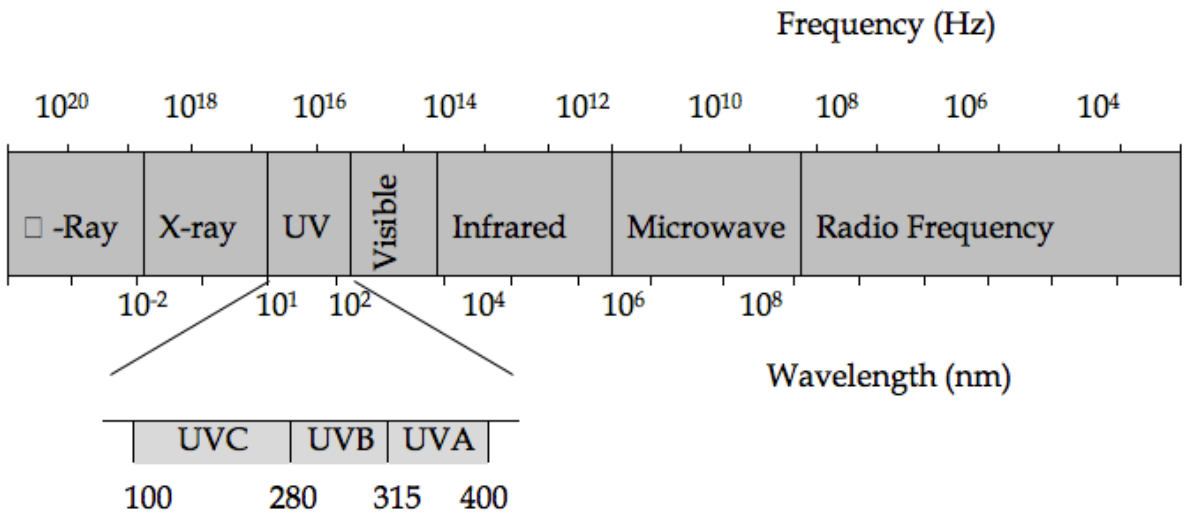

Figure 2.10. Electromagnetic Spectrum

The low intensity used in photografting is less penetrating into the sample, making it highly effective in targeting the surface of the polymers materials. Photografting typically requires simple equipment, can prepare grafted samples in a short amount of time, and has a much lower cost compared to other grafting techniques [94]. The UV spectrum can be further split up into three more categories: UVA, UVB, and UVC representing wavelengths of 315 - 400 nm, 280-315 nm, and 100-280 nm, respectively. The selection of a specific bulb for the photografting experiments is dependent on the photoinitiator used in the solution.

In order for a photografting procedure to occur, a photoinitiator or photosensitizer must be used to initiate the reaction. Photoinitiators are light sensitive, typically at a specific wavelength of light, and create free radicals that initiate the polymerization of the monomer. A photosensitizer is used primarily to speed up the reaction and is not consumed in the reaction. It can also be used to adjust the range in which the photoinitiator absorbs photons, adjusting it towards long wavelengths [104].

Other components can be present in the solution to aid in the photografting process, such as coinitiators or synergists. Some systems require the use of a coinitiator to aid the photoinitiator in producing radicals to initiate polymerization. If the coinitiator is not an indispensible part of the reaction and also enhances the efficiency of the process it is considered a synergist. Amines are common synergists for benzophenone photoinitiator as it improves the efficiency of the reaction but are not required for the photoinitiator to work [105].

The rate of photoinitiation is affected by many factors. For photoinitiation certain characteristics of the system must be correct:

1. The initiator molecules are sensitive to the particular wavelength of light under which they are exposed
2. There are no components presents that absorb photons at the same wavelength as the photoinitiator
3. There are no chain terminating molecules present in solution
4. An appropriate quantum yield is achieved

The quantum yield, Equation , of the reaction describes the ratio between the number of events that occur for each UV photon absorbed. This is dependent on many factors including the concentration of reactants and products, the temperature of the system, and the wavelength of light [104]. For the event of photografting,

$$\text{Quantum Yield } (\Phi) = \frac{\text{\# of reactants consumed}}{\text{\# of photon absorbed}} \qquad \textbf{(2.12)}$$

In order for photoinitiation to proceed, there must be more reactant molecules consumed than UV photons absorbed. Thus, $\Phi \geq 1$.

Oxygen in the environment in which the photoinitiation is taking place can not only quench the triplet state of the photoinitiator but also react with the radicals. Both situations prevent chain initiation from occurring because the monomers are unable to react with the radicals. This can be prevented by performing the procedures in a vacuum or in a nitrogen

atmosphere. This is difficult, as it means that the entire UV set up must be enclosed in an inert atmosphere. Other methods have also been suggested for preventing oxygen inhibition, such as the addition of water in the grafting solution [106], [107].

There are many different photoinitiators available and many different mechanisms for the initiation of the reaction. Photoinitiation can occur through fragmentation, ionic initiation, photocrosslinking reactions, triplet energy transfer reactions, or hydrogen abstraction. Benzophenone (and derivatives of the molecule) is one of the most commonly used photoinitiators used in photografting procedures, [102].

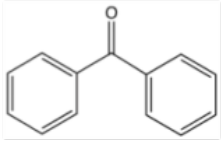

Figure 2.11. Benzophenone molecule

It is an aromatic ketone that reacts through hydrogen abstraction to create surface free radicals. The photoinduced excitation in which benzophenone, BP, is elevated to its singlet state occurs at 340 nm. The photoinitiator remains in its triplet state for only 10^{-6} seconds before producing radical ions. Several factors can cause the photoinitiator to no longer remain in the triplet state. The triplet state can become quenched by the monomer if no chain initiation occurs or oxygen present in the environment. The formation of other complexes or photolysis products can also cause the deactivation of the triplet states. If this occurs than proper chain initiation will not continue since the radical ions will not be produced [105].

2.4.2 Chemical Surface Modification

2.4.2.1 Ceric Salts

Cerium ion has been extensively studied for its strong oxidizing properties in redox-initiated polymerizations [62], [63], [77], [108], [109]. Cerium is a rare earth metal in the lanthanide family that is found in abundance in the earth's crust. Cerium ion is stable in both +3 and +4 oxidation states but is more stable as in the +4, cerium(IV), because of its vacant f shell. Cerium(IV) has a high reduction potential of 1.6 V vs normal hydrogen electrode which makes it an efficient oxidizing agent, it has the ability to accept electrons [110].

Some of the earliest work done in the area of ceric salt initiated grafting was performed by Mino and Kaizerman in 1958 [77]. The authors found that when ceric salts, specifically ceric ammonium nitrate and sulfate, were mixed with suitable organic reducing agents they formed redox systems. The reducing agents used in the study included alcohols, glycerols, mono and disaccharids, thiols, aldehydes, and amines. Mino and Kaizerman [77] proposed a single electron transfer mechanism, in which a free radical is produced on the reducing agent. If the reducing agent is a polymer and a monomer is present in the grafting solution, a free radical is produced on the polymer backbone and becomes the grafting site for the monomer present. In this particular study, acrylamide, acrylonitrile, and methyl acrylate were grafted onto polyvinyl alcohol under nitrogen.

Few changes have been made to the ceric ion grafting process since the early studies. Extensive studies have been done on investigating the kinetics of ceric ion initiated grafting reactions [78], [108], [111], [112]. In one such study by Odian and Kho [113], the rate of grafting vinyl-acetate acrylonitrile to PVA initiated by ceric ammonium nitrate was a first order reaction with respect to the monomer and polymer concentrations. The authors found that at varying CAN and monomer concentrations, all grafting percentages leveled off after 20 minutes, which they attributed to consumption of the ceric ions. The grafting percentage was found to be independent of ceric ion concentration above .002 M.

Ceric ammonium nitrate and sulfate (CAN, CAS) are the two most common ceric salt molecules used for redox initiated grafting. Ceric ammonium nitrate, Figure 2.12, dissociates

in a strong acid medium and the tetravalent cerium ion is available to accept electrons. The polymerization of the monomers via ceric salt initiation proceeds by initiation of the radical site, propagation of the monomer to the grafting site, and termination of the radicals[63]. Ceric ions are used primarily to initiate polymerization of vinyl monomers [76], [111], [113], [114], [115]as well as cellulose [62], [63], [79].

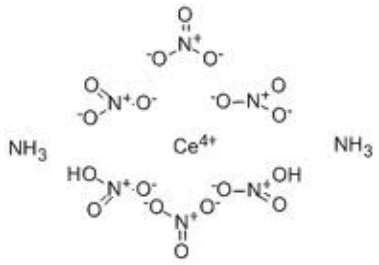

Figure 2.12. Ceric Ammonium Nitrate molecule

Haworth and Holker [116] investigated the grafting of acrylic acid on nylon fibers via ceric ammonium nitrate and sulphate initiation. The use of mineral acid additives was also investigated as a means of speeding up the reaction. 8.7 – 50.3% grafting was reported after 1 – 7 hours, respectively. With the addition of sulfuric acid in the grafting solution this was increased to 80% grafting percentage after 1 hour. The reactions were performed in closed flasks in the dark, but no nitrogen was flushed through the reaction.

2.5 Functionalization

The grafted monomer must then be modified by chemically bonding acidic or basic functional groups. The attached functional group determines the selectivity of the material. It was previously mention that strongly acidic groups are most often sulfonic acid, $-SO_3^-$, and weak acid groups are carboxylic acid, $-COO^-$. While, strongly basic groups are commonly quaternary ammonium groups, $-NR_3OH$, and weak base anion exchangers are tertiary amine

groups, $-N(CH_3)_2$, but can also contain primary and secondary amines as well. Sulfonation is the most common functionalization technique as it is very simple and the least expensive process[28]. Compounds such as sulfuric acid, sodium sulfite, sulfates, and variations of complexes have been used as the sulfonating agents[117]. Currently there are no known continuous functionalization processes. Therefore, all chemical processes are done in batch type operations in a reaction kettle with the sulfonating agents and materials[28].

2.6 Surface Modification of PET

As previously discussed, surface modification of polyethylene terephthalate (PET) is difficult due to its highly ordered structure and lack of reactive groups[2]. Achieving an efficient, cost effective method of surface modification of PET would have a profound impact on the functional fiber industry. Modifications allow for tailoring of the reactivity of the PET fibers, while taking advantage of the positive physical properties of the material. Some methods of modification of the PET structure have been reported in the literature[3], [5], [118], [119], [120]. However, to the best of our knowledge, there are no commercial functionalized PET materials currently available.

Somanathan et al.[2] grafted methylacrylic acid on PET fiber by swelling the fibers in solvent and exposing them to the MMA monomers in the presence of an initiator at elevated temperature. Gupta et al.[120] used radiation to initiate the grafting of acrylic acid to PET textured knit yarns. Gao et al.[7] used UV radiation to modify the surface of PET films. The films were exposed to UV and submerged in functional solutions. Improved adhesion of the films was experienced after functionalization. In a similar study, improved flame retardancy of PET woven fabrics was experienced using UV initiated grafting of glycidyl methacrylate with benzophenone photoinitiator. The glycidyl methacrylate is then functionalized with a flame retardant group[121].

Although limited, some reports of redox initiation of monomers to PET films and fibers are available in the literature. Chansook and Kiatkamjornwong[118] performed surface modification of PET yarns using ceric ion initiation. The experiments were performed in

batch operations under nitrogen. Acrylic acid was used as the grafting monomer. Grafting percentages of 50% were experienced after 60 minutes of reaction time. The use of other redox initiators such as potassium bromate-thiourea[3] and potassium-permanganate-oxalic[4] have also been reported to be successful methods of modifying the PET surface.

2.7 Removal of Copper Ions

Although certain amounts of some heavy metal ions are essential for human existence, the concentration of these metals is often much higher in drinking water and serious efforts need to be made to recover and remove these metals from water. Heavy metals are considered to be any metal with a density above 5 g/cm^3, but arsenic, cadmium, chromium, copper, nickel, lead, and mercury are considered to be some of the most harmful to both the environment and living organisms. Copper in particular can lead to liver damage, Wilson disease, and insomnia at exposure levels of just .25 mg/L [122]. Water sources are polluted with heavy metals from common industrial waste such as mining, electronics, metal finishing, and electroplating [87].

Common heavy metal ion removal techniques include flotation, adsorption, ion exchange, and most commonly chemical precipitation. Chemical precipitation involves the addition of chemicals to the waste water to bring the water to a basic pH and bind with the metal ions. This process produces a large amount of a high density, toxic sludge that must then be removed and disposed of. Due to these disadvantages, other options are being considered as acceptable alternatives to chemical precipitation. Ion exchange is a potential process to replace chemical precipitation, however, the capacity and selectivity of commercially available ion exchangers need to be increased[122].

2.8 References

[1] I. Hutten, “Handbook of nonwoven filter media,” Elsevier, Ltd., pp. 151–152.

[2] N. Somanathan, B. Balasubramaniam, and V. Subramaniam, “Grafting of Polyester Fibers,” *J. Macromol. Sci. Part*, vol. 32, no. 5, pp. 1025–1036, May 1995.

[3] M. K. Mishra, B. L. Sar, and A. K. Tripathy, “Potassium Bromate-Thiourea Redox Initiated Grafting of Methyl Methacrylate onto Polyethylene Terephthalate,” *J. Macromol. Sci. Part - Chem.*, vol. 18, no. 4, pp. 565–573, Sep. 1982.

[4] A. K. Pradhan, N. C. Pati, and P. L. Nayak, “Grafting vinyl monomers onto polyester fibers. III. Graft copolymerization of methyl methacrylate onto poly(ethylene terephthalate) using potassium permanganate–oxalic acid redox system,” *J. Appl. Polym. Sci.*, vol. 27, no. 6, pp. 2131–2138, Jun. 1982.

[5] R. Coşkun and S. Akdeniz, “Functinalization of poly(ethylene terephthalate) fibers by grafting of maleic acid/methacrylamide monomer mixture,” *Fibers Polym.*, vol. 11, no. 8, pp. 1111–1118, Dec. 2010.

[6] D. Praschak, T. Bahners, and E. Schollmeyer, “Excimer UV lamp irradiation induced grafting on synthetic polymers,” *Appl. Phys. Mater. Sci. Process.*, vol. 71, no. 5, pp. 577–581, Nov. 2000.

[7] S. L. Gao, R. Häßler, E. Mäder, T. Bahners, K. Opwis, and E. Schollmeyer, “Photochemical surface modification of PET by excimer UV lamp irradiation,” *Appl. Phys. B*, vol. 81, no. 5, pp. 681–690, Aug. 2005.

[8] L. Yu, S. Zhang, W. Liu, X. Zhu, X. Chen, and X. Chen, “Improving the flame retardancy of PET fabric by photo-induced grafting,” *Polym. Degrad. Stab.*, vol. 95, no. 9, pp. 1934–1942, Sep. 2010.

[9] F. Pazzagli and M. Pracella, “Reactive compatibilization of polyolefin/PET blends by melt grafting with glycidyl methacrylate,” *Macromol. Symp.*, vol. 149, no. 1, pp. 225–230, Jan. 2000.

[10] M. Pracella and D. Chionna, "Reactive compatibilization of blends of PET and PP modified by GMA grafting," *Macromol. Symp.*, vol. 198, no. 1, pp. 161–172, August.

[11] S. Batra, M. Thompson, E. Vaughn,, and L. Wadsworth, *INDA Nonwovens Glossary*. Cary, NC: Association of the Nonwovens Fabrics Industr, 2002.

[12] N. Anantharamaiah and B. Pourdeyhimi, "Durable Nonwoven Fabrics via Fracturing Bicomponent Islands-in-the-Sea Filaments," *J. Eng. Fibers Fabr.*, vol. 3, no. 3, pp. 1–9.

[13] W. Goddard, *Handbook of nanoscience, engineering, and technology*, 2nd ed. Boca Raton FL: CRC Press, 2007.

[14] M. Lewin, *Handbook of fiber science and technology*. New York: Dekker, 1996.

[15] N. Fedorova and B. Pourdeyhimi, "High strength nylon micro- and nanofiber based nonwovens via spunbonding," *J. Appl. Polym. Sci.*, vol. 104, no. 5, pp. 3434–3442, Jun. 2007.

[16] C. Sun, D. Zhang, Y. Liu, and J. Xiao, "Bicomponent Meltblown Nonwovens and Fibre Splitting," *J. Ind. Text.*, vol. 34, no. 1, pp. 17–26, Jul. 2004.

[17] N. V. Fedorova, "Investigation of the utility of islands-in-the-sea bicomponent fiber technology in the spunbond process," 2007.

[18] A. Durany, N. Anantharamaiah, and B. Pourdeyhimi, "High surface area nonwovens via fibrillating spunbonded nonwovens comprising Islands-in-the-Sea bicomponent filaments: structure–process–property relationships," *J. Mater. Sci.*, vol. 44, no. 21, pp. 5926–5934, Sep. 2009.

[19] F.-L. Zhou and R.-H. Gong, "Manufacturing technologies of polymeric nanofibres and nanofibre yarns," *Polym. Int.*, vol. 57, no. 6, pp. 837–845, Jun. 2008.

[20] D. Groitzsch and G. Schaut, "Medical Bandaging Material," 6,448,462.

[21] J. Gillespie, "Meltspun multicomponent thermoplastic continuous filaments, products made therefrom, and methods therefor," 5,783,503.

[22] C. (Qin) Sun, D. Zhang, Y. Liu, and R. Xiao, "Preliminary study on fiber splitting of bicomponent meltblown fibers," *J. Appl. Polym. Sci.*, vol. 93, no. 5, pp. 2090–2094, Sep. 2004.

[23] D. Zhang, G. Bhat, S. Malkan, and L. Wadsworth, "Structure and properties of polypropylene filaments in a spunbonding process," *J. Therm. Anal.*, vol. 49, no. 1, pp. 161–167, Jul. 1997.

[24] E. Shim, B. Pourdeyhimi, and M. Latifi, "Three-dimensional analysis of segmented pie bicomponent nonwovens," *J. Text. Inst.*, vol. 101, no. 9, pp. 773–787, Sep. 2010.

[25] S. Malkan, "An overview of spunbonding and meltblowing technologies," *Tappi J.*, vol. 78, no. 6, pp. 185–190, Nov. 1994.

[26] G. D. Considine, Ed., "Ion-Exchange Resins," in *Van Nostrand's Scientific Encyclopedia*, Hoboken, NJ, USA: John Wiley & Sons, Inc., 2007.

[27] A. Wachinski, *Ion exchange treatment for water*. Denver CO: American Water Works Association, 2006.

[28] F. G. Helfferich, *Ion exchange*. New York: Dover Publications, 1995.

[29] D. L. Owens, *Practical principles of ion exchange water treatment*. Voorhees, NJ: Tall Oaks Pub., 1985.

[30] T. Xu, "Ion exchange membranes: State of their development and perspective," *J. Membr. Sci.*, vol. 263, no. 1–2, pp. 1–29, Oct. 2005.

[31] T. Sata, "Ion exchange membranes preparation, characterization, modification and application," 2004. [Online]. Available: http://dx.doi.org/10.1039/9781847551177. [Accessed: 08-Apr-2013].

[32] A. Zagorodni, *Ion exchange materials : properties and applications*. Amsterdam ;;London: Elsevier, 2007.

[33] The Dow Chemical Company, "AMBERLYST™," *Dow - Products and Services*, 2011. [Online]. Available: http://www.amberlyst.com/sac.htm. [Accessed: 18-Jul-2011].

[34] I. M. Huxham, L. Tetley, B. Rowatt, and D. C. Sherrington, "Comparison of porosity characteristics of macroporous poly(styrene?divinylbenzene) resins determined from mercury intrusion data and image analysis of transmission electron micrographs," *J. Mater. Chem.*, vol. 4, no. 2, p. 253, 1994.

[35] A. Klingenberg and A. Seubert, "Sulfoacylated poly(styrene-divinylbenzene) copolymers as resins for cation chromatography. Comparison with sulfonated, dynamically coated and silica gel cation exchangers," *J. Chromatogr. A*, vol. 946, no. 1–2, pp. 91–97, Feb. 2002.

[36] S. Howdle, "Reversibly collapsible macroporous poly(styrene-divinylbenzene) resins," *Polymer*, vol. 41, no. 19, pp. 7273–7277, Sep. 2000.

[37] The Dow Chemical Company, "AMBERLITE™," *Dow - Products and Services*, 2011. [Online]. Available: http://www.amberlyst.com/wac.htm. [Accessed: 18-Jul-2011].

[38] The Dow Chemical Company, "Dowex," *Strong Acid Cation Exchange Resins*, 2013. [Online]. Available: http://msdssearch.dow.com/PublishedLiteratureDOWCOM/dh_0202/0901b80380202d

8f.pdf?filepath=liquidseps/pdfs/noreg/177-01728.pdf&fromPage=GetDoc. [Accessed: 02-May-2013].

[39] The Dow Chemical Company, "AMBERJET™," *Dow - Products and Services*, 2011. [Online]. Available: http://www.amberlyst.com/sba.htm. [Accessed: 18-Jul-2011].

[40] Y. Bai and B. Bartkiewicz, "Removal of Cadmium from Wastewater Using Ion Exchange Resin Amberjet 1200H Columns," *Pol. J. Environ. Stud.*, vol. 18, no. 6, pp. 1191–1195, 2009.

[41] The Dow Chemical Company, "AMBERJET™ 1200 H," *Dow - Products and Services*, 2011.[Online].Available: http://www.dow.com/products/product_detail.page?product=1120843&application=1120783. [Accessed: 18-Jul-2011].

[42] E. Pehlivan and T. Altun, "The study of various parameters affecting the ion exchange of Cu2+, Zn2+, Ni2+, Cd2+, and Pb2+ from aqueous solution on Dowex 50W synthetic resin," *J. Hazard. Mater.*, vol. 134, no. 1–3, pp. 149–156, Jun. 2006.

[43] J. Economy, L. Dominguez, and C. L. Mangun, "Polymeric Ion-Exchange Fibers," *Ind. Eng. Chem. Res.*, vol. 41, no. 25, pp. 6436–6442, Dec. 2002.

[44] L. Dominguez, "Design of high efficiency fibers for ion exchange and heavy metal removal," Dissertation, University of Illinois at Urbana-Champaign, Illinois, 2001.

[45] Z. Yue, C. Mangun, J. Economy, P. Kemme, D. Cropek, and S. Maloney, "Removal of Chemical Contaminants from Water to below USEPA MCL Using Fiber Glass Supported Activated Carbon Filters," *Environ. Sci. Technol.*, vol. 35, no. 13, pp. 2844–2848, Jul. 2001.

[46] Z. Yue, C. L. Mangun, and J. Economy, "Preparation of fibrous porous materials by chemical activation," *Carbon*, vol. 40, no. 8, pp. 1181–1191, Jul. 2002.

[47] J. E. Greenleaf, J. Lin, and A. K. Sengupta, "Two novel applications of ion exchange fibers: Arsenic removal and chemical-free softening of hard water," *Environ. Prog.*, vol. 25, no. 4, pp. 300–311, Dec. 2006

[48] F. Pazzagli and M. Pracella, "Reactive compatibilization of polyolefin/PET blends by melt grafting with glycidyl methacrylate," *Macromol. Symp.*, vol. 149, no. 1, pp. 225–230, Jan. 2000.

[49] H. Park and C. Na, "Preparation of anion exchanger by amination of acrylic acid grafted polypropylene nonwoven fiber and its ion-exchange property," *J. Colloid Interface Sci.*, vol. 301, no. 1, pp. 46–54, Sep. 2006.

[50] M. Kim, "Radiation-induced graft polymerization and sulfonation of glycidyl methacrylate on to porous hollow-fiber membranes with different pore sizes," *Radiat. Phys. Chem.*, vol. 57, no. 2, pp. 167–172, Feb. 2000.

[51] K. Fujiwara, "Separation functional fibers by radiation induced graft polymerization and application," *Nucl. Instruments Methods Phys. Res. Sect. B Beam Interactions Mater. Atoms*, vol. 265, no. 1, pp. 150–155, Dec. 2007.

[52] V. Soldatov, A. Shunkevich, and G. Sergeev, "Synthesis, structure and properties of new fibrous ion exchangers⋆," *React. Polym. Ion Exch. Sorbents*, vol. 7, no. 2–3, pp. 159–172, Jan. 1988.

[53] V. S. Soldatov, A. A. Shunkevich, I. S. Elinson, J. Johann, and H. Iraushek, "Chemically active textile materials as efficient means for water purification," *Desalination*, vol. 124, no. 1–3, pp. 181–192, Nov. 1999.

[54] M. V. Bazunova, S. V. Kolesov, and A. V. Korsakov, "Preparation of ion-exchange fiber from polypropylene waste with grafted polyacrylic acid," *Russ. J. Appl. Chem.*, vol. 79, no. 5, pp. 853–855, May 2006.

[55] F. Loh, "Structural studies of polyethylene, poly(ethylene terephthalate) and polystyrene films modified by near u.v. light induced surface graft copolymerization," *Polymer*, vol. 36, no. 1, pp. 21–27, Jan. 1995.

[56] W. Huang and J. Jang, "Hydrophilic modification of PET fabric via continuous photografting of acrylic acid (AA) and hydroxyethyl methacrylate (HEMA)," *Fibers Polym.*, vol. 10, no. 1, pp. 27–33, Mar. 2009.

[57] Z. P. Yao and B. Rånby, "Surface modification by continuous graft copolymerization. III. Photoinitiated graft copolymerization onto poly(ethylene terephthalate) fiber surface," *J. Appl. Polym. Sci.*, vol. 41, no. 78, pp. 1459–1467, Jan. 1990.

[58] X. Zhang, K. Jiang, Z. Tian, W. Huang, and L. Zhao, "Removal of arsenic in water by an ion-exchange fiber with amino groups," *J. Appl. Polym. Sci.*, vol. 110, no. 6, pp. 3934–3940, Dec. 2008.

[59] H. An, C. Shin, and G. G. Chase, "Ion exchanger using electrospun polystyrene nanofibers," *J. Membr. Sci.*, vol. 283, no. 1–2, pp. 84–87, Oct. 2006.

[60] K. C. Gupta and K. Khandekar, "Ceric(IV) ion-induced graft copolymerization of acrylamide and ethyl acrylate onto cellulose," *Polym. Int.*, vol. 55, no. 2, pp. 139–150, Feb. 2006.

[61] H. Kubota and S. Suzuki, "Comparative examinations of reactivity of grafted celluloses prepared by u.v.- and ceric salt-initiated graftings," *Eur. Polym. J.*, vol. 31, no. 8, pp. 701–704, Aug. 1995.

[62] K. C. Gupta and K. Khandekar, "Graft copolymerization of acrylamide onto cellulose in presence of comonomer using ceric ammonium nitrate as initiator," *J. Appl. Polym. Sci.*, vol. 101, no. 4, pp. 2546–2558, Aug. 2006.

[63] D. J. McDowall, B. S. Gupta, and V. T. Stannett, "Grafting of vinyl monomers to cellulose by ceric ion initiation," *Prog. Polym. Sci.*, vol. 10, no. 1, pp. 1–50, Jan. 1984.

[64] C. Tyagi, L. K. Tomar, and H. Singh, "Surface modification of cellulose filter paper by glycidyl methacrylate grafting for biomolecule immobilization: Influence of grafting parameters and urease immobilization," *J. Appl. Polym. Sci.*, vol. 111, no. 3, pp. 1381–1390, Feb. 2009.

[65] H. H. Sokker, S. M. Badawy, E. M. Zayed, F. A. Nour Eldien, and A. M. Farag, "Radiation-induced grafting of glycidyl methacrylate onto cotton fabric waste and its modification for anchoring hazardous wastes from their solutions," *J. Hazard. Mater.*, vol. 168, no. 1, pp. 137–144, Aug. 2009.

[66] Y.-W. Song, H.-S. Do, H.-S. Joo, D.-H. Lim, S. Kim, and H.-J. Kim, "Effect of grafting of acrylic acid onto PET film surfaces by UV irradiation on the adhesion of PSAs," *J. Adhes. Sci. Technol.*, vol. 20, no. 12, pp. 1357–1365, Sep. 2006.

[67] E. Suljovrujic, "Dielectric study of post-irradiation effects in gamma-irradiated polyethylenes," *Radiat. Phys. Chem.*, vol. 79, no. 7, pp. 751–757, Jul. 2010.

[68] M. Ohrlander, A. Wirsen, and A. Albertsson, "The grafting of acrylamide onto poly(epsilon-caprolactone) and poly(1,5-dioxepan-2-one) using electron beam preirradiation. I. Influence of dose and Mohr's salt for the grafting onto poly(epsilon-caprolactone)," *J. Polym. Sci. Part Polym. Chem.*, vol. 37, no. 11, pp. 1643–1649, 1999.

[69] W. T. Yang and B. R�nby, "The role of far UV radiation in the photografting process," *Polym. Bull.*, vol. 37, no. 1, pp. 89–96, Jul. 1996.

[70] R. Chaplin, "The role of partitioning of reagents in grafting and curing reactions initiated by ionizing radiation and UV," *Radiat. Phys. Chem.*, vol. 47, no. 3, pp. 435–437, Mar. 1996.

[71] Y.-W. Song, H.-S. Do, H.-S. Joo, D.-H. Lim, S. Kim, and H.-J. Kim, "Effect of grafting of acrylic acid onto PET film surfaces by UV irradiation on the adhesion of PSAs," *J. Adhes. Sci. Technol.*, vol. 20, no. 12, pp. 1357–1365, Sep. 2006.

[72] G. Oster and O. Shibata, "Graft copolymer of polyacrylamide and natural rubber produced by means of ultraviolet light," *J. Polym. Sci.*, vol. 26, no. 113, pp. 233–234, Nov. 1957.

[73] Z. P. Yao and B. RÅNby, "Surface modification by continuous graft copolymerization. I. Photoinitiated graft copolymerization onto polyethylene tape film surface," *J. Appl. Polym. Sci.*, vol. 40, no. 910, pp. 1647–1661, Nov. 1990.

[74] Y. Liu, "Grafting of Methyl Acrylate onto PET Initiated by Diperiodatocuprate(III).," *J. Macromol. Sci. Pure Appl. Chem.*, vol. 43, no. 8, pp. 1255–1263, Oct. 2010.

[75] Y. Zheng, H. Liu, P. V. Gurgel, and R. G. Carbonell, "Polypropylene nonwoven fabrics with conformal grafting of poly(glycidyl methacrylate) for bioseparations," *J. Membr. Sci.*, vol. 364, no. 1–2, pp. 362–371, Nov. 2010.

[76] I. Kaur, R. Kumar, and N. Sharma, "A comparative study on the graft copolymerization of acrylic acid onto rayon fibre by a ceric ion redox system and a γ-radiation method," *Carbohydr. Res.*, vol. 345, no. 15, pp. 2164–2173, Oct. 2010.

[77] G. Mino and S. Kaizerman, "A new method for the preparation of graft copolymers. Polymerization initiated by ceric ion redox systems," *J. Polym. Sci.*, vol. 31, no. 122, pp. 242–243, Aug. 1958.

[78] I. Casinos, "Mechanisms for the radical graft polymerization of vinyl and/or acrylic monomers on cellulose," *Polymer*, vol. 35, no. 3, pp. 606–615, Feb. 1994.

[79] J. Song, Y. Jin, G. Fu, A. He, and W. Fu, "A facile approach toward surface sulfonation of natural cotton fibers through epoxy reaction," *J. Appl. Polym. Sci.*, vol. 124, no. 2, pp. 1744–1750, Apr. 2012.

[80] A. Bildyukevich, "Fibrous Ion Exchangers," *Institute of Physical Organic Chemistry*. [Online]. Available: http://ifoch.bas-net.by/K4_eng1.htm. [Accessed: 13-Apr-2011].

[81] G. Medyak, A. Shunkevich, A. Polikarpov, and V. Soldatov, "Features of Preparation and Properties of FIBAN K-4 Fibrous Sorbents," *Russ. J. Appl. Chem.*, vol. 74, no. 10, pp. 1658–1663, Feb. 2001.

[82] M. Vuorio, J. A. Manzanares, L. Murtomäki, J. Hirvonen, T. Kankkunen, and K. Kontturi, "Ion-exchange fibers and drugs: a transient study," *J. Controlled Release*, vol. 91, no. 3, pp. 439–448, Sep. 2003.

[83] J. Lehto and R. Harjula, "Experimentation in ion exchange studies - the problem of getting reliable and comparable results," *React. Funct. Polym.*, vol. 27, no. 2, pp. 121–146, Oct. 1995.

[84] C. Gerente, V. Lee, K. Lee, and C. Lee, "Application of Chitosan for the Removal of Metals From Wastewaters by Adsorption—Mechanisms and Models Review," *Crit. Rev. Environ. Sci. Technol.*, vol. 37, no. 1, pp. 41–127, Jan. 2007.

[85] Z. Aksu, G. Eğretli, and T. Kutsal, "A comparative study of copper(II) biosorption on Ca-alginate, agarose and immobilized C. vulgaris in a packed-bed column," *Process Biochem.*, vol. 33, no. 4, pp. 393–400, Mar. 1998.

[86] Y. F. Lasheen, A. F. Seliman, and A. A. Abdel-Rassoul, "Chromatographic separation of certain metal ions using a bifunctional quaternary ammonium-sulfonate mixed bed ion-exchanger," *J. Chromatogr. A*, vol. 1136, no. 2, pp. 202–209, Dec. 2006.

[87] A. Gόrka, J. Zamorska, and D. Antos, "Coupling Ion Exchange and Biosorption for Copper(II) Removal From Wastewaters," *Ind. Eng. Chem. Res.*, vol. 50, no. 6, pp. 3494–3502, Mar. 2011.

[88] S. W. Lee, Y. Bondar, and D. H. Han, "Synthesis of a cation-exchange fabric with sulfonate groups by radiation-induced graft copolymerization from binary monomer mixtures," *React. Funct. Polym.*, vol. 68, no. 2, pp. 474–482, Feb. 2008.

[89] T.-Y. Hsien, Y.-H. Lien, and D.-M. Wang, "Synthesis of novel mixed matrix scaffolds and adsorption of copper ions of waste water," *Desalination Water Treat.*, vol. 17, no. 1–3, pp. 113–119, May 2010.

[90] S. W. Lee, Y. Bondar, and D. H. Han, "Synthesis of a cation-exchange fabric with sulfonate groups by radiation-induced graft copolymerization from binary monomer mixtures," *React. Funct. Polym.*, vol. 68, no. 2, pp. 474–482, Feb. 2008.

[91] F.-C. Wu, R.-L. Tseng, and R.-S. Juang, "Enhanced abilities of highly swollen chitosan beads for color removal and tyrosinase immobilization," *J. Hazard. Mater.*, vol. 81, no. 1–2, pp. 167–177, Jan. 2001.

[92] Y. Sağ and Y. Aktay, "Kinetic studies on sorption of Cr(VI) and Cu(II) ions by chitin, chitosan and Rhizopus arrhizus," *Biochem. Eng. J.*, vol. 12, no. 2, pp. 143–153, Nov. 2002.

[93] W. S. W. Ngah, S. Ab Ghani, and A. Kamari, "Adsorption behaviour of Fe(II) and Fe(III) ions in aqueous solution on chitosan and cross-linked chitosan beads," *Bioresour. Technol.*, vol. 96, no. 4, pp. 443–450, Mar. 2005.

[94] J. Deng, L. Wang, L. Liu, and W. Yang, "Developments and new applications of UV-induced surface graft polymerizations," *Prog. Polym. Sci.*, vol. 34, no. 2, pp. 156–193, Feb. 2009.

[95] N. Kwak, T. Hwang, S. Kim, Y. Yang, and K. Kang, "Synthesis of sulfonated PET-g-GMA fine ion-exchange fibers for water treatment by photopolymerization and their adsorption properties for metal ions," *Polym. Korea*, vol. 28, no. 5, pp. 397–403, Sep. 2004.

[96] Y. Dong, W. S. Lyoo, and J. Jang, "Union dyeing of the photografted PET/wool blend fabrics with dimethylaminopropyl methacrylamide," *Fibers Polym.*, vol. 11, no. 2, pp. 213–217, May 2010.

[97] M. Ulbricht and H. Yang, "Porous Polypropylene Membranes with Different Carboxyl Polymer Brush Layers for Reversible Protein Binding via Surface-Initiated Graft Copolymerization," *Chem. Mater.*, vol. 17, no. 10, pp. 2622–2631, May 2005.

[98] Y. Xie and Q. Yang, "Surface modification of poly(vinyl chloride) for antithrombogenicity study," *J. Appl. Polym. Sci.*, vol. 85, no. 5, pp. 1013–1018, Aug. 2002.

[99] Y.-L. Hsieh and M. Wu, "Residual reactivity for surface grafting of acrylic acid on argon glow-discharged poly(ethylene terephthalate) (PET) films," *J. Appl. Polym. Sci.*, vol. 43, no. 11, pp. 2067–2082, Dec. 1991.

[100] M. R�tzsch, H. Bucka, S. S. Ivanchev, A. M. Mesh, and Khaikine, "Some peculiar features of radiation grafting of monomers of various structures and reactivities onto polyolefins," *J. Appl. Polym. Sci.*, vol. 77, no. 4, pp. 711–718, Jul. 2000.

[101] H. Yasuda, "Plasma for Modification of Polymers," *J. Macromol. Sci. Part*, vol. 10, no. 3, pp. 383–420, Mar. 1976.

[102] C.-M. Chan, *Polymer Surface Modification and Characterization*. Hanser Gardner Publications, 1994.

[103] A. Bell, "Fundamentals of Plasma Polymerization," *J. Macromol. Sci. Part*, vol. 10, no. 3, pp. 369–381, Mar. 1976.

[104] C. Roffey, *Photopolymerization of Surface Coatings*. John Wiley & Sons Australia, Limited, 1982.

[105] H. F. Gruber, "Photoinitiators for free radical polymerization," *Prog. Polym. Sci.*, vol. 17, no. 6, pp. 953–1044, Jan. 1992.

[106] J. Garnett, "Grafting," *Radiat. Phys. Chem. 1977*, vol. 14, no. 1–2, pp. 79–99, 1979.

[107] D. M. Pinkerton and R. H. Stacewicz, "γ-Radiation-induced grafting of methyl methacrylate to polypropylene: The effects of water and mineral acid," *J. Polym. Sci. Polym. Lett. Ed.*, vol. 14, no. 5, pp. 287–291, May 1976.

[108] T. Demappa and Mahadevaiah, "Polymerization of acrylonitrile initiated by cerium (IV)-oxalic acid redox system: A kinetic study," *J. Appl. Polym. Sci.*, vol. 108, no. 3, pp. 1667–1674, May 2008.

[109] N. Chansook and S. Kiatkamjornwong, "Ce(IV)-initiated graft polymerization of acrylic acid onto poly(ethylene terephthalate) fiber," *J. Appl. Polym. Sci.*, vol. 89, pp. 1952–1958, Aug. 2003.

[110] V. Sridharan and J. C. Menéndez, "Cerium(IV) Ammonium Nitrate as a Catalyst in Organic Synthesis," *Chem. Rev.*, vol. 110, no. 6, pp. 3805–3849, Jun. 2010.

[111] V. S. Ananthanarayanan and M. Santappa, "Kinetics of vinyl polymerization initiated by ceric ion in aqueous solution," *J. Appl. Polym. Sci.*, vol. 9, no. 7, pp. 2437–2449, Jul. 1965.

[112] I. Casinos, "Role of ceric ion in the heterogeneous graft polymerization of olefins on cellulose," *Polymer*, vol. 33, no. 6, pp. 1304–1315, Jan. 1992.

[113] G. Odian and J. H. T. Kho, "Ceric Ion Initiated Graft Polymerization onto Poly(vinyl Alcohol)," *J. Macromol. Sci. Part - Chem.*, vol. 4, no. 2, pp. 317–330, Mar. 1970.

[114] T. Amornsakchai and O. Doaddara, "Grafting of Acrylamide and Acrylic Acid onto Polyethylene Fiber for Improved Adhesion to Epoxy Resin," *J. Reinf. Plast. Compos.*, vol. 27, no. 7, pp. 671–682, Jan. 2008.

[115] G. V. Ramana Reddy, J. Arun, and J. Panda, "Kinetic study of the polymerization of ethyl acrylate in an aqueous nitric acid medium," *J. Appl. Polym. Sci.*, vol. 99, no. 1, pp. 218–224, Jan. 2006.

[116] S. Haworth and J. R. Holker, “Oxidation of Some 2,4-Dinitrophenylamines with Ceric Salts,” *Nature*, vol. 208, no. 5006, pp. 184–185, Oct. 1965.

[117] F. Ku?era and J. Jan?�?, “Homogeneous and heterogeneous sulfonation of polymers: A review,” *Polym. Eng. Sci.*, vol. 38, no. 5, pp. 783–792, May 1998.

[118] N. Chansook and S. Kiatkamjornwong, “Ce(IV)-initiated graft polymerization of acrylic acid onto poly(ethylene terephthalate) fiber,” *J. Appl. Polym. Sci.*, vol. 89, no. 7, pp. 1952–1958, Aug. 2003.

[119] Z. Ma, M. Kotaki, T. Yong, W. He, and S. Ramakrishna, “Surface engineering of electrospun polyethylene terephthalate (PET) nanofibers towards development of a new material for blood vessel engineering,” *Biomaterials*, vol. 26, no. 15, pp. 2527–2536, May 2005.

[120] B. Gupta, N. Grover, and H. Singh, “Radiation grafting of acrylic acid onto poly(ethylene terephthalate) fabric,” *J. Appl. Polym. Sci.*, vol. 112, no. 3, pp. 1199–1208, May 2009.

[121] L. Yu, S. Zhang, W. Liu, X. Zhu, X. Chen, and X. Chen, “Improving the flame retardancy of PET fabric by photo-induced grafting,” *Polym. Degrad. Stab.*, vol. 95, no. 9, pp. 1934–1942, Sep. 2010.

[122] M. A. Barakat, “New trends in removing heavy metals from industrial wastewater,” *Arab. J. Chem.*, vol. 4, no. 4, pp. 361–377, Oct. 2011.

Chapter 3

3 Web properties of fractured segmented pie bicomponent fibers

Abstract

The purpose of this study is to investigate structures of high surface area nonwovens consisting of fully fractured segmented pie bicomponent fibers. PET/PE segmented pie fibers with varying numbers of segments as well as PET monofilaments have been produced in the NCRC Pilot Plant. The segmented pie fibers were fully fractured in a jet dying machine and the web structures were evaluated. It was found that increasing the number of segments causes an increase in consolidation of the web. This decreases the pore diameter and increases the solidity of the webs.

3.1 Introduction

Bicomponent fibers are fibers composed of at least two polymers that are extruded into one single filament and share a common interface [1]. Bicomponent fibers have been used for many years as a way of producing nonwoven materials composed of fibers on the micro and nano scale. Electrospinning has traditionally been the method for producing micro and nanofibers. However, electrospinning is a very slow, energy intensive process [2]. Though the splittable bicomponent technology was developed in the mid 1960's [3], Dupont Company made the first commercially available bicomponent fiber in the 1970's [4]. In the past 30 years, much research has been done in the area of bicomponent fibers, looking for ways to make cheaper more efficient high surface area fibers.

When producing bicomponent fibers the selection of polymers is essential to produce fibers with proper adhesion and melt temperature properties. Extruding the two polymers through a spinneret of a particular configuration using a spunlaid process produces the bicomponent fiber webs. The bicomponent webs contain either soluble or splittable fibers.

The soluble bicomponents, such as island-in-the-sea fibers, contain one component that is selectively removed by leaching with a non abrasive solvent, typically sodium hydroxide. Splittable fibers, such as segmented pie fibers, contain two polymers that are fractured by mechanical force, usually high powered water jets [5]. The resulting nonwoven fabric is then composed of high surface area micro and nano sized fibers making them ideal for a variety of applications such as air and water filters, adsorption materials, and medical textiles and can be used for many advanced applications [6].

Unlike meltblowing, the fibers in the spunbond process do not self bond when they reach the forming belt. Spunbonding requires a bonding technique after processing to give the fibrous webs structural integrity [7]. Hydroentanlging is a technique commonly used to fracture bicomponent fibers while simultaneously bonding the webs[8]. In a previous study, Shim et al.[9] investigated the orientation of the fibers in the MD, CD, and TD directions of segmented pie fibers that were fractured in the jet dyeing machine. They found that the orientation of the fibers was not significantly changed after washing in the jet dyeing machine, reducing the effects of jet streaks from hydroentangling. There was also a 40% increase in the fracturing of the fibers through the cross section of the webs when jet dyeing followed hydroentangling. Achieving a high degree of fracture is important to increase the surface area and further increase the ion exchange capacity in later stages of development.

The fractured bicomponent nonwovens in the present study will be used for ion exchange filtration media. The permeability of the webs, as well as the surface area of the webs is important for the future applications of the materials. Bicomponent fiber technology will provide the high surface area necessary for attachment of functional groups to the fiber surface. The more fiber surface available, the more functional groups that can be bonded, thus the higher the ion exchange capacity of the filter media.

In order to provide a more cost efficient substrate than the current commercially available ion exchange fibrous substrates[10], [11], polyethylene terephthalate (PET) will be used as the grafting fiber substrate in the bicomponent nonwovens. Polyethylene (PE) has been chosen as the secondary fiber in the bicomponent nonwovens due to its low reactivity; it

should not be involved in the reaction. Due to the large difference in melt temperature between PET and PE (260°C vs 110°C, respectively)[12], PET and PE are not typically used in combination as bicomponent fibers [13], although successful spinning of sheath core fibers has been reported in the literature [13], [14]. The effects of the number of segments on the web properties after fracturing will be investigated.

3.2 Experimental

3.2.1 Materials

The bicomponent webs were composed of segmented pie fibers of 4, 8 and 16 segments and polymer ratios of 60/40 and 80/20 of Polyethylene terephthalate (PET) to Polyethylene (PE).

Polymer 1: Eastman F61HC polyethylene terephthalate (PET) from Eastman Chemicals with a melting temperature of 260 °C

Polymer 2: ASPUN™ 6850A polyethylene (PE) from Dow Chemical Company which melts at 131 °C and has a density of 0.955 g/cm^3

3.2.2 Fabric Formation

The Nordson Fiber Systems/Hills Inc. spunbond machine, in the Nonwoven's Cooperative Research Center Partner's Pilot lab at NC State University was used to produce the segmented pie PET/PE nonwovens[15]. The segmented pie cross section is seen below in **Figure 3.1**.

Figure 3.1. Segmented Pie Cross Section

3.2.3 Fabric Bonding

Hydroentangling is used to bond the spunbond webs. Since the intention is to evaluate the structure of the webs based solely on the fracturing of the fibers, it is necessary to reduce the effects of any jet streaks from the hydroentangling. Therefore, it was important to use low water pressures to entangling the fibers but not fracture the fibers. The fibers will be fractured using the jet dyeing machine.

The Fleissner Aquajet 2000 Hydroentangling machine in the NCRC Parnter's Pilot Lab was used for the hydroentangling process[15]. The water jet pressures for the 5 manifolds were set at: 30, 175, 220, 220, and 200 bars of pressure, respectively. The first 3 manifolds are projected on the top of the fabric and the last two hit the bottom of the fabric. The webs were passed through the hydroentangling machine one time at 10 m/min. One pass was enough to entangle the fibers and reduce the amount of fracturing that occurred. The samples were then fed into the Through Air Dryer at 115° C to dry the samples before being wrapped on the take up roll.

3.2.4 Fiber Fracturing

Fracturing was done in the Mathis JFO Jet Dyeing Machine shown in **Figure 3.2**, in the College of Textiles Pilot Plant.

Figure 3.2. Image of Mathis JFO Jet Dyeing Machine in Pilot Plant [28]

The Mathis JFO has a single high powered water jet that is concentrated on the looped fabric sample. The fabric is wrapped over a motor and through the circular jet opening and sewn together to form a continuous loop. The motor is set to a specific speed that controls the speed at which the fabric circulates. However, the pressure of the jet also increases the rate of circulation of the fabric.

The material circulation speed of 10 m/min was chosen, as it is the same as the belt speed of the hydroentangling machine, with a water flow rate of 70,000 L/min. 5 liters of water for 5 meters of 100 g/m^2 material was added to the wash tank. The water temperature was 90 °C, 20 degrees lower than the melting temperature of polyethylene (approximately 110 °C). This causes sufficient softening of the polymers without any degradation. Through preliminary studies, it was found that 120 minutes run time was sufficient to achieve 100% fracturing.

3.2.5 Analytical Methods

The following analytical techniques were employed to analyze the web structure of the materials with varying numbers of segments.

3.2.5.1 Air Permeability

An Air Permeability tester, model FX330, from TexTest Instruments was used to investigate the permeability of the materials with a 1 in^2 sample holder in the Analytical Lab of the Nonwovens Institute. Three repetitions were performed on each sample.

3.2.5.2 BET Surface Area Analysis

BET (available through the Material Science and Engineering department at NC State University) was used to investigate the surface area of the PET/PE fractured bicomponent fibers.

3.2.5.3 Solidity

The solidity is known as the packing density or volume fraction. It is the volume of fibers in a given volume of the web. It is described as,

$$Solidity = (\%PET)\frac{(\rho_{web})}{(\rho_{PET})} + (\%PE)\frac{(\rho_{web})}{(\rho_{PE})} \qquad \textbf{(3.1)}$$

where *%PET* is the ratio of PET in the original fiber (60% or 80%) , *%PE* is the ratio of PE in the original fiber (40% or 20%), ϱ_{PET} is the density of PET polymer (1.41 g/cm^3), ϱ_{PE} is the density of PE polymer (.955 g/cm^3), and the density of the web is defined as a ratio of Basis Weight (g/cm^2) and Thickness (cm):

$$\rho_{web} = \frac{BasisWeight}{Thickness} \qquad \textbf{(3.2)}$$

3.2.5.4 Pore Diameter

The small, mean, and large pore diameters of the samples were calculated using a PMI, Inc. Capillary Flow Porometer, model CFP-1100-Ax, in the Analytical Lab of the Nonwovens Institute. Galwick™ (surface tension 15.9 dynes/com) was applied to the samples. One replication of each sample was done.

3.2.5.5 Scanning Electron Microscopy

The Hitachi Scanning Electron Microscope (SEM), available in the Analytical Instrumentation Facility at NC State, was employed to investigate the degree of fracture of the fractured samples.

3.2.5.6 Web Thickness

The thickness test was done with an AMES 99-0697 thickness tester in the NCRC Physical and Mechanical Testing laboratory. 5 measurements were recorded for each sample.

3.2.5.7 Basis Weight

The basis weight of the samples was calculated from the average of 5 samples with 100 cm^2 of area cut using a die.

3.2.5.8 Percent Shrinkage

The percent shrinkage was calculated by marking a 144 in^2 area on the material along the machine and cross directions. The area was measured after fracturing in the jet dyeing machine and the difference was calculated.

$$\%Shrinkage = \frac{(Original - Fractured)}{Original} \times 100\% \qquad \textbf{(3.3)}$$

3.2.5.9 Tensile Test

The mechanical strength of the nonwovens was tested using the XX strip tensile tester available in the Nonwovens Institute's Testing Services lab. 1" by 8" samples were cut in the machine and cross directions of the nonwovens. 5 samples for each nonwoven were tested to failure.

3.2.5.10 Flexural Rigidity

The resistance to bending was calculated doing the cantilever beam test available in the Nonwovens Institute's Testing Services lab. 1" by 8" samples were cut in the machine and cross directions of the nonwovens. The average of the four edges of each samples were averaged and the average of 5 tests were used to represent the final value. Overhang length

and flexural rigidity were calculated according to ASTM D-5732-95 where the bending length is half the overhang length:

$$c = O / 2 \tag{3.4}$$

where c (mm) is the bending length and O (mm) is the overhang length. The flexural rigidity is calculated using the bending length:

$$G = Mc^3 \tag{3.5}$$

where G (N* m) is the flexural rigidity, M (g/m^2) is the fabric mass per unit area, and c (mm) is the bending length.

3.3 Results and Discussion

3.3.1 Degree of fracture and Surface Area

The degree of fracture is difficult to quantify. SEM images of the cross section were done to visually assess the degree of fracture through the cross section of the webs as well as measure the diameter of the fiber segments to calculate the theoretical surface area.

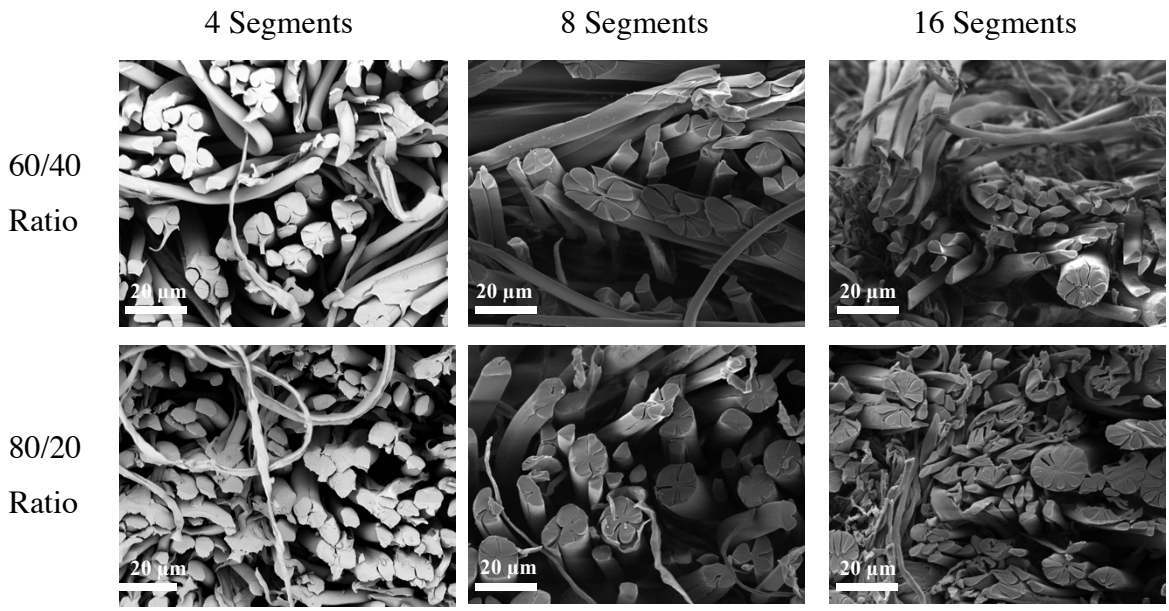

Figure 3.3. SEM images of bicomponent fibers with 4, 8, and 16 segments and polymer ratios of PET/PE of 60/40 and 80/20

The SEM images showed that most fibers had fully fractured, while some were partially fractured. The fiber diameter was measured digitally using imaging software. SEM is only looking at a very small portion of the cross section of these materials so other techniques should be used to confirm the degree of fracture, such as BET surface area analysis.

The theoretical specific surface area of the web was calculated using the following equation:

$$\frac{SA}{V} = \frac{2}{r} + \frac{2n}{\pi r} \qquad \textbf{(3.6)}$$

where r is the radius of the original unfractured fiber and n is the number of segments in the fiber. A radius of 5 µm was used based on the fiber diameters that were measured using SEM.

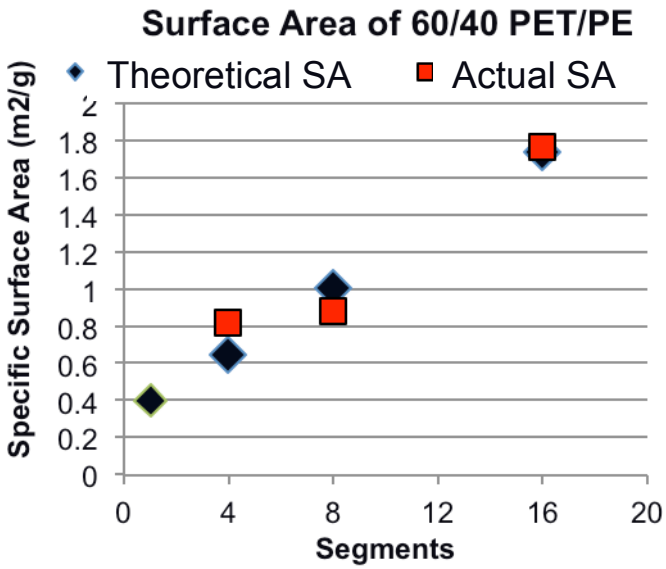

Figure 3.4. Effect of the number of segments on the surface area of the web

The surface area of the 60/40 PET/PE samples is comparable to the theoretical surface area if 100% fracturing of the fibers occurs, indicating that a high degree of fracture of the fibers has occurred. Although in the SEM images some fibers appeared to be only partially fractured, the BET results indicate that the surface area is still available as if all fibers are fully fractured. If some fibers are still intact, the surface area is probably the result of fibrillation of fiber segments.

3.3.2 Effect of number of segments on material properties

Changes in both the thickness and weight of the web were measured to evaluate the effects of the fiber fracturing on the web, Figure 3.5. The changes in the structure of the web were evaluated based on the webs with different number of segments. The results were compared to a control samples containing PET homocomponent fibers with a diameter of 12-15 μm.

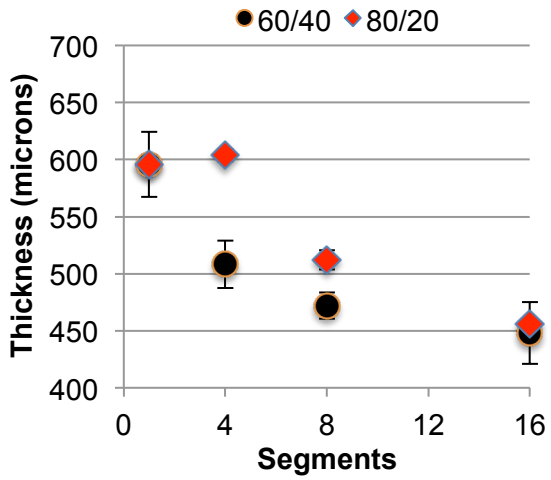

Figure 3.5. Effects of the number of segments on the changes in the web thickness

As the number of segments in the fibers of the web increases, the web thickness decreases in both the 80/20 and 60/40 PET/PE ratio webs. When the original fiber is split into more segments, the fiber diameter of the resulting segments decreases. Fibers with smaller fiber diameters are able to pack more closely together. Therefore, the webs composed of fibers with 16 segments will have the smallest fibers after fracturing and thus the smallest web thickness due to increased packing density.

The 80/20 ratio samples have larger web thicknesses than the 60/40 in all of the samples. This difference is much more evident in the samples with less segments. Although the average fiber diameter will be the same in webs with the same number of segments but different polymer ratios, the 80/20 fibers have a bimodal distribution in size. This ratio creates large and small fibers, as is evident in the SEM images. The large PET fibers support the structure and prevent consolidation, thus thicker webs result.

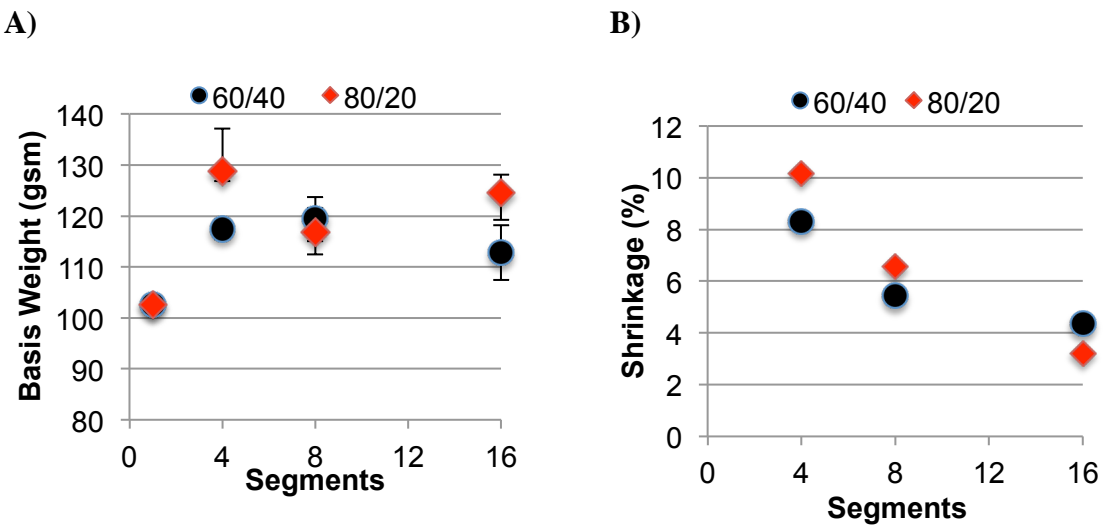

Figure 3.6. Effect of number of segments on the a) basis weight and B) Shrinkage of the samples

When the fibers are fractured into multiple segments, shrinkage of the web occurs and results in an increase in the basis weight of the material. The shrinkage is partly due to the consolidation of the web, but also due to the shrinkage of the PET fibers during washing in the jet dyeing machine. This shrinkage also increases the basis weight of the samples. Since the thickness of the web decreases with increasing number of segments, the basis weights increases, but then levels off around 120 gsm for both the 80/20 and 60/40 ratios.

3.3.3 Effect of number of segments on solidity

The solidity, or packing density, is a measure of the volume of the solid material in the volume of web. The solidity of each was calculated based on the ratio between the density of the web and the density of the fibers, **Figure 3.7**.

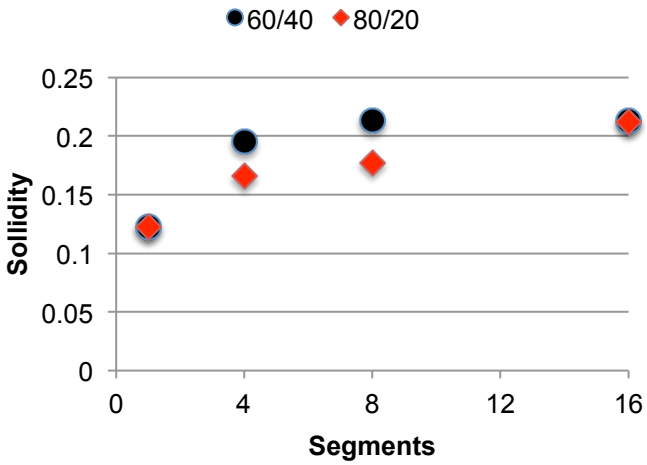

Figure 3.7. Effect of number of segments on the Solidity

The solidity of the web increases with increasing number of segments. Since the density of the fibers is staying the same, the increase in the solidity is due to the consolidation of the web that increases with increasing number of segments. This trend is consistent with the results of the thickness and shrinkage of the webs. For both the thickness and shrinkage the 80/20 samples with 4 and 8 segments were slightly higher than the 60/40 samples. The solidity of these samples is slightly lower than the 60/40 samples, indicating that slightly less consolidation has occurred.

3.3.4 Effect of number of segments on the Pore Structure

The decrease in the pore diameter with increasing numbers of segments was calculated with a porometer, **Figure 3.8**.

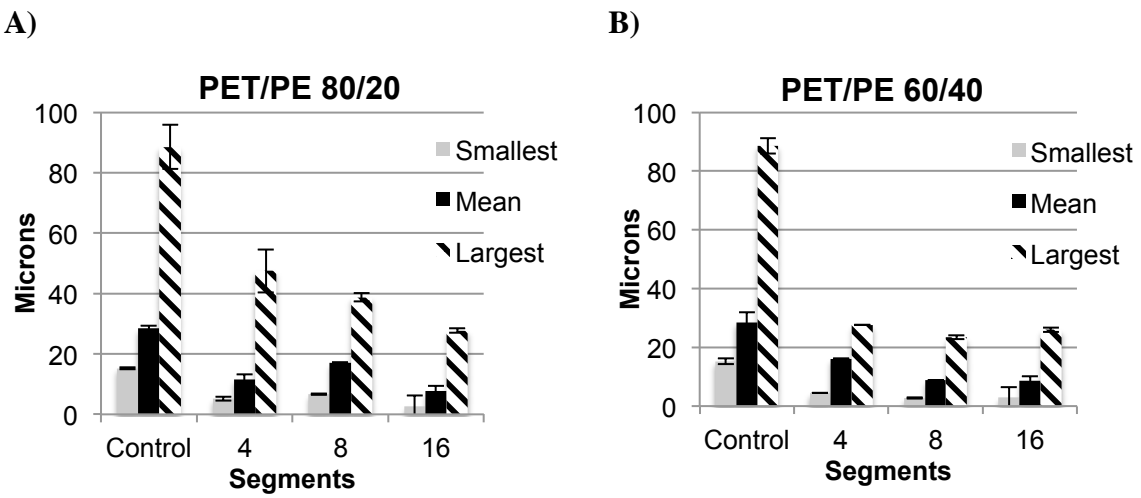

Figure 3.8. The effect of the number of segments on the pore diameter of the a) PET/PE 80/20 ratio and the b) PET/PE 60/40 ratio

The mean pore diameters, as well as the smallest and largest detected pores, of the samples with varying numbers of segments are seen in . In both of the polymer ratios, the smallest, mean, and largest pore diameters all decrease with increasing number of segments. This is true except for the 80/20 8 segmented pie nonwovens. In the 80/20 8 segmented pie nonwoven, the mean pore size is slightly larger than the mean pore size of the 4 segmented pie nonwoven. This indicates that the 80/20 8 segmented pie nonwoven may have not fully fractured in the jet dyeing machine.

3.3.5 Effect of the number of segments on the permeability

The air permeability of the samples were tested to evaluate the changes in porosity of the materials. This will be important, as these materials will be used as liquid filtration media and the pore size will affect the ability of the liquid to flow through the media.

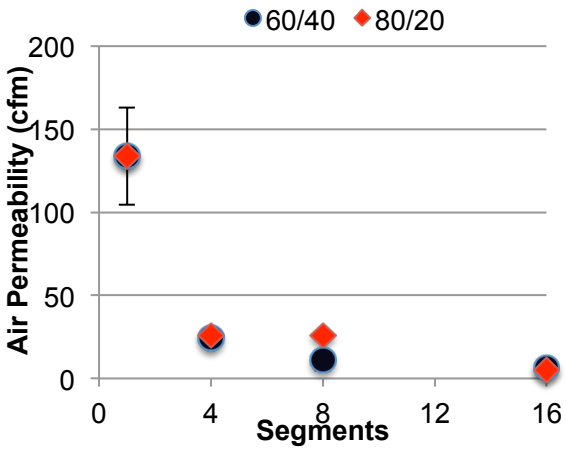

Figure 3.9. Effect of number of segments on air permeability

Figure 3.9 shows that the air permeability significantly decreases as the number of segments increases. This is a result of the packing of the fibers that occurs when the fibers are fractured into the individual segments. This decreases the size of the pores, making it more difficult for air to flow through the sample. This permeability decreases with more segments in the fibers. There is little difference between the two polymer ratios.

3.3.6 Effect of Number of Segments on Mechanical Properties

Upon fracturing of segmented pie fibers, a large amount of consolidation occurs in which the fibers pack tightly together. It is important to balance the degree of web consolidation with the mechanical properties. The percent strain at break of the 80/20 and 60/40 PET/PE ratio fibers were compared to the PET homocomponent nonwovens, **Figure 3.10**.

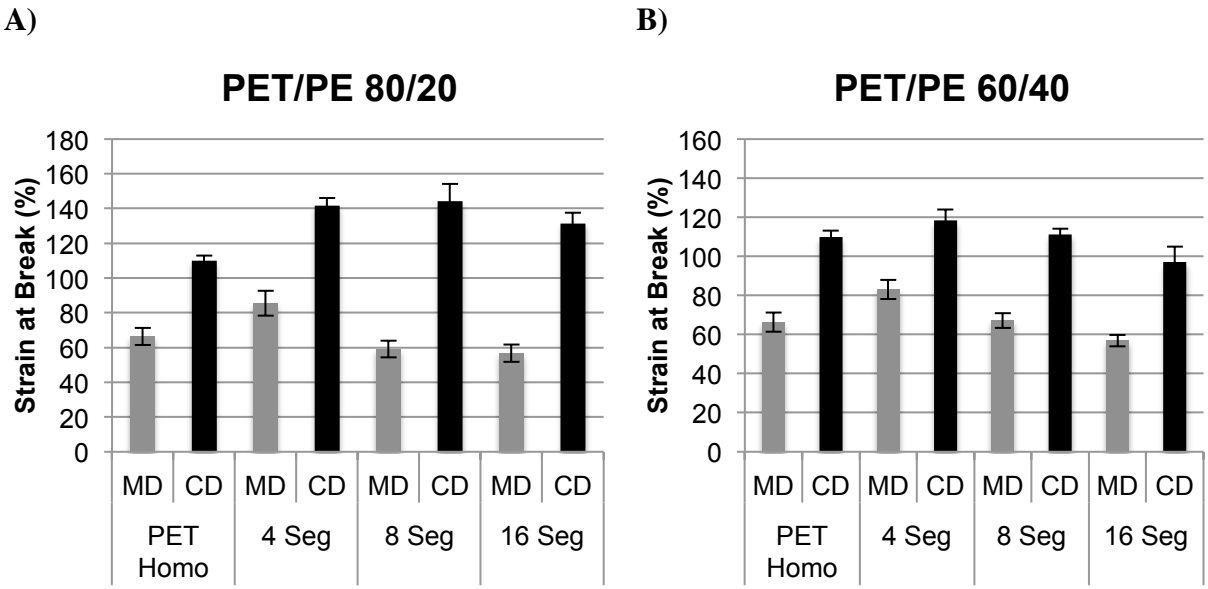

Figure 3.10. Effect of number of segments on strain at break with polymer ratios A) 80/20 PET and B) 60/40 PET/PE

The 80/20 polymer ratio had improved percentage strain at break in the cross direction but a decrease in the machine direction compared to the PET homocomponent nonwoven. The percent strain at break decreased with increasing number of segments in both material directions. The same behavior occurred with the 60/40 polymer ratio as well. The bicomponent nonwovens have more fiber entanglements due to the fracturing by the water jet dyeing machine, increasing the elongation by allowing the fibers to move past each other. However, increasing the number of segments decreases the diameter of the fibers thus decreasing the percent elongation. There is a higher orientation of fibers in the machine direction, decreasing the amount of elongation that can occur from the fiber slippage, relying more on the elongation of individual fibers, and therefore leading to a decrease in the elongation in the machine direction compared to the cross direction.

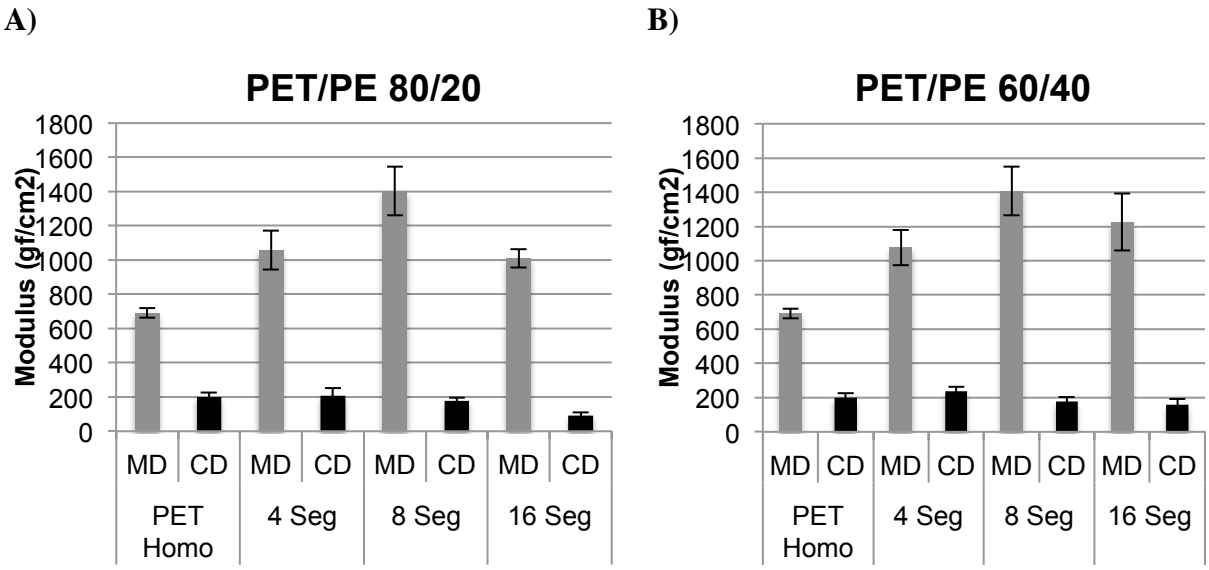

Figure 3.11. Effect of number of segments on Modulus with polymer ratios of A) PET/PE 80/20 and B) PET/PE 60/40

The modulus, or tensile strength, of the bicomponent nonwovens was compared to the PET homocomponent nonwoven. The modulus in the machine direction for all the bicomponent nonwovens was improved compared to the homocomponent nonwoven. This superior performance is due to the fiber entanglements that occur during the fracturing in the jet dyeing machine. High strength is experienced in the fiber direction, resulting in high strength in the machine direction. Overall, the bicomponent nonwovens have improved mechanical performance with the segments up to 16.

3.3.7 Effect of Number of Segments on Flexibility

The bending length, **Figure 3.12**, of the samples was calculated using a cantilever beam, as a way of evaluating the flexibility, and the flexural rigidity, **Figure 3.13**, of the nonwovens was determined based on the weight of the sample.

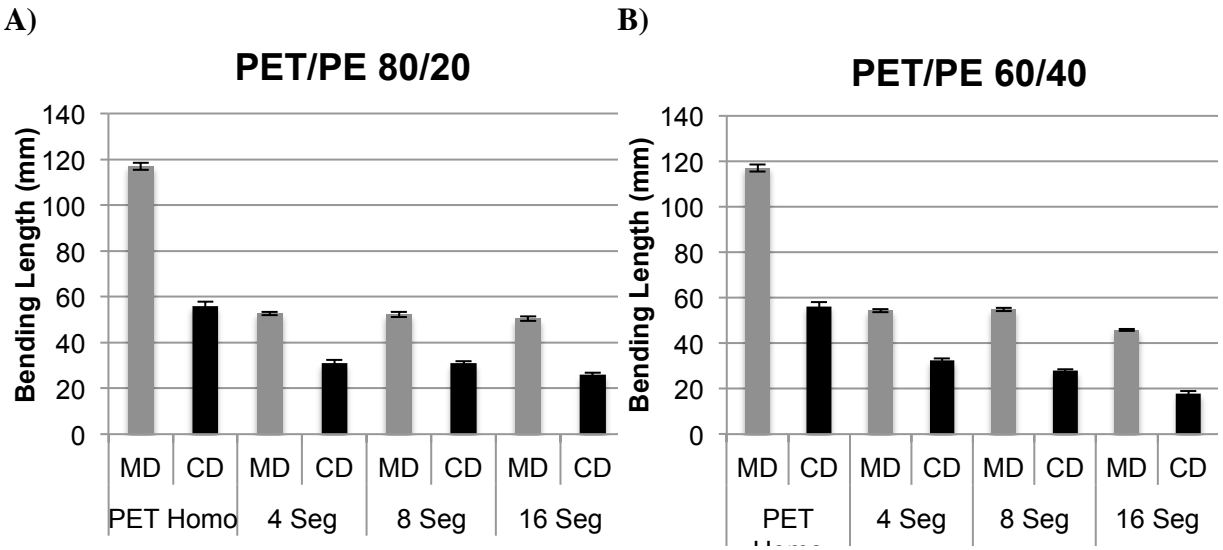

Figure 3.12. Effect of number of segments on the overhang length of the A) 80/20 and B) 60/40 polymer ratios

The length of the bend of the sample on the cantilever beam can provide information about the flexibility of the materials, the shorter the bending length the more flexible the material. All of the bicomponent samples have a lower bending length than the PET homocomponent samples, indicating a greater flexibility. This is due to the smaller diameters of the fibers in the bicomponent samples.

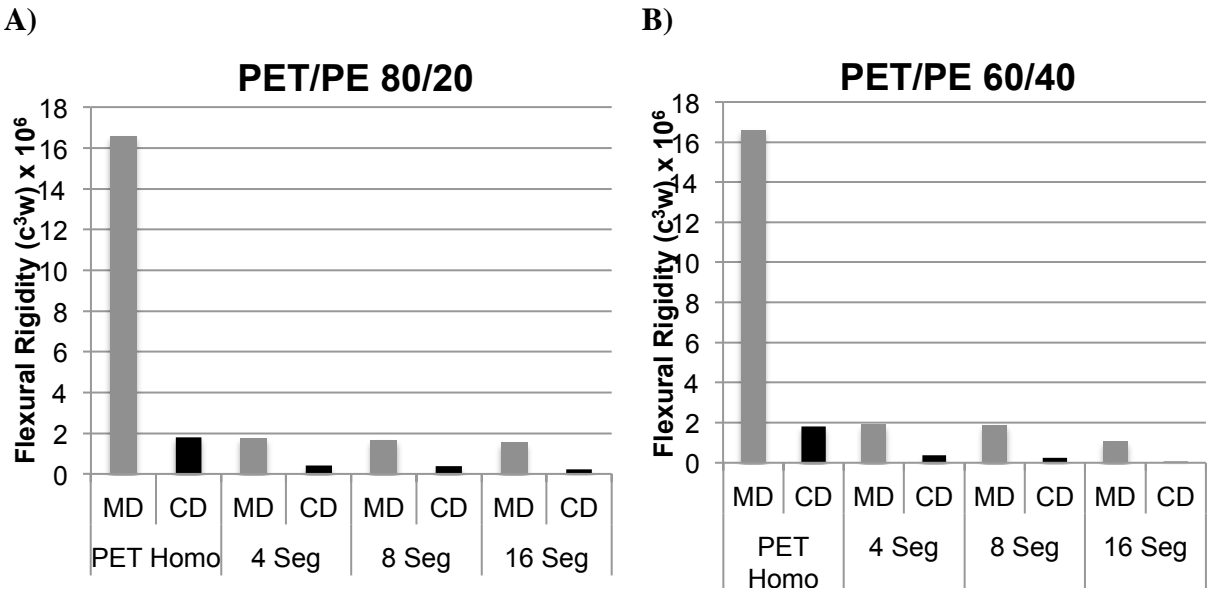

Figure 3.13. Effect of number of segments on the flexural rigidity of the A) 80/20 and B) 60/40 plymer ratios

The flexural rigidities of the bicomponent samples were tested using a cantilever beam and compared to the homocomponent nonwoven. There is a significant decrease in the flexural rigidity of the bicomponent samples compared to the homocomponent. The stiffness of the samples decreases with increasing number of segments. Increasing the number of segments in the original fiber decreases the diameter of the fibers after fracturing. Fibers with smaller diameters have a higher flexibility and less resistance to bending. The flexible nature of the fractured bicomponent materials makes them good candidates for a variety of applications.

3.4 Conclusion

PET/PE segmented pie bicomponent nonwovens were produced with varying number of segments and polymer ratios. These materials will later be functionalized to produce ion exchange nonwovens with a high surface area. Therefore, the permeability, porosity, and surface area of the materials are important. The nonwovens were washed in a jet dyeing

machine to ensure they had been fully fractured. There was little difference between the material properties of the two polymer ratios with different numbers of segments, but slightly less consolidation of the 80/20 samples with 4 and 8 segments. Both polymer ratios with 16 segments had nearly the exact sample properties. It was found that increasing the number of segments in the fiber increased the surface area of the material and increased the consolidation of the web. This consolidation resulted in a decrease in the permeability and pore size, while increasing the packing density. Upon fracturing of the bicomponent nonwovens a large increase in entanglements occurred, improving the mechanical strength of the materials. The smaller fiber diameters also increased the flexibility of the samples. These properties are important for understanding the effects of increasing the number of segments and how this will change the properties of the materials.

3.5 References

[1] S. Batra, M. Thompson, E. Vaughn,, and L. Wadsworth, *INDA Nonwovens Glossary*. Cary, NC: Association of the Nonwovens Fabrics Industr, 2002.

[2] N. Anantharamaiah and B. Pourdeyhimi, "Durable Nonwoven Fabrics via Fracturing Bicomponent Islands-in-the-Sea Filaments," *J. Eng. Fibers Fabr.*, vol. 3, no. 3, pp. 1–9.

[3] W. Goddard, *Handbook of nanoscience, engineering, and technology*, 2nd ed. Boca Raton FL: CRC Press, 2007.

[4] M. Lewin, *Handbook of fiber science and technology*. New York: Dekker, 1996.

[5] N. Fedorova and B. Pourdeyhimi, "High strength nylon micro- and nanofiber based nonwovens via spunbonding," *J. Appl. Polym. Sci.*, vol. 104, no. 5, pp. 3434–3442, Jun. 2007.

[6] C. Sun, D. Zhang, Y. Liu, and J. Xiao, "Bicomponent Meltblown Nonwovens and Fibre Splitting," *J. Ind. Text.*, vol. 34, no. 1, pp. 17–26, Jul. 2004.

[7] Dong Zhang, G. Bhat, M. Sanjiv, and L. Wadsworth, "Evolution of Structure and Properties in a Spunbonding Process," *Text. Res. J.*, vol. 68, no. 1, pp. 27–35, Jan. 1998.

[8] N. Anantharamaiah,, S. Verenich,, and B. Pourdeyhimi,, "Durable Nonwoven Fabrics via Fracturing Bicomponent Islands-in-the-Sea Filaments," *Jeff J.*, vol. 3, no. 3, pp. 1–9, 2008.

[9] E. Shim, B. Pourdeyhimi, and M. Latifi, "Three-dimensional analysis of segmented pie bicomponent nonwovens," *J. Text. Inst.*, vol. 101, no. 9, pp. 773–787, Sep. 2010.

[10] M. Vuorio, J. A. Manzanares, L. Murtomäki, J. Hirvonen, T. Kankkunen, and K. Kontturi, "Ion-exchange fibers and drugs: a transient study," *J. Controlled Release*, vol. 91, no. 3, pp. 439–448, Sep. 2003.

[11] V. Soldatov, A. Shunkevich, and G. Sergeev, "Synthesis, structure and properties of new fibrous ion exchangers⋆," *React. Polym. Ion Exch. Sorbents*, vol. 7, no. 2–3, pp. 159–172, Jan. 1988.

[12] I. Hutten, "Handbook of nonwoven filter media," Elsevier, Ltd., pp. 151–152.

[13] M. Dasdemir, B. Maze, N. Anantharamaiah, and B. Pourdeyhimi, "Influence of polymer type, composition, and interface on the structural and mechanical properties of core/sheath type bicomponent nonwoven fibers," *J. Mater. Sci.*, vol. 47, no. 16, pp. 5955–5969, Apr. 2012.

[14] H. H. Cho, K. H. Kim, Y. A. Kang, H. Ito, and T. Kikutani, "Fine structure and physical properties of polyethylene/poly(ethylene terephthalate) bicomponent fibers in high-speed spinning. I. Polyethylene sheath/poly(ethylene terephthalate) core fibers," *J. Appl. Polym. Sci.*, vol. 77, no. 10, pp. 2254–2266, Sep. 2000.

[15] Nonwovens Cooperative Research Center, “The Nonwovens Institute.” North Carolina State University, 2009.

[16] Werner Mathis AG, “Mathis Overflow Jet Färbeapparat Typ JFO Brochure.” .

Chapter 4

4 SURFACE GRAFTING OF NONWOVENS VIA UV INITIATION

Abstract

Surface grafting behavior of PET homocomponent nonwovens was investigated. The conditions contributing to the extensive homopolymer formation, specifically the drying process were studied in UV initiated grafting. The effects of oxygen scavenging and solution application methods were also investigated. PBT nonwovens were treated and the results are compared with PET. It was found that the addition of sulfuric acid as a catalyst lead to extremely high homopolymer formation at low reaction times. Mohr's salt did not prevent the formation of homopolymer. Different application methods and drying techniques were used to reduce the amount of homopolymer on the samples. No techniques were found to reduce the homopolymer and pore blockage of the samples after grafting. Other grafting techniques should be investigated.

4.1 Introduction

Surface grafting techniques are often performed on polymers to control the physical and chemical properties of the polymer. Surface grafting can be used to improve the wearability, wettability, biocompatibility, dyeability, adhesion, as well as physical strength of polymers [1], [2], [3]. Several different surface grafting techniques can be used to attach monomers to the surface of the polymer chains, including irradiation techniques, chemical modification, and plasma treatments. All of these techniques have their own advantages and disadvantages.

Glow discharge, flame treatment, and corona discharge are all types of plasma treatments to be used in surface modification. Generally, plasma treatment is less penetrating than other modification techniques and is therefore effective in targeting the modification of the surface of the polymers rather than affecting the bulk properties of the polymer [4]. Although plasma treatments result in a fairly uniform modification, the need for a vacuum

makes operation costly and it is difficult to control the exact amount of functional groups that are attached to the surface [5].

Radiation grafting employs an energy source to induce grafting between the substrate and the monomer, typically in the presence of a solvent. Radiation grafting is split up into two main categories, ionization and photografting, based on the intensity of the source. Ionization radiation includes electron beam radiation, γ radiation, and X-rays. The study of these techniques is known as radiation chemistry. Grafting done by UV and visible light is photografting; the study of which is photochemistry. The primary difference between photografting and ionization radiation is the high amounts of energy that are used in ionization radiation compared to photografting, Figure **4.1**. Ionization radiation produces a large amount of excited and ionized molecules and its high intensity makes it very difficult to be selective [5].

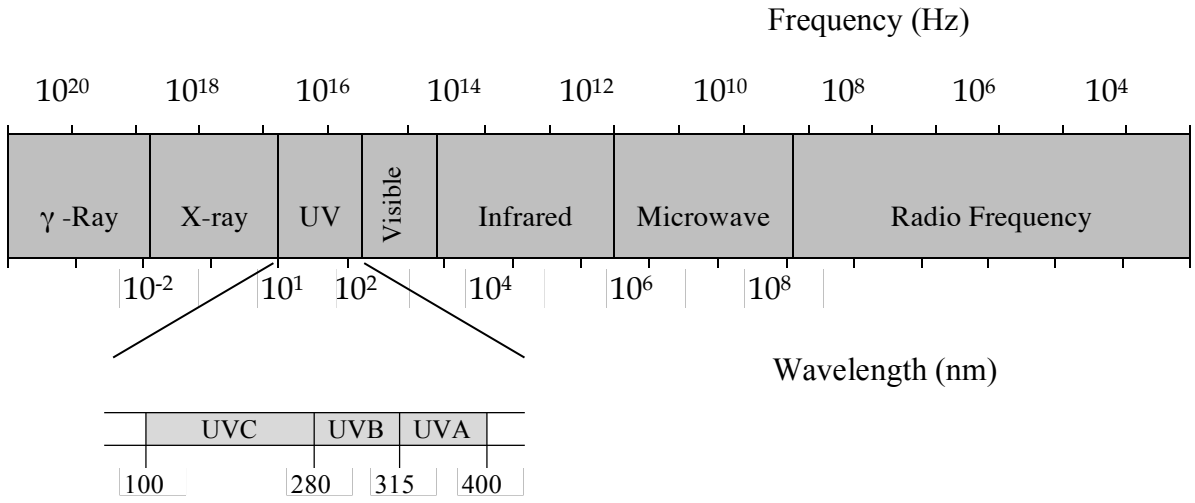

Figure 4.1. Electromagnetic Spectrum

The low intensity used in photografting is less penetrating into the sample, making it highly effective in targeting the surface of the polymeric materials. Photografting typically requires simple equipment, can prepare grafted samples in a short amount of time, and has a much lower cost compared to other grafting techniques [6]. The UV spectrum can be further split up into three more categories: UVA, UVB, and UVC representing wavelengths of 315 - 400 nm, 280-315 nm, and 100-280 nm, respectively. The selection of a specific bulb for the photografting experiments is dependent on the photoinitiator used in the solution.

In order for a photografting procedure to occur, a photoinitiator or photosensitizer must be used to initiate the reaction. A photosensitizer is used primarily to speed up the reaction and is not consumed in the reaction, while a photoinitiator is used to initiate the polymerization and is consumed during the process. Photoinitiators are light sensitive, typically at a specific wavelength of light, and create free radicals that initiate the polymerization of the monomer. Photoinitiation will occur if:

1 The initiator molecules have sensitivities to the particular wavelength of light under which they are exposed.
2 There are no chain terminating molecules present in solution.
3 An appropriate quantum yield is achieved.

The quantum yield of the reaction describes the ratio between the number of events that occur for each UV photon absorbed. This is dependent on many factors including the concentration of reactants and products, the temperature of the system, and the wavelength of light [7]. For the event of photografting,

$$\text{Quantum Yield } (\Phi) = \frac{\text{\# of reactants consumed}}{\text{\# of photon absorbed}}$$

In order for photoinitiation to proceed, there must be more reactant molecules consumed than UV photons absorbed. Thus, $\Phi \geq 1$.

There are many different photoinitiators available and many different mechanisms for the initiation of the reaction. Benzophenone (and derivatives of the molecule) is one of the most commonly used photoinitiators used in photografting procedures [5]. It is an aromatic ketone that reacts through hydrogen abstraction to create surface free radicals. The photoinduced excitation in which benzophenone (BP) is elevated to its singlet state occurs at 340 nm. The suggested reaction mechanism of glycidyl methacrylate (GMA) monomer grafted to PET polymers initiated with BP photoinitiator is shown in Figure **4.2**.

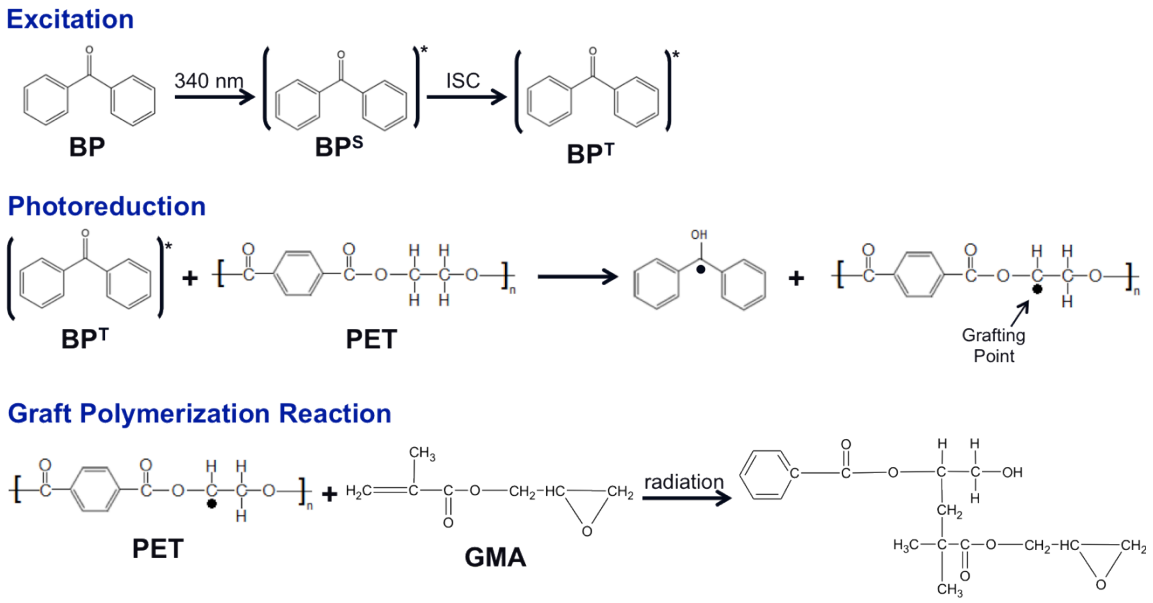

Figure 4.2. Reaction scheme of the grafting and sulfonation of PET with BP photoinitiator

With the absorption of a UV photon at 340 nm, BP is excited to its short lifetime singlet state, $[BP]^S$, and then relaxes to its triplet state, $[BP]^T$[7]. This movement from the singlet to the triplet state is known as intersystem crossing and only occurs with direct absorption of a photon [8]. The carbon-hydrogen bond of the methylene which connects to

the ester group of the PET backbone is the weakest bond of the PET molecule. Therefore, BP in its excited state abstracts a hydrogen atom from this site [9], [10]. The abstraction of the hydrogen from PET provides a surface free radical that allows for the initiation of graft polymerization of the GMA molecules onto the PET backbone. The surface radicals become the attachment sites for the GMA monomers [11]. The epoxy rings of the GMA monomers can later be opened through sulfonation reactions and become the attachment site for sulfonate groups to produce functionalized fibers.

Glycidyl methacrylate (GMA) was chosen as the grafting monomer because of the ease in which it can be grafted to synthetic polymers using BP photoinitiator. An abundance of literature can be found in which GMA is used as a grafting monomer with the aid of BP photoinitiator [12], [13], [14], [15]. The grafting efficiency of the monomer on the fibrous substrates is consistently reported as a function of weight increase of the sample. In the literature, the grafting behavior is then confirmed through FTIR analysis (the addition of epoxy groups) and SEM imaging [1], [11], [13], [14], [15], [16], [17].

Zheng et al. [15] investigated the conditions for grafting GMA on polypropylene nonwoven samples using BP photoinitiator with a UV pretreatment process. After exposure to UV in air in the presence of benzophenone samples were then sprayed with GMA in butanol solution containing benzophenone initiator and exposed to UV radiation. The group found that increased conformity in the attachment of the functional groups was due to the increased adsorption of BP due to the pretreatment process. Tests were done to investigate the effects of pretreatment time and immersion time on the BP adsorption. It was found that increased pretreatment time and increased immersion improved the adsorption of BP. Increased pretreatment time leads to increased polar groups which leads to dipole dipole interactions between the BP. BP can be removed from the surface with butanol which means that it is not covalently bonded on the surface of the sample.

Polybutylene Terephthalate, PBT, is a synthetic polymer with a similar structure to PET, but is known to be highly reactive to UV grafting procedures, Figure **4.3**. To investigate

whether the difficulty in grafting was due to the PET material or the UV system, PBT was also considered as a possible substrate for photografting.

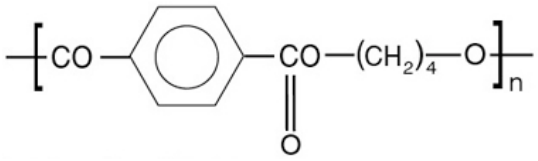

Figure 4.3. Structure of Polybutylene Terephthalate

4.2 Experimental Procedure

The grafting of GMA monomers using UV initiation onto the surface of PBT and PET nonwovens is investigated. The effectiveness of additives in the grafting solution, such as Mohr's salt and sulfuric acid in preventing homopolymer formation and speeding up the reaction, is also evaluated.

4.2.1 Materials

Polyethylene terephthalate, PET, and Polybutylene terephthalate, PBT, homocomponent spunbond substrates were produced in the Pilot Plant facility of the Nonwovens Institute at NC State University. Both materials had 100 gsm basis weight and were hydroentangled to entangle the materials.

Table 4.1. Properties of PET substrate (Eastman F61HC polyethylene terephthalate (PET) from Eastman Chemicals with a melting temperature of 260 °C) and the PBT substrate

Polymer	Ratio	Basis Weight (gsm)	Hydros
PET	Monofilament	100	1 (750 psi)
PBT	Monofilament	100	1 (750 psi)

Inhibitors were removed from glycidyl methacrylate prior to use with the inhibitor remover column from Sigma Aldrich. All solutions were made just prior to grafting procedures or used as received.

Table 4.2. List of the chemicals and solutions used for all grafting procedures

Solution	Acronym	Company	Purpose
Glycidyl Methacrylate	GMA	Sigma Aldrich	Monomer
Benzophenone	BP	Sigma Aldrich	Photoinitiator
Methanol	CH_3OH	Sigma Aldrich	Solvent
Mohr's Salt	Mohr's Salt	Sigma Aldrich	Homopolymer Suppressor
Sulfuric Acid	H_2SO_4	Sigma Aldrich	Grafting Accelerator
Tetrahydrofuran	THF	Sigma Aldrich	Washing

4.3 Analytical Methods

4.3.1 Grafting Percentage

The grafting efficiency of the monomer on the fibrous substrates is reported as a function of weight increase of the sample. This is defined as,

$$GP(\%) = \frac{W_1 - W}{W} \times 100\%$$

where W is the weight of the sample before grafting and W_1 is the weight after grafting.

4.3.2 Scanning Electron Microscopy

Scanning Electron Microscopy (SEM) was used to evaluate the degradation of the grafted samples, as well as the grafting behaviors after UV exposure. The SEM was available through the College of Textiles at NC State University.

4.4 Surface Grafting of Nonwovens

PET and PBT samples of A variety of solution compositions were used to investigate the effect of Mohr's Salt, sulfuric acid, and water in the grafting solutions with GMA monomer and BP photoinitiator, Table **4.3**.

Table 4.3. Compositions of the grafting solutions used for all UV grafting procedures

GMA : Methanol: H_2O (wt%)	**BP (M)**	**Mohr's Salt (mM)**	**H_2SO_4**
30:50:20	.1	0	0
40:40:20			
50:30:20		5	0.1
20:40:40			
50:50:0			

In an effort to reduce the degree of homopolymer formation that results after grafting, three different application methods were used to apply the grafting solution to the samples:

Control – Samples were submerged in the grafting solution until saturated (about 10 seconds)

Pad- Samples were submerged in grafting solution until saturated and padded between two paper towels to remove excess solution from between the pores

Spray – A small spray bottle was used to spray an even coating of solution on the surface of the samples

The samples were weighed before and after to ensure a consistent wet pick-up.

The grafting procedure was performed in a Fusion UV System, Figure **4.4**A, with a UVA bulb emitting light at 340 nm. The Fusion UV System is a bench top conveyor set up composed of a Kevlar belt that passes under a mounted UV lamp. Samples were placed between two glass slides, on top of a stainless steel mesh, and placed on the belt, Figure **4.4**B. The exposure times for all UV grafting procedures reported here were 10, 30, and 50 seconds.

A) **B)**

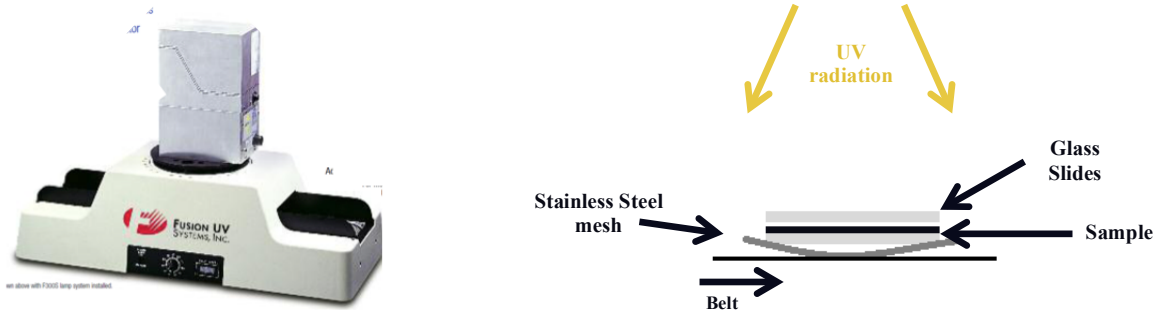

Figure 4.4. A) Fusion UV System used for photografting procedure and B) experimental set up for grafting procedures

After exposure to UV light and prior to washing, the samples were dried completely, either in air for 18 hours or in an oven at 100 ºC for 10 minutes. After the samples were dried completely, the unreacted monomer and homopolymer were washed off with a 30 minute sonication treatment in tetrahydrofuran, THF, solvent followed by 60 minute sonication treatment in methanol. The samples were then washed in DI water, dried completely, and weighed to calculate grafting percentages.

4.5 Results and Discussion

The effect of the grafting solution, experimental procedure, and grafting substrate on the grafting percentage was evaluated and SEM was used to evaluate the level of homopolymer.

4.5.1 Effect of Additives

Mohr's salt and sulfuric acid were added to a GMA, methanol, BP photoinitiator solution. The effect of the additives on the grafting percentage were calculated, Figure **4.5**. The grafting solutions were applied by submerging the samples in the solution followed by UV exposure.

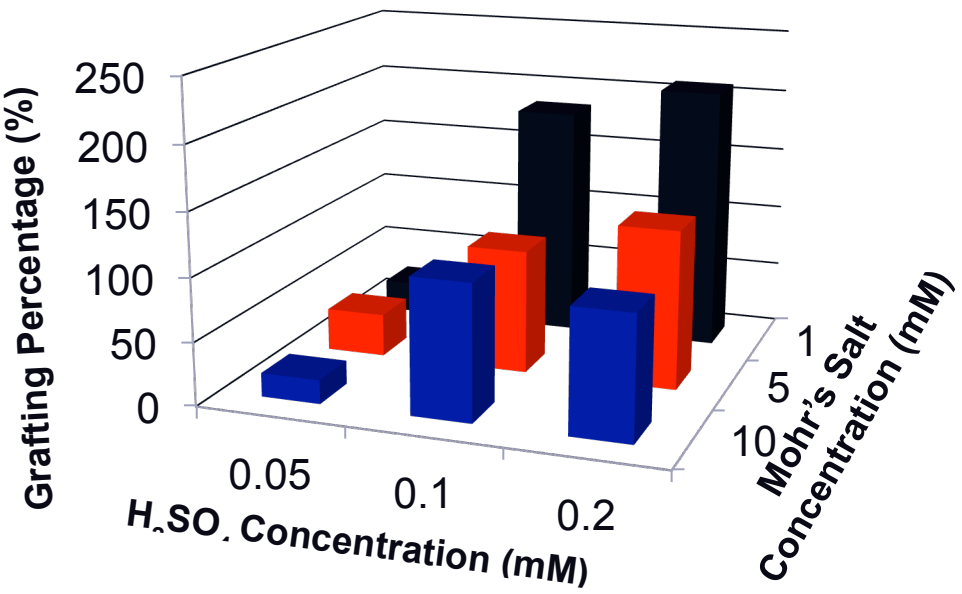

Figure 4.5. Effect of Additives on Grafting Percentage with 50:50 wt% GMA:Methanol with 0.1M BP and 50 second UV exposure

Mohr's salt is added to the grafting solution to inhibit the formation of homopolymer, while sulfuric acid is added as a catalyst to speed up the reaction [18], [19]. At low acid concentrations and high Mohr's salt concentrations the grafting percentage is reasonable, around 18%. However, the grafting percentage increases quickly, up to 200%, with increasing sulfuric acid concentrations. Even with the addition of a high level of Mohr's salt, the grafting percentage reaches 100%, likely due to a high levels of homopolymer formation. The homopolymer formation was monitored using SEM, Figure **4.6**.

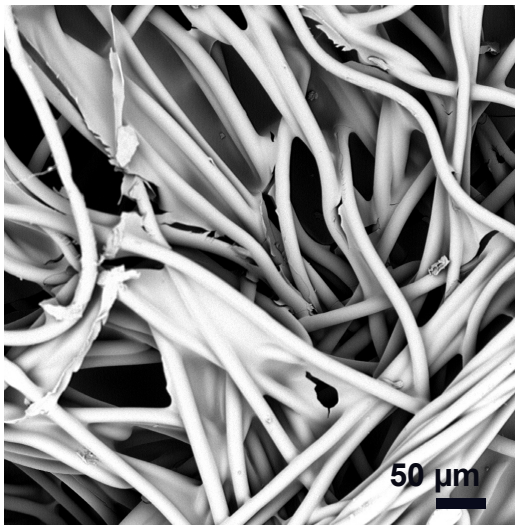

Figure 4.6. SEM image of grafted PET nonwoven with 184% GP grafted with 1 mmol/L Mohr's Salt, 0.1 mol/L H_2SO_4 for 50 seconds

The SEM image of the high grafting percentage nonwoven showed that the grafting resulted in high homopolymer formation that clearly blocks the pores of the sample. This was consistent with all samples that were grafted using UV initiation. It is possible that there is to much grafting solution in the pores of the sample after application causing the homopolymer to form between the pores. Other application methods should be investigated.

4.5.2 Effect of Solution Application Method

In an effort to reduce the homopolymer formation, different application methods of the solution on the PET substrates were used. Ideally, these application methods will reduce the amount of solution on the surface of the samples and reduce the pore blockage that occurs after grafting, Figure **4.7**.

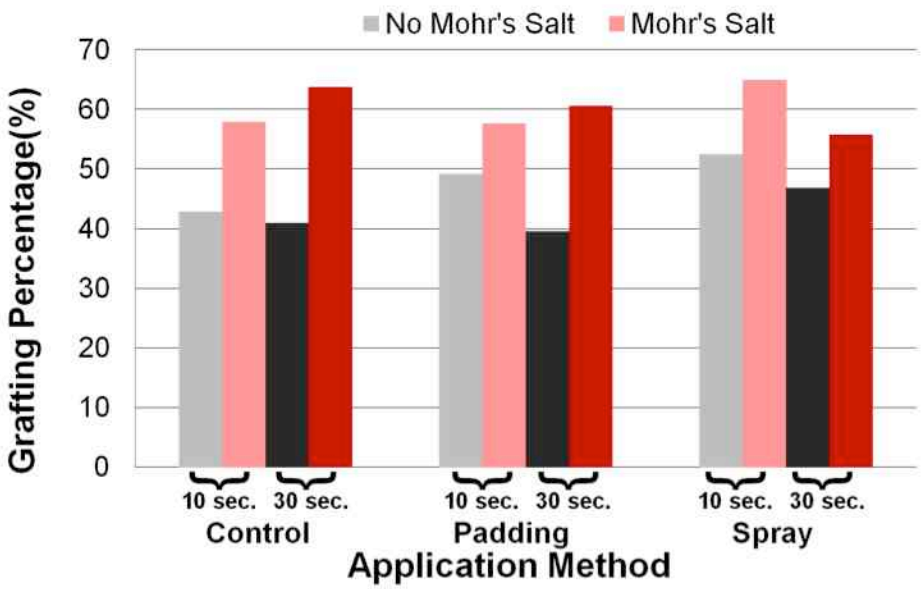

Figure 4.7. Effect of Application Method with and without Mohr's Salt

There was very little difference between the three application methods. In Figure **4.7**, the solutions that contained Mohr's salt are represented by the grey and black bars, while the solutions without Mohr's Salt are represented in the pink and red bars. For all application methods and at both 10 and 30 seconds, there was a 10-20% difference between grafting percentages of solutions that did and did not contain Mohr's Salt. Only one replication was done with each solution, due to time constraints. Therefore, the results are not statistically significant. However, the higher grafting percentage of the solutions containing Mohr's Salt is likely due to the prevention of homopolymer formation. With the same solution and exposure time, there is very little difference between the 3 application methods. SEM images were taken to investigate the surface morphology of the grafted samples, Figure **4.8**.

a) 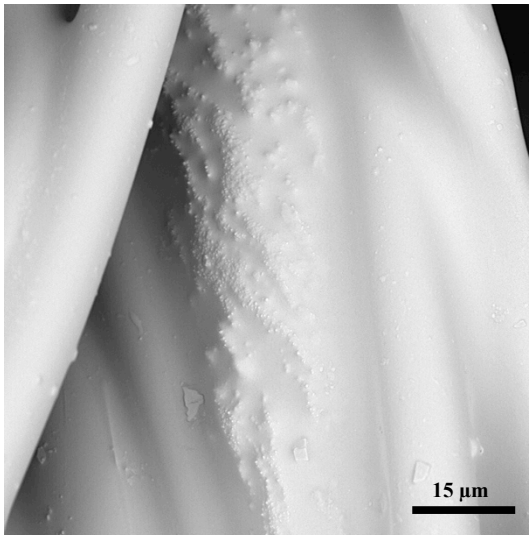

b) 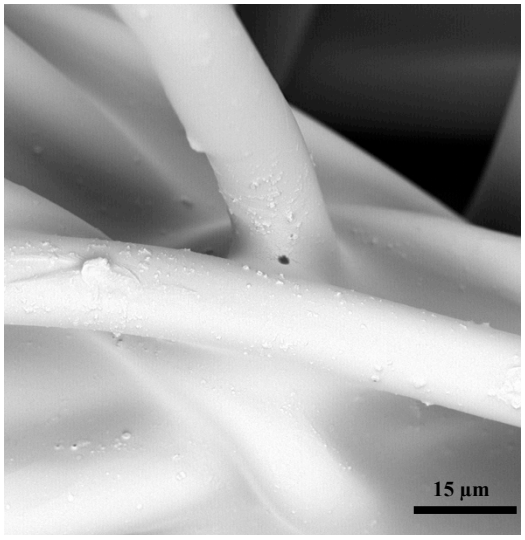

Figure 4.8. SEM images of a) Padded Sample, 30 Seconds exposure time w/Mohr's Salt - 60 GP%, b) Sprayed Sample, 10 second exposure time w/Mohr's Salt

Fibers in the samples have experienced obvious surface morphology changes after grafting. However, the extent of the changes can still not be investigated fully due to the homopolymer layer that is coating the individual fibers. The homopolymer film is also between the fibers in the web, creating a large amount of pore blockage.

The homopolymer layer has strongly adhered to the surface of all the samples. After analysis of the SEM images, there did not appear to be much of a difference between the three application methods. Based on these results, the control method was used for the rest of the UV grafting procedures. Since there is still the issue of homopolymer adherence and pore blockage, it is necessary to look at the various factors in the grafting procedure that could be causing this bond, one of which being the drying process.

4.5.3 Effect of Drying Technique after Grafting

For all of the application methods the samples that were not exposed to UV light and dried had 20-70% grafting percentage, Figure **4.9**.

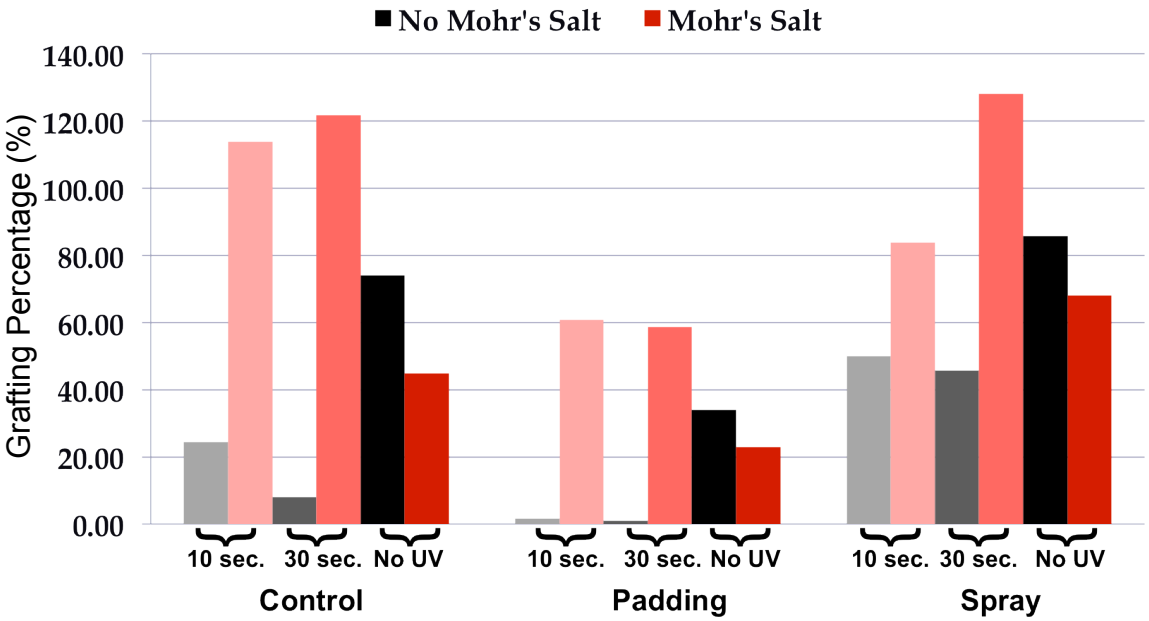

Figure 4.9. Effect of UV and Curing for various application methods

The grafting should be initiated by the photoinitiator component of the solution, benzophenone. Radicals on the PET backbone are created when the benzophenone absorbs UV photons and abstracts a hydrogen atom. If the samples are not exposed to UV light, no grafting should occur. However, with all of the application methods, the samples still had a grafting percentage of at least 25% with no exposure to UV light. Therefore, the grafting percentage of the third sample set (with no UV light exposure) must be due to homopolymer adhesion caused by the drying process. This is likely the cause of the high grafting percentage of the other samples. Looking at the samples under SEM gives an indication of the level of homopolymer formation.

A) **B)**

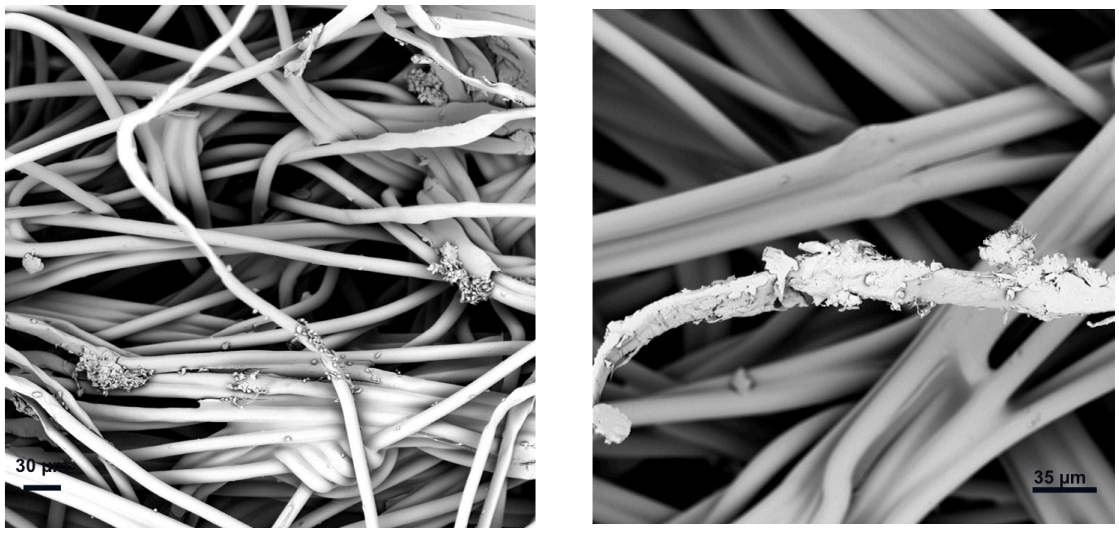

Figure 4.10. SEM images of A) sprayed sample with Mohr's Salt 10 second exposure time – 83% GP and B) padded sample with Mohr's Salt with no UV exposure – 33% GP

Figure **4.10**A shows grafting beads that have formed on the surface of the sprayed sample after 10 seconds of UV exposure, along with a large amount of homopolymer. Figure **4.10**B shows a sample that had the grafting solution containing Mohr's Salt applied via the padding method but was not exposed to UV light and was dried at 100 °C for 10 minutes. The fibers of these samples have significant homopolymer adhered to the surface even after washing in THF sonication. This is likely due to the high temperature of the drying step causing the homopolymer to bond to the surface of the fibers. The high temperature drying is likely causing what was perceived to be high grafting percentages at the low UV exposure times.

4.5.4 Effect of UV Grafting with Air Drying

The grafted weights of the samples were all exactly the same at their initial weights; no change in basis weight occurred. This indicated that the drying process was curing the homopolymer to the surface of the polymers which was being reported as high grafting

percentages. Since the samples had no weight gain, indicating no grafting had occurred, the other parameters of the process and components of the solution must be investigated.

One possible complication is that the grafting is not being performed in an inert atmosphere. Oxygen in the atmosphere could be reacting with the radicals produced on the PET backbone by the benzophenone photoinitiator [20]. Pinkerton and Stacewicz [21] found that adding water to the grafting solution would lower the oxygen equilibrium concentration in the solution. This allows grafting to commence sooner than when the grafting was performed in air with no water in the solution.

4.5.5 Effect of Water in the Grafting Solution

To investigate the effects of oxygen scavenging that could be inhibiting the grafting reactions from occurring, water was added to the grafting solutions. Solutions with 4 different concentrations of GMA monomer, methanol, and water were used. All solutions contained 20 vol% DI water with varying concentrations of methanol, and GMA monomer, Figure **4.11**.

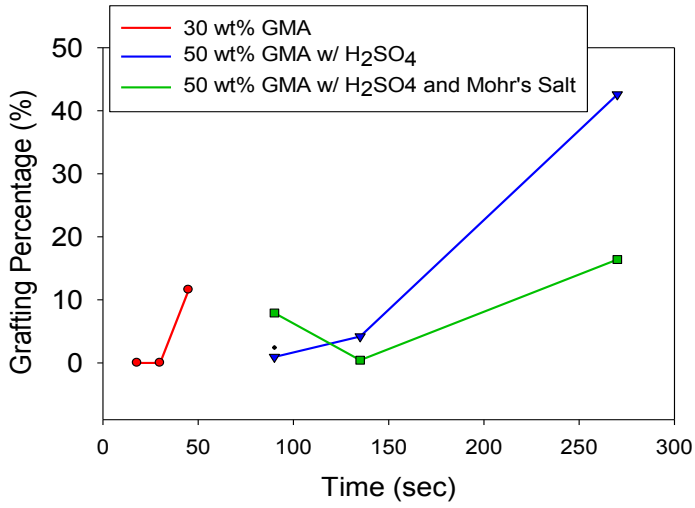

Figure 4.11. Grafting Percentage of grafted samples with 20:40:40 GMA: CH3OH: H2O, .1 M H2SO4, 5 mM Mohr's Salt

Samples with the solutions containing sulfuric acid were destroyed after 4.5 minutes of UV exposure, Figure **4.11**. Therefore, lower exposure times were used for these samples. The samples with solutions that did not contain sulfuric acid were beginning to degrade after about 4.5 minutes. Water did encourage grafting at low exposure times. However, the results were highly inconsistent and difficult to control.

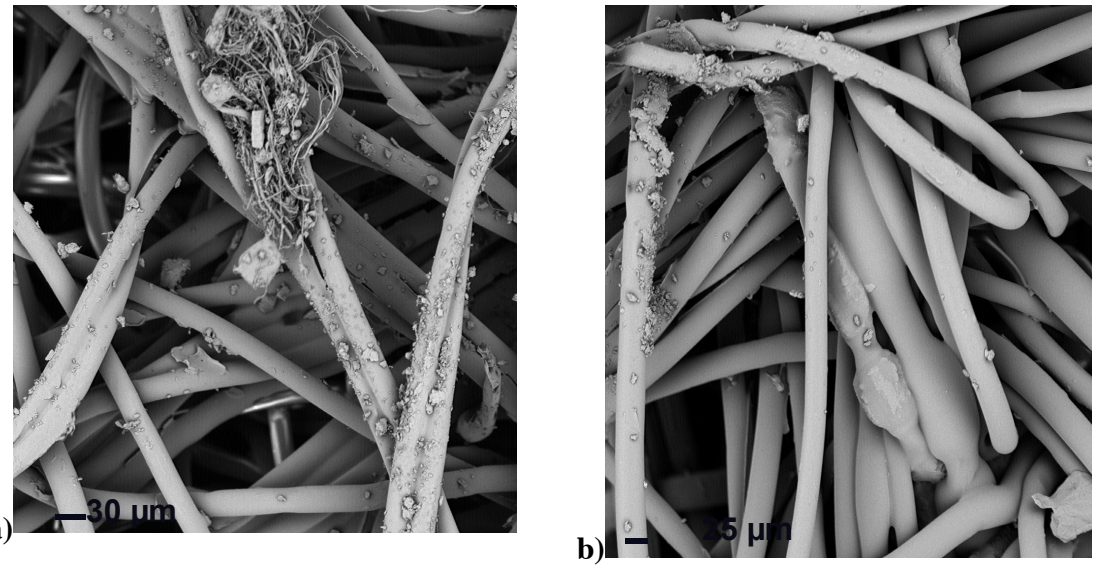

Figure 4.12. 20:40:40 GMA:CH3OH:H2O with .1M H2SO4 for a) 135 seconds and 5 mM Mohr's Salt and b) for 90 seconds with no Mohr's Salt

Using SEM imaging analysis, Figure **4.12**, it was evident that a high level of homopolymer formation remained on the surface of the sample. The samples with solution that contained Mohr's Salt had lower grafting percentages than those without Mohr's Salt. This is likely due to the reduction in the amount of homopolymer on the samples. It is

expected that a significant portion of the change in weight of the samples is due to the homopolymer.

UV grafting of PET with the Fusion UV machine has produced highly inconsistent results with large amounts homopolymer formation that has proven to be nearly impossible to remove from the surface of the sample. It was expected that PET would prove to be a difficult polymer to graft functional groups. However, the results have been very inconsistent and other means of grafting may need to be investigated.

4.5.6 Effect of Nonwoven Substrate

The grafting percentages of the PBT and PET nonwovens were considered for each grafting solution at increasing time of UV exposure, Figure **4.13**.

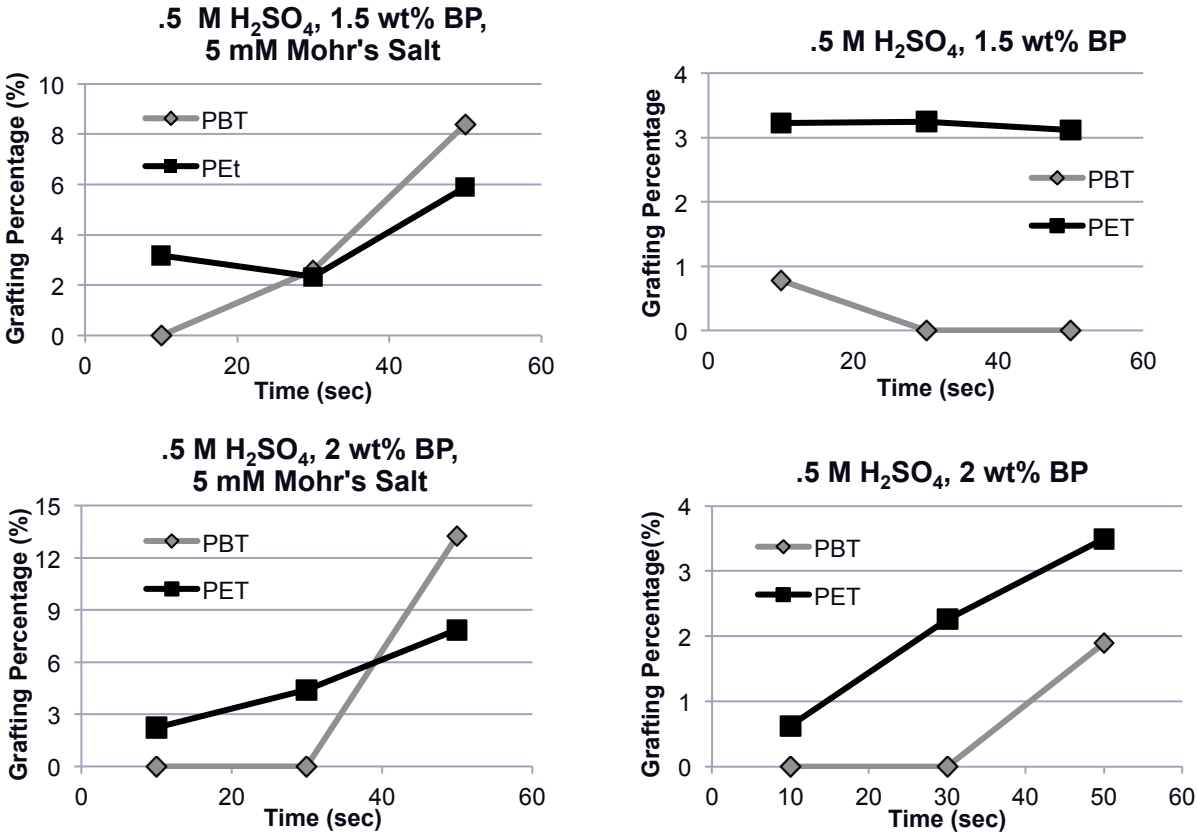

Figure 4.13. Effect of varying grafting solution concentrations on the grafting percentage of PBT and PET

There is not a significant difference in the two fiber types over the 10-50 second UV exposure times. Under these grafting conditions, the PET and PBT nonwovens have very low grafting percentages, all less that 12% and most under 4%. SEM analysis was done to investigate the changes in the fiber surface morphology, Figure **4.14**.

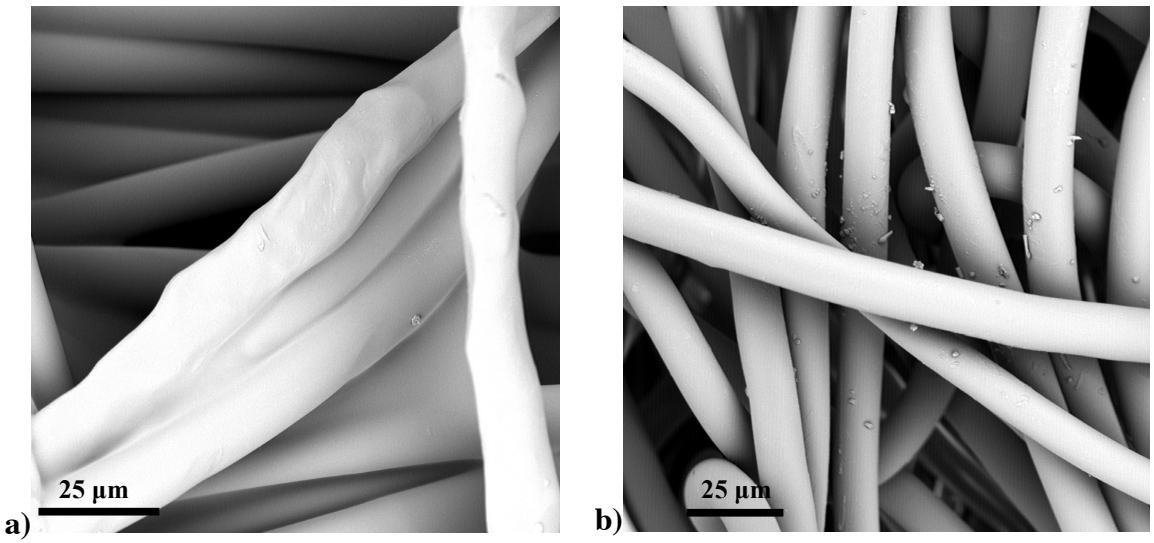

Figure 4.14. SEM images of nonwovens in solution containing 2 wt% BP photoinitiator and 5 mM Mohr's Salt with 50 second UV exposure times for a) 100% PBT and b) 100% PET nonwovens

It is evident from the SEM images that at the same exposure times and with the same solution concentrations, the PBT nonwoven sample has a significantly higher degree of homopolymer on the surface compared to the PET sample. Under these testing conditions, the PET samples had low grafting percentages but also had low degrees of homopolymer formation (based on subjective evaluation of the SEM images). After comparison of the fiber surface topologies and the differences in mean grafting percentages under various grafting conditions, it was concluded that the grafting behaviors of PET fibers should continue to be investigated and the use of this material should not be overlooked. However, other grafting techniques should be considered as the use of UV initiated grafting was proven to be inconsistent.

4.6 Conclusions

The grafting behavior of PET spunbond nonwoven materials using UV initiation was investigated. Trials were run to determine the cause for the high degree of homopolymer on the surface of the samples. Different applications methods were used to reduce the grafting

solution in the pores of the sample. There was no difference between the three application methods, so the samples continued to be saturated in solution prior to grafting. It was found that the drying of the samples in the oven after grafting was causing the homopolymer to adhere to the surface of the samples. The effects of oxygen scavenging were investigated with the addition of DI water to the grafting solution. Although low amounts of grafting occurred using this process, the grafting percentages between trials was highly inconsistent. The grafting of PBT was investigated to determine the efficiency of the Fusion UV set up. There was not a significant difference between the grafting results of PBT and PET, indicating that the UV experimental set up could be causing the difficulties with grafting. Therefore, due to the inconsistency in the grafting results other methods of grafting were investigated.

4.7 References

[1] F. Severini, L. Di Landro, L. Galfetti, L. Meda, G. Ricca, and G. Zenere, "Flame surface modification of polyethylene sheets," *Macromol. Symp.*, vol. 181, no. 1, pp. 225–244, May 2002.

[2] W. Huang and J. Jang, "Hydrophilic modification of PET fabric via continuous photografting of acrylic acid (AA) and hydroxyethyl methacrylate (HEMA)," *Fibers Polym*, vol. 10, no. 1, pp. 27–33, Mar. 2009.

[3] G. Oster and O. Shibata, "Graft copolymer of polyacrylamide and natural rubber produced by means of ultraviolet light," *J. Polym. Sci.*, vol. 26, no. 113, pp. 233–234, Nov. 1957.

[4] H. Yasuda, "Plasma for Modification of Polymers," *J. of Macromolecular Sc., Part A*, vol. 10, no. 3, pp. 383–420, Mar. 1976.

[5] C.-M. Chan, *Polymer Surface Modification and Characterization*. Hanser Gardner Publications, 1994.

[6] J. Deng, L. Wang, L. Liu, and W. Yang, "Developments and new applications of UV-induced surface graft polymerizations," *Progress in Polymer Science*, vol. 34, no. 2, pp. 156–193, Feb. 2009.

[7] C. Roffey, *Photopolymerization of Surface Coatings*. John Wiley & Sons Australia, Limited, 1982.

[8] J. Rabek, *Mechanisms of photophysical processes and photochemical reactions in polymers: theory and applications*. the University of Michigan: Wiley, 1987.

[9] N. Chansook and S. Kiatkamjornwong, "Ce(IV)-initiated graft polymerization of acrylic acid onto poly(ethylene terephthalate) fiber," *Journal of Applied Polymer Science*, vol. 89, pp. 1952–1958, Aug. 2003.

[10] M. M. Nasef, "Gamma radiation-induced graft copolymerization of styrene onto poly(ethyleneterephthalate) films," *Journal of Applied Polymer Science*, vol. 77, pp. 1003–1012, Aug. 2000.

[11] Y.-W. Song, H.-S. Do, H.-S. Joo, D.-H. Lim, S. Kim, and H.-J. Kim, "Effect of grafting of acrylic acid onto PET film surfaces by UV irradiation on the adhesion of PSAs," *j adhes sci technol*, vol. 20, no. 12, pp. 1357–1365, Sep. 2006.

[12] M. Ulbricht, "Photograft-polymer-modified microporous membranes with environment-sensitive permeabilities," *Reactive and Functional Polymers*, vol. 31, no. 2, pp. 165–177, Sep. 1996.

[13] M. Ulbricht and H. Yang, "Porous Polypropylene Membranes with Different Carboxyl Polymer Brush Layers for Reversible Protein Binding via Surface-Initiated Graft Copolymerization," *Chem. Mater.*, vol. 17, no. 10, pp. 2622–2631, May 2005.

[14] Y. Zheng, P. V. Gurgel, and R. G. Carbonell, "Effects of UV Exposure and Initiator Concentration on the Spatial Variation of Poly(glycidyl methacrylate) Grafts on Nonwoven Fabrics," *Ind. Eng. Chem. Res.*, vol. 50, no. 10, pp. 6115–6123, May 2011.

[15] Y. Zheng, H. Liu, P. V. Gurgel, and R. G. Carbonell, "Polypropylene nonwoven fabrics with conformal grafting of poly(glycidyl methacrylate) for bioseparations," *Journal of Membrane Science*, vol. 364, no. 1–2, pp. 362–371, Nov. 2010.

[16] N. Kwak, T. Hwang, S. Kim, Y. Yang, and K. Kang, "Synthesis of sulfonated PET-g-GMA fine ion-exchange fibers for water treatment by photopolymerization and their adsorption properties for metal ions," *Polymer (Korea)*, vol. 28, no. 5, pp. 397–403, Sep. 2004.

[17] L. Yu, S. Zhang, W. Liu, X. Zhu, X. Chen, and X. Chen, "Improving the flame retardancy of PET fabric by photo-induced grafting," *Polymer Degradation and Stability*, vol. 95, no. 9, pp. 1934–1942, Sep. 2010.

[18] W. Chappas and J. Silverman, "The effect of acid on the radiation-induced grafting of styrene to polyethylene," *Radiation Physics and Chemistry (1977)*, vol. 14, no. 3–6, pp. 847–852, 1979.

[19] J. L. Garnett and N. T. Yen, "Effect of acid on the radiation-induced grafting of monomers to polyolefins," *J. Polym. Sci. B Polym. Lett. Ed.*, vol. 12, no. 4, pp. 225–229, Apr. 1974.

[20] J. Garnett, "Grafting," *Radiation Physics and Chemistry (1977)*, vol. 14, no. 1–2, pp. 79–99, 1979.

[21] D. M. Pinkerton and R. H. Stacewicz, "γ-Radiation-induced grafting of methyl methacrylate to polypropylene: The effects of water and mineral acid," *J. Polym. Sci. B Polym. Lett. Ed.*, vol. 14, no. 5, pp. 287–291, May 1976.

Chapter 5

5 Surface Grafting of PET Homocomponent and Bicomponent Webs Via Ceric Salts

Abstract

In this study, PET/PE fractured bicomponent nonwovens and PET homocomponent nonwovens were grafted with Glycidyl Methacrylate (GMA), an epoxy containing monomer. The grafting conditions of GMA via ceric salt redox reactions were defined and the grafting results of the high surface area bicomponent nonwovens were compared to those of the PET homocomponent nonwovens. The effects of the surface area and web structure on the grafting efficiency were defined. It was found that the dense web structure of the fractured bicomponent webs required longer grafting times but the high surface area resulted in higher grafting percentages. The presence of epoxy rings after grafting was confirmed and uniform grafting was observed on the bicomponent nonwovens.

5.1 Introduction

Polyethylene terephthalate, PET, is a widely used and readily available material used in a multitude of applications. PET is hydrophobic and does not contain any chemically reactive groups. This makes dyeing and water absorption very difficult [1]. Applying functionality to the PET backbone increases the versatility of the fibers and broadens the applications that PET can be useful. Surface modification of polyethylene terephthalate (PET) is difficult due to its highly ordered structure and lack of reactive groups[1]. Achieving an efficient, cost effective method of surface modification of PET would have a profound impact on the functional fiber industry. Modifications allow for tailoring of the reactivity of the PET fibers, while taking advantage of the positive physical properties of the material. Different surface modification techniques are available to bond functional groups to polymer structures using techniques just as redox reactions [1], [2], [3], [4], UV radiation [5], [6], [7], and melt state

modification [8], [9]. Some methods of modification of the PET structure have been reported in the literature[2], [4], [10], [11], [12]. However, to the best of our knowledge, there are no commercial functionalized PET materials currently available.

Cerium ion has been extensively studied for its strong oxidizing properties in redox-initiated polymerizations [13], [14], [15], [16], [17]. Cerium is a rare earth metal in the lanthanide family that is found in abundance in the earth's crust. Cerium ion is stable in both +3 and +4 oxidation states but is more stable as in the +4, cerium(IV), because of its vacant f shell. Cerium(IV) has a high reduction potential of 1.6 V vs. normal hydrogen electrode which makes it an efficient oxidizing agent [18].

Some of the earliest work done in the area of ceric salt initiated grafting was performed by Mino and Kaizerman in 1958 [89]. The authors found that when ceric salts, specifically ceric ammonium nitrate and sulfate, were mixed with suitable organic reducing agents they formed redox systems. The reducing agents used in the study included alcohols, glycerols, mono and disaccharids, thiols, aldehydes, and amines. Mino and Kaizerman [89] proposed a single electron transfer mechanism, in which a free radical is produced on the reducing agent. If the reducing agent is a polymer and a monomer is present in the grafting solution, a free radical is produced on the polymer backbone and becomes the grafting site for the monomer present. In this particular study, acrylamide, acrylonitrile, and methyl acrylate were grafted onto polyvinyl alcohol under nitrogen.

Few changes have been made to the ceric ion grafting process since the early studies. Extensive studies have been done on investigating the kinetics of ceric ion initiated grafting reactions [16], [19], [20], [21]. In one such study by Odian and Kho [22], the rate of grafting vinyl-acetate acrylonitrile to PVA initiated by ceric ammonium nitrate was a first order reaction with respect to the monomer and polymer concentrations. The authors found that at varying CAN and monomer concentrations, all grafting percentages leveled off after 20 minutes, which they attributed to consumption of the ceric ions. The grafting percentage was found to be independent of ceric ion concentration above .002 M.

Haworth and Holker [23] investigated the grafting of acrylic acid on nylon fibers via ceric ammonium nitrate and sulphate initiation. The use of mineral acid additives was also investigated as a means of speeding up the reaction. 8.7 – 50.3% grafting was reported after 1 – 7 hours, respectively. With the addition of sulfuric acid in the grafting solution this was increased to 80% grafting percentage after 1 hour. The reactions were performed in closed flasks in the dark, but no nitrogen was flushed through the reaction.

The suggested reaction scheme for the interaction between cerium and PET to initiate grafting of GMA is seen in Figure 5.1. Cerium ions act as strong oxidizers when in acidic solution. An electron transfer of a hydrogen atom occurs from the PET backbone to Ce(IV) to produce Ce(III). This hydrogen abstraction creates a radical on the PET which becomes the grafting site of the GMA monomer [22].

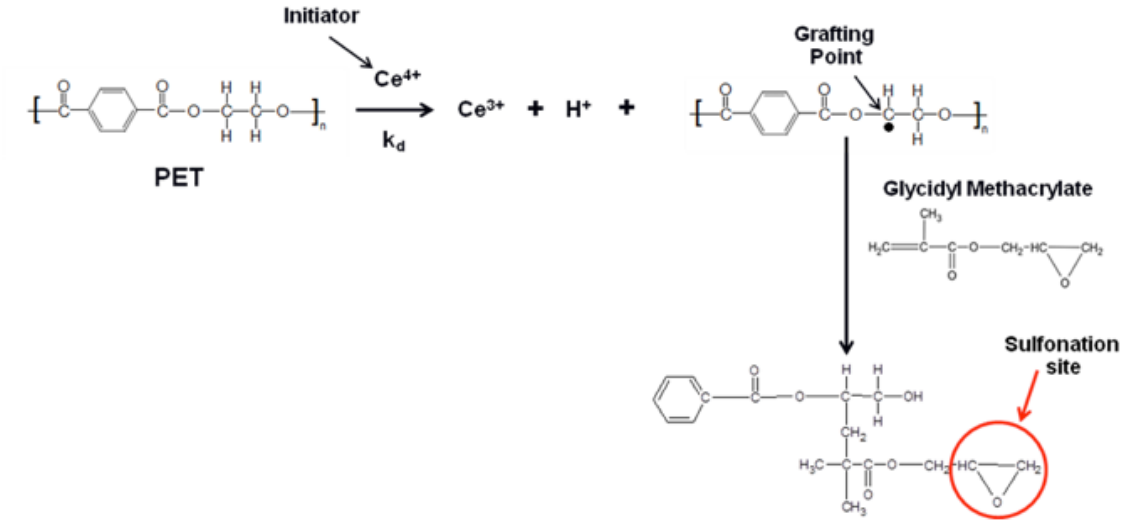

Figure 5.1. Suggested reactions scheme of the GMA grafting on PET initiated with cerium ion

Glycidyl Methacrylate is an epoxy containing monomer often used to give functionality to polyolefins [24], [25], [26], [27], [28], [29]. The monomer contains an acrylic backbone giving it strength and the epoxy ring provides the functionality[30]. The epoxy ring of the glycidyl methacrylate monomer is highly reactive and will readily accepts functional groups [30]. Grafting GMA monomers to a fiber substrate using ceric salt has also been reported[31], [32]. The epoxy rings of the GMA monomers can later be opened through either sulfonation or amination reactions and become the attachment site for reactive groups to produce functionalized fibers.

5.2 Experimental Procedure

5.2.1 Materials

For all of the following experiments, nonwovens composed of 80/20 PET/PE 16 segmented pie bicomponent fibers and a PET homocomponent were used, Table 5.1. The materials had a basis weight of 100 grams/meter^2 and were passed through the hydroentangling machine for one pass at 750 psi. These materials were made in the Pilot Plant of the Nonwoven's Institute. The PET/PE bicomponent fiber was fractured in the Jet Dyeing Machine for 120 minutes to achieve 100% fracture of the bicomponent fibers.

Table 5.1. Characteristics of nonwoven used for the experiments

Polymer	Ratio	Segments	Basis Weight (gsm)	Hydros	Fractured Time (mins)
PET	Homocomponent	1	100	1 (750 psi)	0
PET/PE	80/20	16	100	1 (750 psi)	90

For all of the grafting procedures, hydroquinone is removed from Glycidyl Methacrylate, GMA, prior to all experiments using an inhibitor remover column obtained from Sigma Aldrich. All other chemicals are used as received, Table **5.2**.

Table 5.2. List of the chemicals and solutions used for all grafting procedures

Solution	Acronym	Company	Purpose
Glycidyl Methacrylate	GMA	Sigma Aldrich	Epoxy containing monomer
Ceric Ammonium Nitrate	CAN	Fisher Scientific	Grafting Initiator
Nitric Acid	NHO_3	Fisher Scientific	Grafting Acid
Methanol	CH_3OH	Sigma Aldrich	Washing Solvent

5.2.2 Grating of PET Fibers

The nonwoven samples were cut into 8x8 inch samples, washed in acetone for 24 hours, and dried completely before weighing. The grafting initiator, CAN, was dissolved in 100 mL of Nitric Acid, HNO_3. Distilled water was added to a 500 mL round bottom flask to bring the total solution volume to 400 mL and flushed with nitrogen for 5 minutes. The CAN/HNO_3 solution, sample, and stirring rod were then added to the flask. The flask was lowered into a mineral oil bath at 60 ºC and the solution was flushed with nitrogen for 15 minutes. The GMA monomer was then added to the flask to begin the reaction. Reaction times ranged from 10-30 minutes. The concentrations of GMA and CAN are found in **Table 5.3**.

Table 5.3. Concentrations of Grafting solutions

GMA Concentration (wt%)			CAN Concentration		
2	4	6	2	4	6

After the specified reaction time the PET-g-GMA samples are washed in methanol on a mechanical shaker at 60 ºC for 4 hours, then washed for 3 hours in methanol with a probe sonicator. The samples were rinsed in DI water and dried until a constant weight was achieved.

5.3 Analytical Technique

Several analytical techniques were used to monitor the reactions. No analytical technique is perfect and all are used together to get an overall idea of the effects of the grafting.

5.3.1 Grafting Percentage

The grafting efficiency of the monomer on the fibrous substrates is reported as a function of the weight increase of the sample, Equation 5.1:

$$GP(\%) = \frac{W_g - W}{W} \times 100\% \qquad \textbf{(5.1)}$$

where W is the weight of the sample before grafting and W_g is the weight after grafting.

The major problem experienced with graft polymerization reactions is in the formation of homopolymer that adheres to the grafting substrate. This homopolymer is a product of the monomers reacting with each other rather than the grafting substrate[33], [34]. Therefore, the grafting percentage value includes grafting monomer as well as any remaining homopolymer.

5.3.2 Air Permeability

An Air Permeability tester, model FX330, from TexTest Instruments was used to investigate the permeability of the materials with a 1 in^2 sample holder in the Analytical Lab of the Nonwovens Institute. Three repetitions were performed on each sample.

5.3.3 BET Surface Area Analysis

BET (available through the Material Science and Engineering department at NC State University) was used to investigate the surface area of the PET/PE fractured bicomponent fibers.

5.3.4 Solidity

The solidity is known as the packing density or volume fraction. It is the volume of fibers in a given volume of the web. It is described as,

$$Solidity = (\%PET)\frac{(\rho_{web})}{(\rho_{PET})} + (\%PE)\frac{(\rho_{web})}{(\rho_{PE})} \qquad \textbf{(5.2)}$$

where *%PET* is the ratio of PET in the original fiber (60% or 80%) , *%PE* is the ratio of PE in the original fiber (40% or 20%), ϱ_{PET} is the density of PET polymer (1.41 g/cm^3), ϱ_{PE} is the density of PE polymer (.955 g/cm^3), and the density of the web is defined as a ratio of Basis Weight (g/cm^2) and Thickness (cm):

$$\rho_{web} = \frac{BasisWeight}{Thickness} \qquad \textbf{(5.3)}$$

5.3.5 Pore Diameter

The small, mean, and large pore diameters of the samples were calculated using a PMI, Inc. Capillary Flow Porometer, model CFP-1100-Ax, in the Analytical Lab of the Nonwovens Institute. Galwick™ (surface tension 15.9 dynes/com) was applied to the samples. One replication of each sample was done.

5.3.6 FTIR

The change in the surface chemistry of the samples after grafting was monitored with FTIR. The Thermo Electron FTIR with a Nexus 470 bench in the Analytical Lab of the College of Textiles of NCSU was used for the analysis. 64 scans were done of each sample at a resolution of 4.

5.3.7 TOF-SIMS

The TOF-SIMS analysis was done in the Analytical Instrumentation Facility at NCSU with an ion TOF-SIMS 5 machine. 124 scans were done for each sample at a resolution of 50 nm.

5.4 Results and Discussion

An Analysis of Variance (ANOVA) was run using JMP statistical software was used to analyze the results of the grafting reactions and identify statistically significant interactions between the factors of the grafting reactions and the resulting grafting percentages. The results of the Effects Test are found in Table 5.4.

Table 5.4. Factoring Significantly affecting the grafting percentage

Effect Tests

Source	Nparm	DF	Sum of Squares	F Ratio	Prob > F
Material	1	1	792.4589	37.3998	<.0001*
GMA (wt%)	2	2	3616.5835	85.3416	<.0001*
CAN (mM)	2	2	1525.4598	35.9967	<.0001*
Time (mins)	2	2	22.1913	0.5237	0.5987
Material *GMA (wt%)	2	2	150.1022	3.5420	0.0442*
Material *CAN (mM)	2	2	545.1760	12.8647	0.0001*
GMA (wt%)*CAN (mM)	4	4	1645.6663	19.4166	<.0001*
Material *Time (mins)	2	2	20.2486	0.4778	0.6257
GMA (wt%)*Time (mins)	4	4	65.2975	0.7704	0.5547
CAN (mM)*Time (mins)	4	4	35.8470	0.4229	0.7906

The significant factors affecting the grafting percentage are the nonwoven structure, the GMA concentration, and the CAN concentration, as well as the material used at varying GMA and CAN concentrations and the GMA and CAN concentrations. The interactions between these factors can be found in .

5.4.1 Effect of Grafting Conditions

The grafting of the glycidyl methacrylate monomers to the PET fibers was performed with varying concentrations of the GMA monomer and the ceric ammonium nitrate initiator. Understanding the relationship between these two components is important in improving the efficiency of the grafting process and reducing the homopolymer formation during the process.

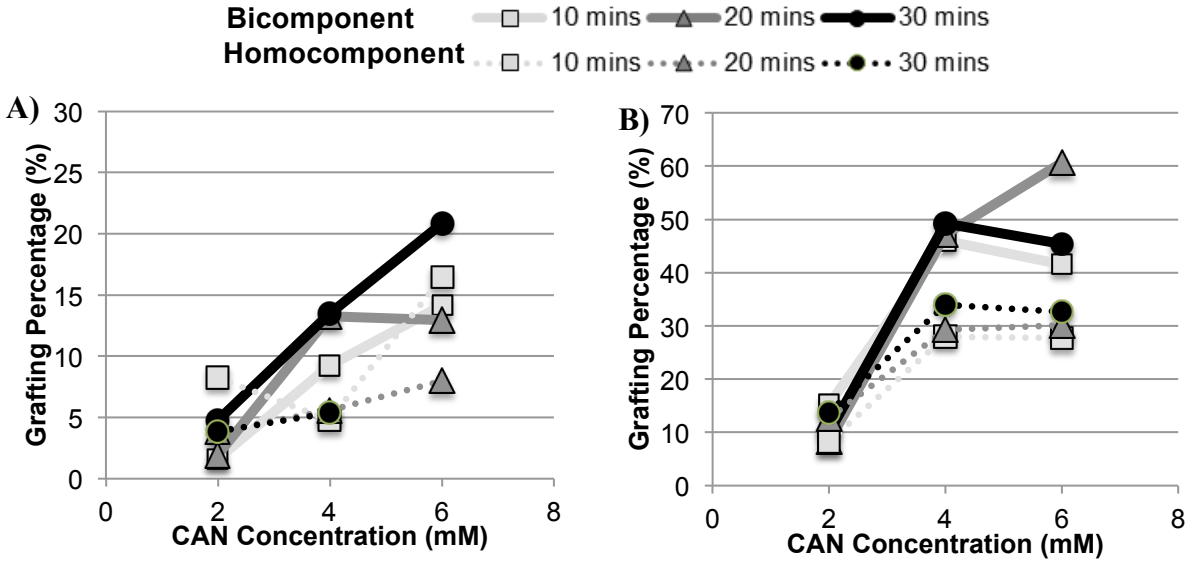

Figure 5.2. Grafting percentages of bicomponent and homocomponent samples at increasing CAN initiator concentrations and a) 2 wt% GMA monomer concentration and b) 6 wt% GMA monomer concentration

At a low monomer concentration of 2 wt%, Figure 5.2, the grafting percentage of both the homocomponent and bicomponent samples continues to increase with increasing initiator concentrations. The continuous increase indicates that an equilibrium has not been reached and the maximum grafting possible has not been achieved. However, at a high monomer concentration of 6 wt% GMA, B, the grafting percentage reaches a maximum at 4

mM CAN initiator concentration and levels off after this concentration. This behavior is consistent at all reaction time and for both the bicomponent and homocomponent samples, indicating that the initiator is likely producing the maximum number of radical sits on the PET backbone.

5.4.2 Effect of Nonwoven Structure on Grafting Percentage

To investigate the effect of the web structure on the grafting behavior, PET homocomponent and 80/20 PET/PE 16 segmented pie webs are grafted under the same conditions and the resulting grafting percentages are compared. The homocomponent webs are much more open than the 16 segmented pie webs and have far less graftable surface area.

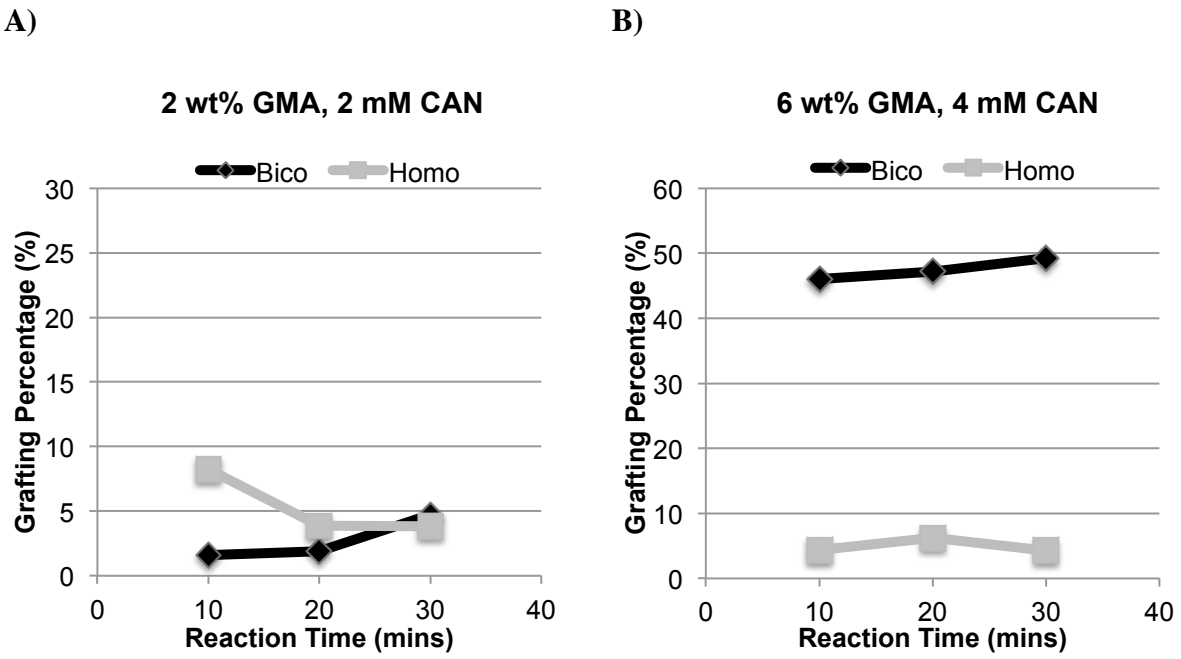

Figure 5.3. Effect of time on the grafting percentage for the bicomponent and homocomponent nonwovens at a) low grafting concentrations and b) ideal grafting concentration

The two web structures behave quite differently under the same grafting conditions, resulting in varying grafting percentages. At low grafting concentrations, the grafting percentage of the PET homocomponent is higher than the PET/PE bicomponent nonwovens at lower grafting reaction times. Both nonwovens have low grafting percentages even after long reaction times. However, with the ideal grafting concentrations, the concentration where an equilibrium in the grafting percentage was reached indicating the monomer and initiator were being fully utilized, the grafting percentage of the bicomponent nonwoven experiences a large increase while the extent of grafting of the homocomponent nonwoven remains low. Under these conditions, the grafting reaction is initiated and completed very quickly, in less than 10 minutes. These low reaction times make this a very favorable process to be used in an industrial application.

The large difference in grafting percentage of the two materials can be explained by investigating the difference in the two web structures, Figure 5.4.

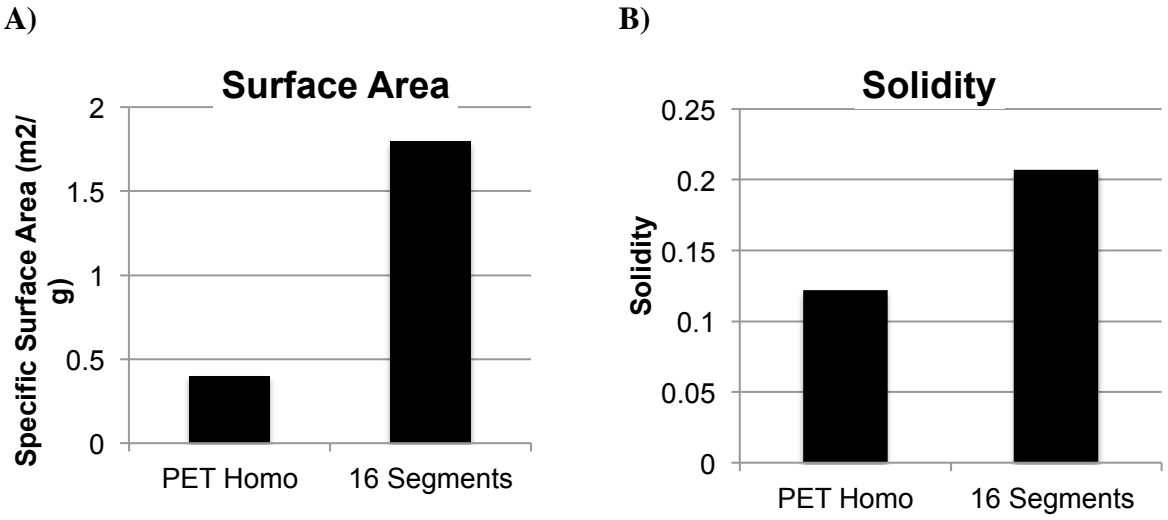

Figure 5.4. WEb properties of the PET Homocomponent Nonwoven compared to the 80/20 PET/PE 16 segmented pie nonwoven based on a)Surface area and B)Solidity

The PET/PE 16 segmented pie web has nearly 4.5 times the amount of surface area as the PET homocomponent, 80% of that being the PET graft-able area, A. In addition to this increase in surface area, the solidity of the bicomponent web is nearly twice that of the homocomponent web, B, due to consolidation of the web after the splitting of the fibers. Under the ideal conditions, the process takes advantage of the higher surface area in the bicomponent web and the extent of grafting is much higher in the bicomponent compared to the homocomponent.

5.4.3 Changes in Morphology and Pore Structure After Grafting

Scanning Electron Microscopy was done to investigate changes to the morphology of the fibers and the formation of homopolymer in the structure of the web, Figure 5.5.

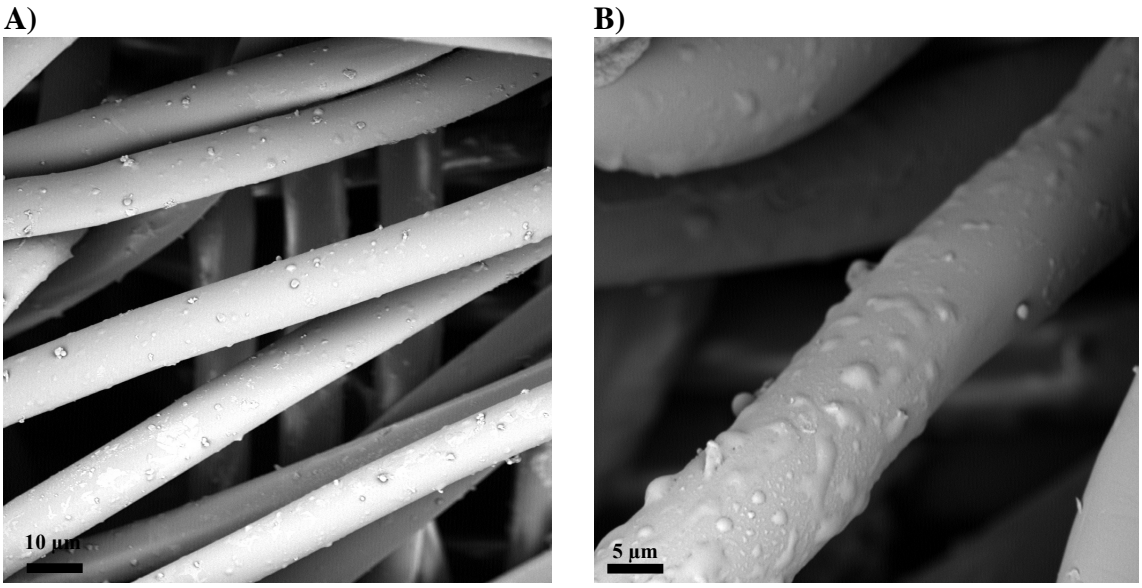

Figure 5.5. SEM images of CAN initiated grafted PET samples with 6 vol% GMA and 4 mM CAN after a) 10 minutes - 5.18% GP and b) 20 minutes - 14.23% GP

The SEM images showed very little homopolymer formation and fairly uniform grafting on the surface of the fibers. These grafting bumps, due to the grafted GMA chains, on the surface of the fibers are consistent with GMA grafting found in the literature [25].

High degrees of grafting could lead to changes in the pore structure of the materials, particularly blockage of the pores. Considering these materials for industrial filtration applications, it is important that the pore structure is maintained and that no significant decrease in the permeability has occurred.

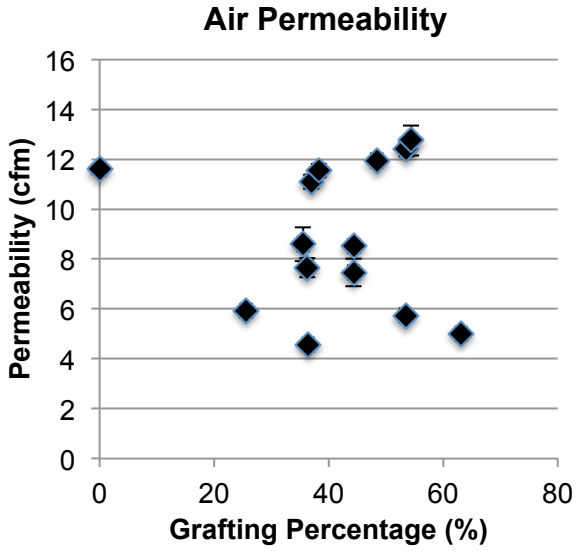

Figure 5.6. Air Permeability of PET/PE 80/20 16 segmented pie fibers at high grafting percentages

The air permeability, Figure 5.6, of the grafted samples decreases with increasing grafting percentage, as is expected. High levels of grafting indicate that long chains of grafting GMA polymers are present, likely causing a slight degree of pore blockage, resulting

in lower permeability. However, the decrease in permeability is not drastic and this behavior is simply important to be aware of when considering these materials for future applications, such as filtration.

5.4.4 Confirmation of the Presence of Epoxy Groups

The grafting procedure was monitored using both FTIR and TOF-SIMS. Both characterization techniques are qualitative and used simply to confirm the presence of epoxy groups available for functionalization and their distributions on the surface.

5.4.5 FTIR

Figure 5.7 shows the spectrum of grafted PET/PE samples, (PET/PE)-g-GMA. A, B, C, and D, represent the sprectra of the PET/PE control sample, as sample grafted for 10 minutes (GP of 44.4%), 20 minutes (GP of 53.5%), and 30 minutes (GP of 36%), respectively.

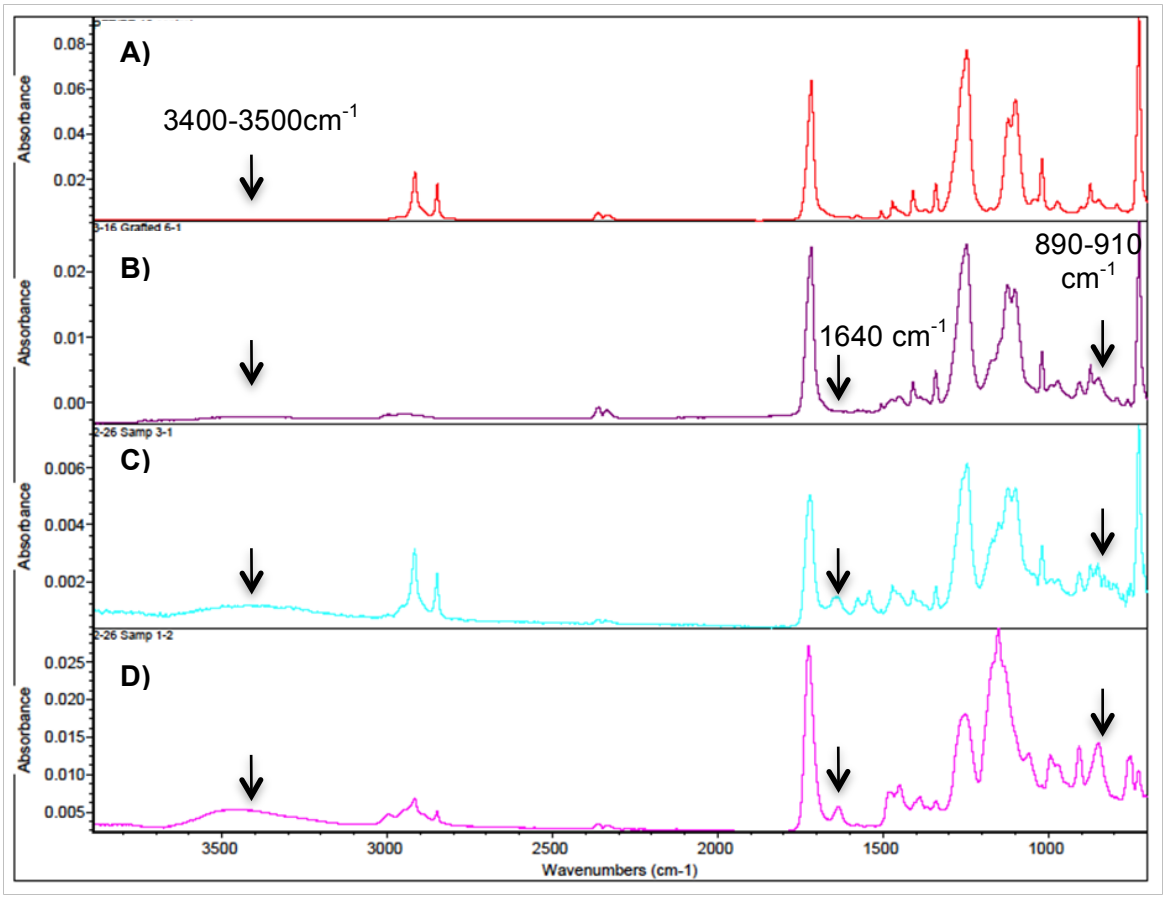

Figure 5.7. FTIR spectra of a) PET/PE Control b) 44.4% GP after 10 mins grafting C) 53.5% Grafting after 20 mins and D) 36% after 30 mins grafting

The absorption bands at 890-910 cm^{-1} represents the epoxy ring vibrations of the GMA monomers [7], [28]. This indicates that GMA has covalently bonded to the PET polymers and the epoxy ring remained intact. The absorption band at 3400-3500 cm^{-1} is assigned to –OH stretching [28]. This indicates that some epoxy rings may have opened during the grafting reactions. These –OH groups could possibly be reactive to functional groups. In C and B the absorption band at 1640 cm^{-1} is present. The band is assigned to

carbon double bond stretching (C=C) from the GMA monomer. This indicates that some GMA monomers have not covalently bonded to the PET backbone through this carbon double bond. It is likely that these are present due to homopolymer remaining on the surface or some monomers have grafted via the epoxy ring.

5.4.6 TOF-SIMS

TOF-SIMS was used to investigate the grafting behavior of the PET/PE bicomponent nonwovens. Looking for unique peaks in the TOF-SIMS spectra of the grafted bicomponent nonwovens compared to the control bicomponent nonwovens can provide information on the grafting mechanisms in the bicomponent samples with the added PE component, Figure 5.8.

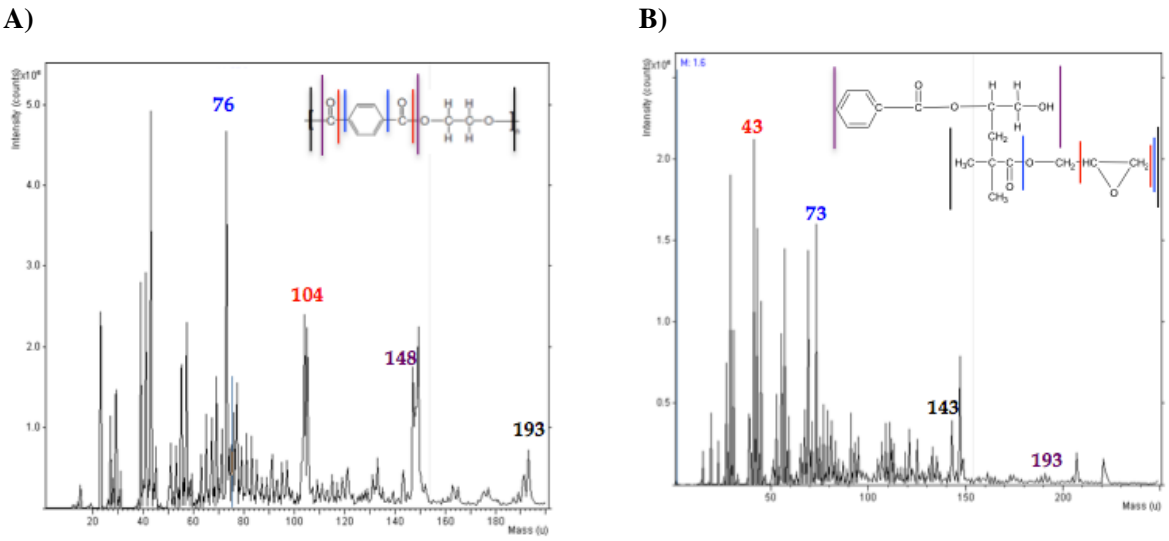

Figure 5.8. TOF-SIMS spectra of A)PET/PE Control and B) 53% Grafted PET/PE bicomponent nonwoven

The identifying peaks of PET dominate the spectrum of the PET/PE control sample. The peak at 76 is assigned to the aromatic ring of the PET backbone. Since this is unique to PET, it will be used as the marker for the PET fibers in the spectra of the samples as well as

the surface images. Peak 104 and 148 are also strong peaks, which are assigned to different segments of the PET backbone. 193 is the weight of the entire PET repeat unit. Comparing the spectrum of the control sample, A, to the spectrum of the grafted PET/PE sample, Figure 5.8B, it is possible to recognize unique peaks and assign them to the GMA monomer.

The peak at 73 is unique to the bicomponent spectrum. It is assigned to the "tail" end of the GMA monomer grafted to the PET backbone. Although both spectra contain a strong peak at 43, the PET peaks identified in the control samples, A, are not present in the bicomponent spectrum, Figure 5.8B. The absence of these identifying peaks indicates the surface of the grafted sample is likely dominated by grafted GMA monomers and the PET fragments cannot be detected. Therefore, the peak at 43 in the grafted sample is most likely due to the epoxy ring of the GMA monomer and not a fragment of the PET backbone. This can be confirmed by looking at the surface images of the samples and how they relate to the spectra.

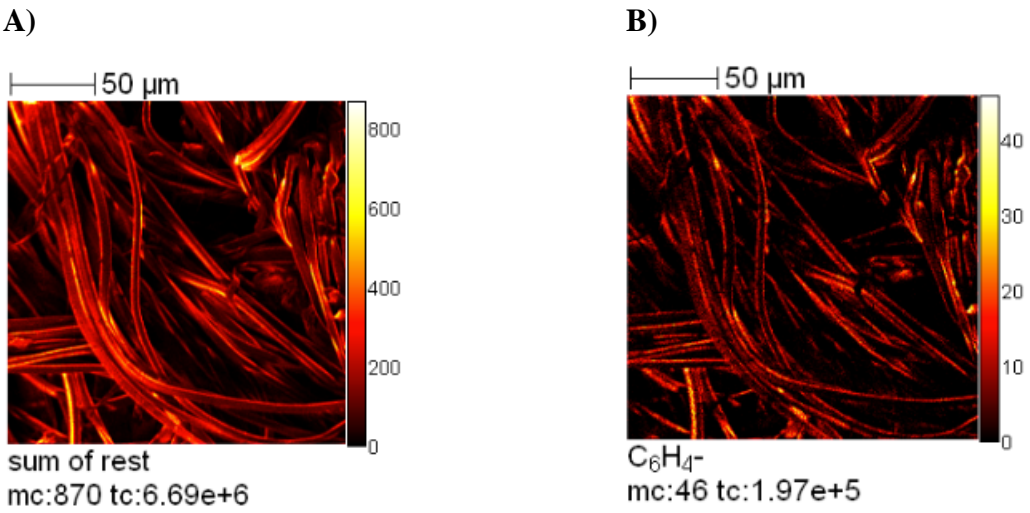

Figure 5.9. TOF-SIMS surface images of the PET/PE Control sample a) total ion, b) Benzene ring of PET

Figure 5.9 shows the TOF SIMS surface images of the PET/PE Control sample. The bar on the right of each image shows the ion count as it is represented by the intensity of the color. A is the total ion count of the PET/PE 16 segment control sample. The fiber structures are clearly defined in this image. B is 76 and assigned to C_6H_4 aromatic ring in the PET structure. Since this fragment is unique to PET it will be used as a marker for identifying PET in the grafted and sulfonated samples. In these images it is difficult to identify the PE component other than the negative strips that occur over the PET fibers in Figu

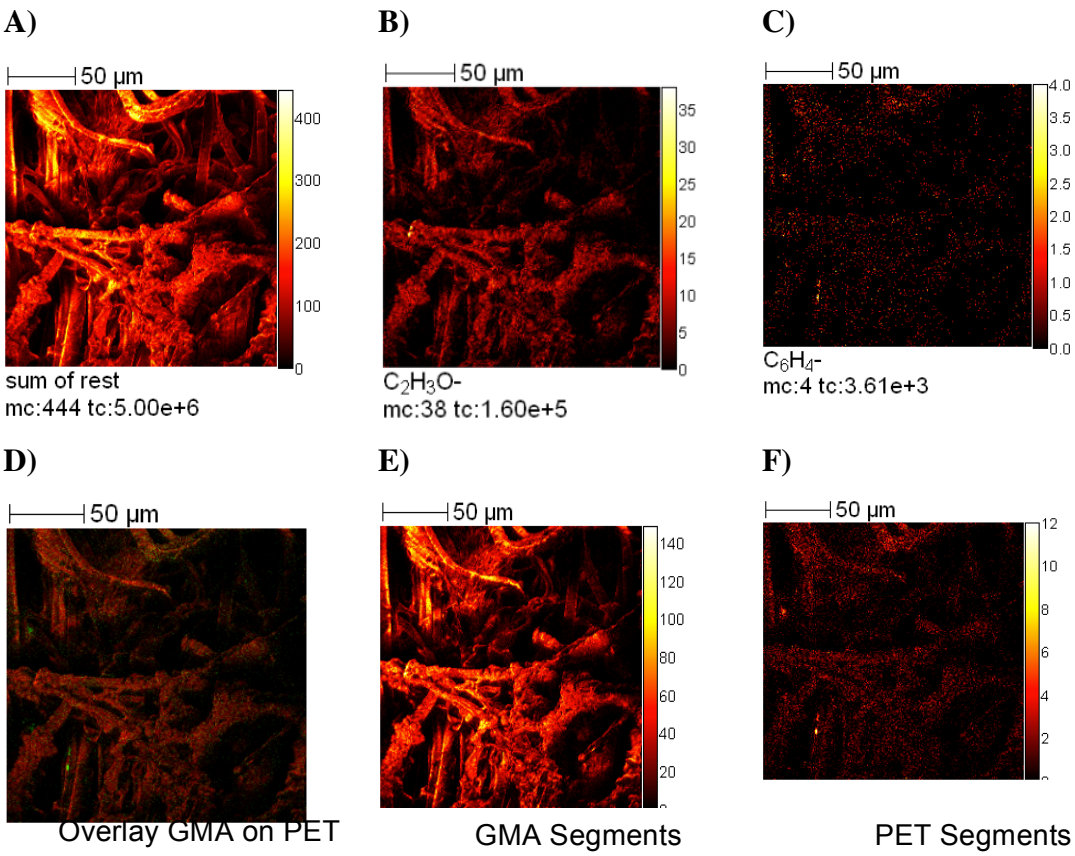

Figure 5.10 TOF-SIMS images of 53% Grafted PET/PE sample of A) TOTAl image b)Epoxy Rings c) PET aromatic ring d) Combined GMA Overlayed on Combined PET Image e) Combined GMA segments and f) Combined PET segments

Figure 5.10 shows the TOF-SIMS surface images of a PET/PE segmented pie nonwoven with 53% grafting. The epoxy ring, C_2H_3O, is the unique feature of the grafted GMA monomer, therefore the peak at 43 is used as the marker to identify GMA. B represents the epoxy peak of the grafted GMA monomers. Comparing the image of the epoxy rings to the total ion count, A, it is evident that the surface of the fibers is dominated by GMA monomers. C represents the aromatic ring of the PET polymers, the unique marker of PET. The aromatic ring count is very low compared to the epoxy ring count, indicating that the surface of the PET is nearly covered with GMA monomers. These two identifiers were used to piece together the other images extracted from the TOF-SIMS surface analysis.

Figure 5.10 E represents peak 149, the combined fragments of the GMA monomer, while F represents peak 193, the combined fragments of the PET main chain. The image of the combined PET fragments is the opposing image of the GMA combined fragments; the areas where GMA is not grafted to the surface can be seen in the small red areas of the PET combined image. To emphasize the large level of GMA present on the surface of the PET fibers, the combined GMA image is overlain on the combined PET image, represented by D. In this image, the red areas are the epoxy containing GMA monomers, while the green area is the PET fiber surface. The green PET fiber areas are nearly nonexistent, indicating that GMA is nearly covering the entire surface of the fibers. Most importantly, the epoxy ring ion intensity in B is very strong, indicating that many epoxy rings are present and available for functionalization.

5.5 Conclusion

PET homocomponent and 80/20 PET/PE 16 segmented pie nonwovens were grafted. The grafting behaviors of the two materials were compared and related to the difference in web structure. It was found that the grafting percentage can be maximized by using an ideal ratio of GMA monomer to CAN initiator, 6 wt% GMA and 4 mM CAN. At this concentration the reaction occurs rapidly; the maximum grafting percentage was reached by 10 minutes. The high surface area of the PET/PE bicomponent nonwoven leads to higher grafting percentages

compared to the PET homocomponent nonwoven. The presence of epoxy groups was confirmed using FTIR and TOF-SIMS. The FTIR spectrum had strong peaks at 890-910 cm^{-1} that was assigned to the presence of epoxy groups from the grafted GMA monomers. TOF-SIMS was used to further confirm the presence of epoxy groups and the grafting of the GMA monomers via the carbon-carbon double bond rather than the epoxy ring. Understanding the grafting behaviors of these materials based on their web structure will be important for functionalization.

5.6 References

[1] N. Somanathan, B. Balasubramaniam, and V. Subramaniam, "Grafting of Polyester Fibers," *J. Macromol. Sci. Part*, vol. 32, no. 5, pp. 1025–1036, May 1995.

[2] M. K. Mishra, B. L. Sar, and A. K. Tripathy, "Potassium Bromate-Thiourea Redox Initiated Grafting of Methyl Methacrylate onto Polyethylene Terephthalate," *J. Macromol. Sci. Part - Chem.*, vol. 18, no. 4, pp. 565–573, Sep. 1982.

[3] A. K. Pradhan, N. C. Pati, and P. L. Nayak, "Grafting vinyl monomers onto polyester fibers. III. Graft copolymerization of methyl methacrylate onto poly(ethylene terephthalate) using potassium permanganate–oxalic acid redox system," *J. Appl. Polym. Sci.*, vol. 27, no. 6, pp. 2131–2138, Jun. 1982.

[4] R. Coşkun and S. Akdeniz, "Functinalization of poly(ethylene terephthalate) fibers by grafting of maleic acid/methacrylamide monomer mixture," *Fibers Polym.*, vol. 11, no. 8, pp. 1111–1118, Dec. 2010.

[5] D. Praschak, T. Bahners, and E. Schollmeyer, "Excimer UV lamp irradiation induced grafting on synthetic polymers," *Appl. Phys. Mater. Sci. Process.*, vol. 71, no. 5, pp. 577–581, Nov. 2000.

[6] S. L. Gao, R. Häßler, E. Mäder, T. Bahners, K. Opwis, and E. Schollmeyer, "Photochemical surface modification of PET by excimer UV lamp irradiation," *Appl. Phys. B*, vol. 81, no. 5, pp. 681–690, Aug. 2005.

[7] L. Yu, S. Zhang, W. Liu, X. Zhu, X. Chen, and X. Chen, "Improving the flame retardancy of PET fabric by photo-induced grafting," *Polym. Degrad. Stab.*, vol. 95, no. 9, pp. 1934–1942, Sep. 2010.

[8] F. Pazzagli and M. Pracella, "Reactive compatibilization of polyolefin/PET blends by melt grafting with glycidyl methacrylate," *Macromol. Symp.*, vol. 149, no. 1, pp. 225–230, Jan. 2000.

[9] M. Pracella and D. Chionna, "Reactive compatibilization of blends of PET and PP modified by GMA grafting," *Macromol. Symp.*, vol. 198, no. 1, pp. 161–172, August.

[10] N. Chansook and S. Kiatkamjornwong, "Ce(IV)-initiated graft polymerization of acrylic acid onto poly(ethylene terephthalate) fiber," *J. Appl. Polym. Sci.*, vol. 89, no. 7, pp. 1952–1958, Aug. 2003.

[11] Z. Ma, M. Kotaki, T. Yong, W. He, and S. Ramakrishna, "Surface engineering of electrospun polyethylene terephthalate (PET) nanofibers towards development of a new material for blood vessel engineering," *Biomaterials*, vol. 26, no. 15, pp. 2527–2536, May 2005.

[12] B. Gupta, N. Grover, and H. Singh, "Radiation grafting of acrylic acid onto poly(ethylene terephthalate) fabric," *J. Appl. Polym. Sci.*, vol. 112, no. 3, pp. 1199–1208, May 2009.

[13] K. C. Gupta and K. Khandekar, "Graft copolymerization of acrylamide onto cellulose in presence of comonomer using ceric ammonium nitrate as initiator," *J. Appl. Polym. Sci.*, vol. 101, no. 4, pp. 2546–2558, Aug. 2006.

[14] D. J. McDowall, B. S. Gupta, and V. T. Stannett, "Grafting of vinyl monomers to cellulose by ceric ion initiation," *Prog. Polym. Sci.*, vol. 10, no. 1, pp. 1–50, Jan. 1984.

[15] G. Mino and S. Kaizerman, "A new method for the preparation of graft copolymers. Polymerization initiated by ceric ion redox systems," *J. Polym. Sci.*, vol. 31, no. 122, pp. 242–243, Aug. 1958.

[16] T. Demappa and Mahadevaiah, "Polymerization of acrylonitrile initiated by cerium (IV)-oxalic acid redox system: A kinetic study," *J. Appl. Polym. Sci.*, vol. 108, no. 3, pp. 1667–1674, May 2008.

[17] N. Chansook and S. Kiatkamjornwong, "Ce(IV)-initiated graft polymerization of acrylic acid onto poly(ethylene terephthalate) fiber," *J. Appl. Polym. Sci.*, vol. 89, pp. 1952–1958, Aug. 2003.

[18] V. Sridharan and J. C. Menéndez, "Cerium(IV) Ammonium Nitrate as a Catalyst in Organic Synthesis," *Chem. Rev.*, vol. 110, no. 6, pp. 3805–3849, Jun. 2010.

[19] V. S. Ananthanarayanan and M. Santappa, "Kinetics of vinyl polymerization initiated by ceric ion in aqueous solution," *J. Appl. Polym. Sci.*, vol. 9, no. 7, pp. 2437–2449, Jul. 1965.

[20] I. Casinos, "Mechanisms for the radical graft polymerization of vinyl and/or acrylic monomers on cellulose," *Polymer*, vol. 35, no. 3, pp. 606–615, Feb. 1994.

[21] I. Casinos, "Role of ceric ion in the heterogeneous graft polymerization of olefins on cellulose," *Polymer*, vol. 33, no. 6, pp. 1304–1315, Jan. 1992.

[22] G. Odian and J. H. T. Kho, "Ceric Ion Initiated Graft Polymerization onto Poly(vinyl Alcohol)," *J. Macromol. Sci. Part - Chem.*, vol. 4, no. 2, pp. 317–330, Mar. 1970.

[23] S. Haworth and J. R. Holker, "Oxidation of Some 2,4-Dinitrophenylamines with Ceric Salts," *Nature*, vol. 208, no. 5006, pp. 184–185, Oct. 1965.

[24] K. Sunaga, M. Kim, K. Saito, K. Sugita, and T. Sugo, "Characteristics of Porous Anion-Exchange Membranes Prepared by Cografting of Glycidyl Methacrylate with Divinylbenzene," *Chem. Mater.*, vol. 11, no. 8, pp. 1986–1989, Aug. 1999.

[25] Y. Zheng, H. Liu, P. V. Gurgel, and R. G. Carbonell, "Polypropylene nonwoven fabrics with conformal grafting of poly(glycidyl methacrylate) for bioseparations," *J. Membr. Sci.*, vol. 364, no. 1–2, pp. 362–371, Nov. 2010.

[26] F. Pazzagli and M. Pracella, "Reactive compatibilization of polyolefin/PET blends by melt grafting with glycidyl methacrylate," *Macromol. Symp.*, vol. 149, no. 1, pp. 225–230, Jan. 2000.

[27] S. Al-Malaika and E. Eddiyanto, "Reactive processing of polymers: Effect of bifunctional and tri-functional comonomers on melt grafting of glycidyl methacrylate onto polypropylene," *Polym. Degrad. Stab.*, vol. 95, no. 3, pp. 353–362, Mar. 2010.

[28] Y. V. Bondar, H. J. Kim, and Y. J. Lim, "Sulfonation of (glycidyl methacrylate) chains grafted onto nonwoven polypropylene fabric," *J. Appl. Polym. Sci.*, vol. 104, no. 5, pp. 3256–3260, Jun. 2007.

[29] N. Kwak, T. Hwang, S. Kim, Y. Yang, and K. Kang, "Synthesis of sulfonated PET-g-GMA fine ion-exchange fibers for water treatment by photopolymerization and their adsorption properties for metal ions," *Polym. Korea*, vol. 28, no. 5, pp. 397–403, Sep. 2004.

[30] The Dow Chemical, "Glycidyl Methacrylate - Product Information." .

[31] H. Kubota and S. Suzuki, "Comparative examinations of reactivity of grafted celluloses prepared by u.v.- and ceric salt-initiated graftings," *Eur. Polym. J.*, vol. 31, no. 8, pp. 701–704, Aug. 1995.

[32] C. Tyagi, L. K. Tomar, and H. Singh, "Surface modification of cellulose filter paper by glycidyl methacrylate grafting for biomolecule immobilization: Influence of grafting

parameters and urease immobilization," *J. Appl. Polym. Sci.*, vol. 111, no. 3, pp. 1381–1390, Feb. 2009.

[33] S. Li and J. Wei, "Evaluation of the influence of homopolymerization on the removal of water-insoluble organics by grafted polypropylene fibers," *Mar. Pollut. Bull.*, vol. 64, no. 6, pp. 1172–1176, Jun. 2012.

[34] D. M. Pinkerton and R. H. Stacewicz, "γ-Radiation-induced grafting of methyl methacrylate to polypropylene: The effects of water and mineral acid," *J. Polym. Sci. Polym. Lett. Ed.*, vol. 14, no. 5, pp. 287–291, May 1976.

Chapter 6

6 Functionalization of Grafted PET/PE Bicomponent Nonwovens

Abstract

Cation exchange nonwovens based on PET/PE bicomponent and PET homocomponent nonwovens were produced via grafting of epoxy containing glycidyl methacrylate monomers followed by sulfonation. The effect of the grafting conditions (monomer concentration, initiator concentration, time of the reaction) on the sulfonic acid group density was studied. It was found that low initiator concentration is necessary for achieving high sulfonate group densities. Due to its higher porosity, the homocomponent sample reached higher maximum sulfonate group densities than the bicomponent nonwovens, up to 4.5 meq/g. The high group densities occurred at low grafting percentages (>20%) indicating that high grafting percentage is likely the result of homopolymer formation during the grafting process. Conversion of the epoxy rings to sulfonate functional groups was confirmed with FTIR and uniform surface functionalization was observed using TOF-SIMS. Grafting of glycidyl methacrylate monomers via ceric ammonium nitrate initiation is a successful method of producing functionalized PET media.

6.1 Introduction

Polyethylene terephthalate, PET, is one of the most widely used and readily available material used in a multitude of applications. However, due to its hydrophobicity and lack of functional groups it is difficult to dye and can not be used for absorption applications[1]. Surface modification of polyethylene terephthalate (PET) is difficult due to its highly ordered structure and lack of reactive groups[1]. Achieving an efficient, cost effective method of surface modification of PET would have a profound impact on the functional fiber industry.

Ceric salts have been extensively studied as a method for initiating the grafting of vinyl monomers on cellulose [2], [3], [4], [5]. However, few studies have been done to investigate its effectiveness of grafting onto PET fibers [6]. The suggested reaction scheme for the interaction between cerium ammonium nitrate and PET to initiate grafting of GMA is seen in Figure **6.1**. Cerium ions act as strong oxidizers when in acidic solution. An electron transfer of a hydrogen atom occurs from the PET backbone to Ce(IV) to produce Ce(III). This hydrogen abstraction creates a radical on the PET which becomes the grafting site of the GMA monomer [7].

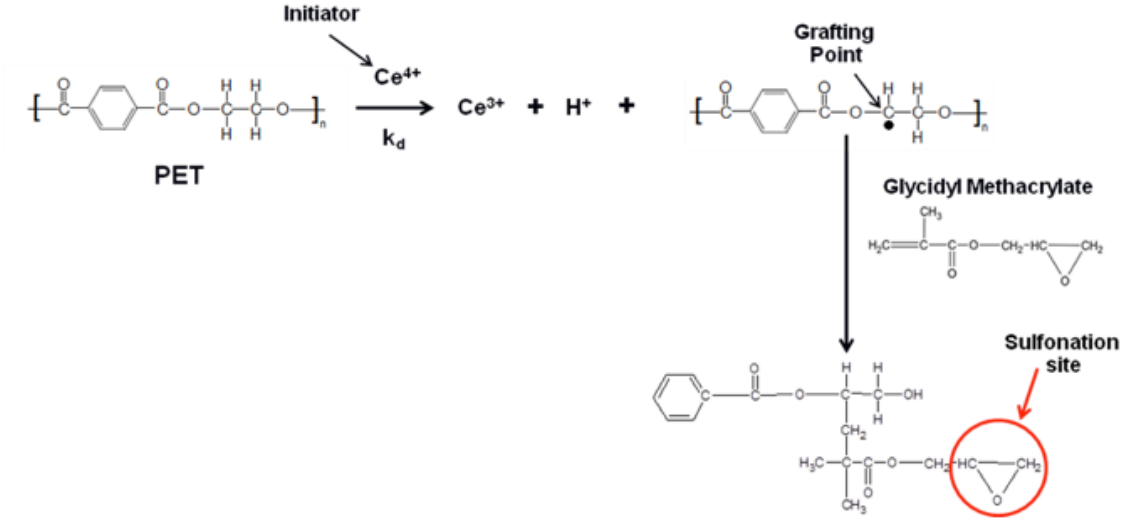

Figure 6.1. Suggested reactions scheme of the GMA grafting on PET initiated with cerium ion

The GMA grafted PET fibers are functionalized via sulfonation reactions. This is a process by which sulfonate, $-SO_3^-$, groups are attached to the epoxy groups of the GMA through a substitution reaction, producing strongly cationic exchange fibers. Strong acid cations can dissociate in both alkaline and acidic solutions, making them very versatile in the solutions in which they can be used and typically have a higher ion exchange capacity then

weak acid cation exchange materials. Therefore, strong acid cation exchangers are the most widely used in industry [8].

Compounds such as sulfuric acid, sodium sulfite, sulfates, and variations of complexes have been used as the sulfonating agents[9]. Currently there are no known continuous functionalization processes. Therefore, all chemical processes are done in batch type operations in a reaction kettle with the sulfonating agents and materials[10].

Sulfonation substitution reactions of GMA epoxy groups have been extensively studied [11], [12], [13], [14], [15], [16]. The suggested reaction between the GMA grafted PET fibers and sodium sulfite is seen in Figure **6.2**.

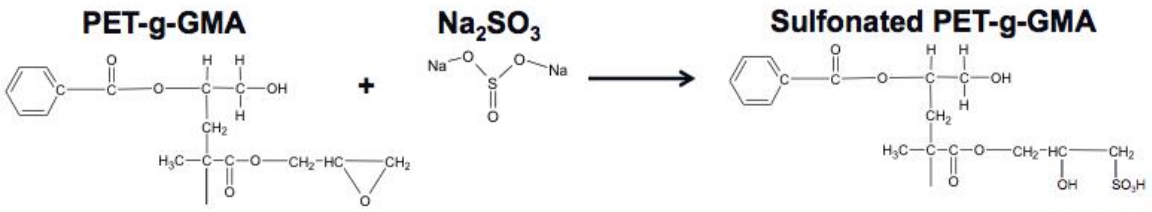

Figure 6.2. Suggested reaction scheme for sulfonation of GMA grafted PET with sodium sulfite as the sufonating agent

6.2 Experimental Procedure

6.2.1 Materials

For all of the following experiments, nonwovens composed of 80/20 PET/PE 16 segmented pie bicomponent fibers and a PET homocomponent were used, **Table 6.1**. The materials had a basis weight of 100 grams/meter^2 and were passed through the hydroentangling machine for one pass at 750 psi. These materials were made in the Pilot

Plant of the Nonwoven's Institute. The PET/PE bicomponent fiber was fractured in the Jet Dyeing Machine for 120 minutes to achieve 100% fracture of the bicomponent fibers.

Table 6.1. Characteristics of nonwoven used for the experiments

Polymer	**Ratio**	**Segments**	**Basis Weight (gsm)**	**Hydros**	**Fractured Time (mins)**
PET	Homocomponent	1	100	1 (750 psi)	0
PET/PE	80/20	16	100	1 (750 psi)	90

For all of the grafting procedures, hydroquinone is removed from Glycidyl Methacrylate, GMA, prior to all experiments using an inhibitor remover column obtained from Sigma Aldrich. All other chemicals are used as received.

Table 6.2. List of the chemicals and solutions used for all grafting procedures

Solution	Acronym	Company	Purpose
Ceric Salt Grafting Solution			
Glycidyl Methacrylate	GMA	Sigma Aldrich	Epoxy containing monomer
Ceric Ammonium Nitrate	CAN	Fisher Scientific	Grafting Initiator
Nitric Acid	NHO_3	Fisher Scientific	Grafting Acid
Methanol	CH_3OH	Sigma Aldrich	Washing Solvent
Sulfonation Reaction Solution			
Sodium Sulfite (anhydrous)	Na_2SO_3	Fisher Scientific	Sulfonation
Isopropyl Alcohol	IPA	Sigma Aldrich	Sulfonation Solvent
Protonation Solution			
Sulfuric Acid	H_2SO_4	Sigma Aldrich	Protonation

6.2.2 Grafting of PET Fibers

The nonwoven samples were cut into 8x8 inch samples, washed in acetone for 24 hours, and dried completely before weighing. The grafting initiator, CAN, was dissolved in 100 mL of Nitric Acid, HNO_3. Distilled water was added to a 500 mL round bottom flask to bring the total solution volume to 400 mL and flushed with nitrogen for 5 minutes. The CAN/HNO_3 solution, sample, and stirring rod were then added to the flask. The flask was lowered into a mineral oil bath at 60 ºC and the solution was flushed with nitrogen for 15 minutes. The GMA monomer was then added to the flask to begin the reaction. Reaction

times ranged from 10-30 minutes. The concentrations of GMA and CAN are found in **Table 6.3**.

Table 6.3. Concentrations of Grafting solutions

GMA Concentration (wt%)			**CAN Concentration**		
2	4	6	2	4	6

After the specified reaction time the PET-g-GMA samples are washed in methanol on a mechanical shaker at 60 ºC for 4 hours, then washed for 3 hours in methanol with a probe sonicator. The samples were rinsed in DI water and dried until a constant weight was achieved.

6.2.3 Functionalization of PET Fiber Via Sulfonation

The grafted PET and PET/PE nonwovens (PET-g-GMA) are sulfonated at 70 ºC on a mechanical shaker in a 10/15/75 weight percent solution of Sodium Sulfite/ Isopropyl Alcohol/ Distilled Water for 4 hours. The samples are then repeatedly washed in DI Water at 70 ºC on a mechanical shaker until the conductivity of the wash water reaches that of DI water and dried completely at 80 ºC.

The sulfonated samples are then protonated (put in the hydrogen form) in 400 mL of 0.5 M H_2SO_4 on a mechanical shaker at 70 ºC for 2 hours. The samples are removed, rinsed in cold DI water until neutral pH, and dried at 80 ºC until a constant weight is achieved.

6.3 Analytical Technique

Several analytical techniques were used to monitor the reactions. No analytical technique is perfect and all are used together to get an overall idea of the effects of the grafting and functionalization.

6.3.1 Grafting Percentage

The grafting efficiency of the monomer on the fibrous substrates is reported as a function of the weight increase of the sample, Equation).

$$GP(\%) = \frac{W_g - W}{W} \times 100\% \qquad \textbf{(6.1)}$$

where W is the weight of the sample before grafting and W_g is the weight after grafting.

The major problem experienced with graft polymerization reactions is in the formation of homopolymer that adheres to the grafting substrate. This homopolymer is a product of the monomers reacting with each other rather than the grafting substrate[17], [18]. Therefore, the grafting percentage value includes grafting monomer as well as any remaining homopolymer.

6.3.2 Percent Sulfonation

The percent sulfonation is typically reported in the literature as a means of monitoring the sulfonation reaction [14], [19], [20]. However, negative values for the percent sulfonation were calculated because of a decrease in the weight of the sample after sulfonation. This decrease in weight is likely due to homopolymer washing off the samples in the sulfonation solution. Because of this decrease, the percent sulfonation cannot be reported. Instead, the total weight gain of the sulfonated samples will be used as a method of monitoring the sulfonic acid group addition. The Total Weight Gain is based on the weight of the entire grafted GMA monomer with the sulfonic acid functional group, Equation ,

$$S_{SO_3H} = \frac{W_{H+} - W_0}{W_{H+} \bullet M_{GMA+SO_3H}} x1000 \qquad \textbf{(6.2)}$$

where W_{H+} is the weight of the sulfonated sample in the hydrogen form, W_0 is the original weight of the sample, and $M_{GMA+SO3H}$ is the molecular weight of the grafted GMA monomer with one sulfonic acid group attached, 223 g/mol.

6.3.3 FTIR

The change in the surface chemistry of the samples after grafting was monitored with FTIR. The Thermo Electron FTIR with a Nexus 470 bench in the Analytical Lab of the

College of Textiles of NCSU was used for the analysis. 64 scans were done of each sample at a resolution of 4.

6.3.4 TOF-SIMS

The TOF-SIMS analysis was done in the Analytical Instrumentation Facility at NCSU with an ion TOF-SIMS 5 machine. 124 scans were done for each sample at a resolution of 50 nm.

6.3.5 Back Titration for Ion Exchange Capacity

The sulfonated samples in the proton form were equilibrated in 100 mL of .05 M sodium hydroxide (NaOH) for 24 hours. The samples were removed, washed in DI water until neutral pH and dried completely at 80 ºC. 10 mL aliquots of NaOH were titrated to the phenolphthalein end point with .1M hydrochloric acid (HCl). Three repetitions were done of each sample. The titration schematic is as follows:

x SO_3H^+ + 10 NaOH = x SO_3Na^+ + (10-x) NaOH +x H_2O

(10-x) NaOH + y HCl = y H_2O + y NaCl

where x is the mmols of SO_3H^+ functional groups on the sample and y is the mmols of HCl added to the unknown concentration of NaOH to change the phenolphthalein indicator from pink to clear. The mmols of functional groups (x) on the sample is calculated as the difference of the mmols of NaOH and the mmols of HCL (y) needed to neutralize it:

$$x=10-y \qquad \textbf{(6.3)}$$

The ion exchange capacity (IEC) of the material is calculated as:

$$IEC(meq/g)=\frac{(.05\times x)}{W_{S_{H+}}}\times 1000 \qquad \textbf{(6.4)}$$

where .05 is the molarity of the NaOH and $W_{S_{H+}}$ is the weight (grams) of the sulfonated sample in the hydrogen form.

6.4 Functionalization of PET Fibers

The homocomponent and bicomponent samples were grafted via ceric salt initiation with varying monomer and initiator concentrations and at varying times. The grafted (PET/PE)-g-GMA samples were then sulfonated for 4 hours in a 10/15/75 Sodium Sulfite/IPA/H_2O solution. The sulfonated samples were then put in the proton form by equilibration in a .1M Sulfuric Acid solution for 2 hours. The functionalized nonwoven materials were dried in an oven at 80 °C for 2 hours and weighed to achieve the sulfonated weight.

6.4.1 Weight Gain

The sulfonated weight was compared to the grafted weights of the samples, Figure **6.3**.

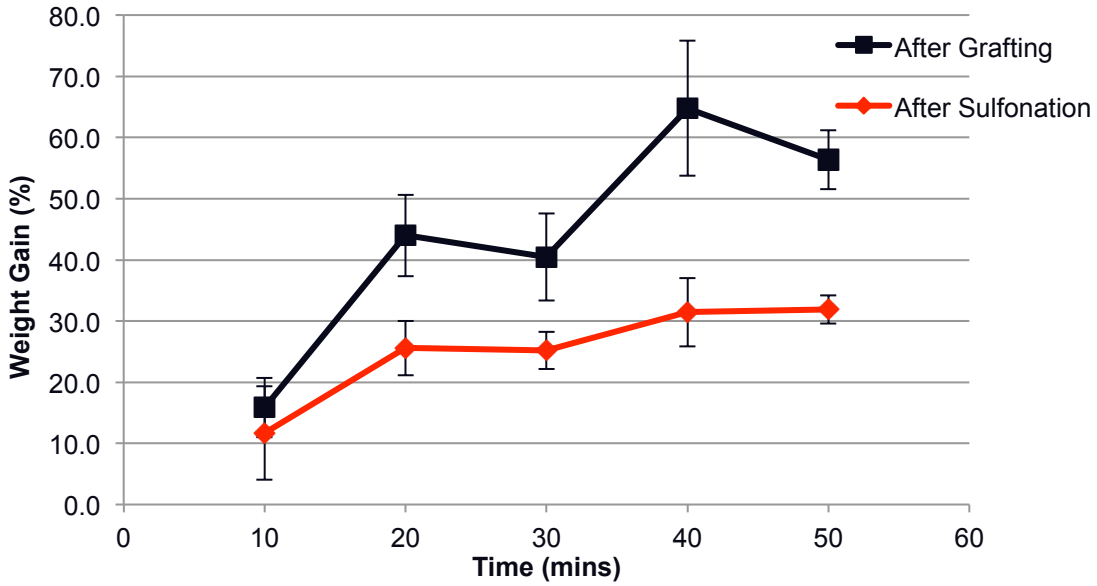

Figure 6.3. Changes in weight gain of samples after grafting (4 wt% GMA and 4 mM CAN) and after sulfonation

During the sulfonation procedure, the epoxy ring of the GMA monomer is opened and a large sulfonate functional group is added. Therefore, an increase in the weight of the samples after sulfonation is expected. However, the sulfonation procedure resulted in a decrease in the weight of the grafted samples. It is likely the result of a large level of homopolymer remaining in the web structure after grafting that is washed out during sulfonation. The decrease in the weight of the sample is higher at longer grafting times, 40 - 50 minutes. It is highly likely that these long grafting times result in higher homopolymer formation and thus more homopolymer is washed out during sulfonation. The competing reaction of homopolymerizatin of the GMA monomers is a well-known issue with most grafting procedures, including UV and gamma irradiation techniques as well as bulk chemical solution [2], [6], [21], [22].

Because of this behavior, the grafted and sulfonated weights will be considered only as a way of monitoring the reactions and will not be used as a way of defining the extent of the functionalization reaction. Other analytical techniques should be used along with weight gain to better understand this process. The grafting of the GMA monomers is an intermediate step to producing functionalized nonwovens. Although it would be relevant to monitor the conversion efficiency of the epoxy groups to sulfonic acid groups, it is difficult to do with homopolymer removal occurring during the sulfonation process. The final weight gain of the sulfonated samples will be used to monitor the efficiency of the entire functionalization process.

6.4.2 FTIR

To confirm the presence of sulfonic acid groups FTIR was used to detect changes in the spectrum of the grafted sample, Figure 6.4.

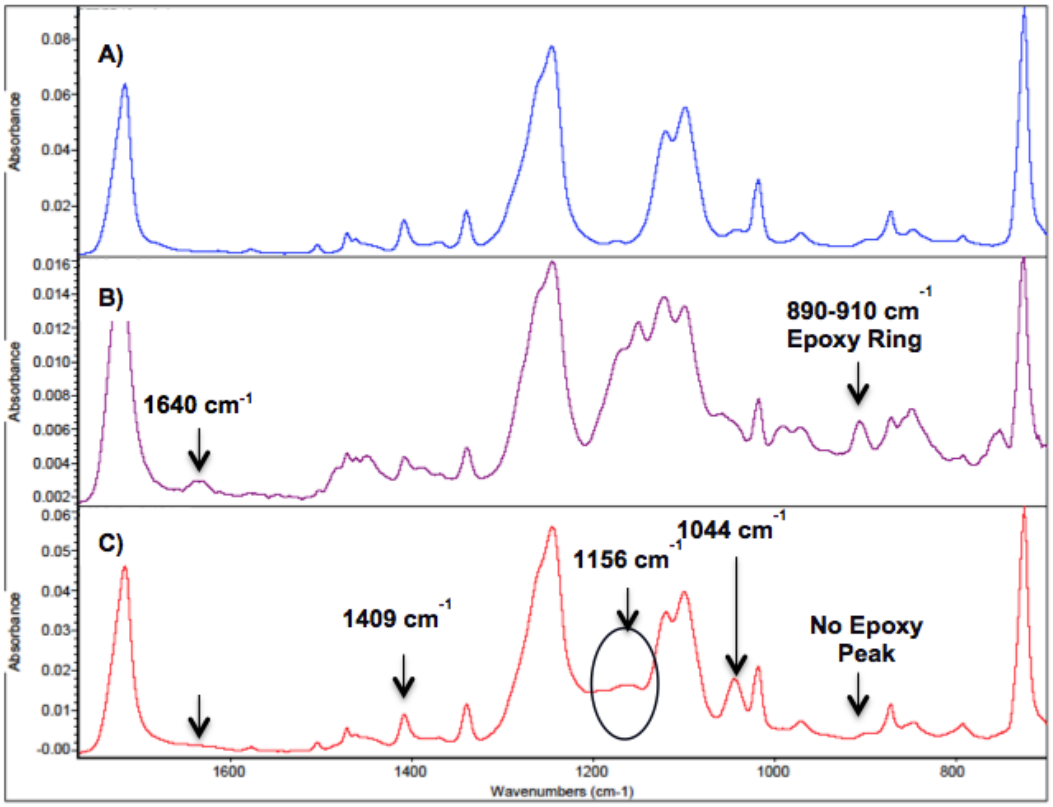

Figure 6.4 FTIR of the a) PET/PE Control B) 48% Grafting PErcentage and c) 12% WEight Gain sulfonated sample

The characteristic absorption bands at 890-910 cm^{-1} represent the epoxy ring vibrations of the GMA monomers [14], [23] and are evident in the spectrum of B. This indicates that GMA has covalently bonded to the PET polymers and the epoxy ring has remained intact. The epoxy ring absorption band is not present in the sulfonated sample C, indicating that the epoxy rings have been converted to sulfonic acid groups. The peaks at 1044 and 1409 cm^{-1} have been assigned to the SO_3 asymmetric and symmetric bending, respectively [44], [39]. The peak at 1156 cm^{-1} represents SO_3 bending. [44]

In spectrum B the absorption band at 1640 cm^{-1} had been assigned to carbon double bond stretching (C=C) from the GMA monomer on the grafted sample. It is hypothesized that this band is due to homopolymer on the surface or some monomers that have grafted at the epoxy ring. This band is not found in spectrum C of the sulfonated sample, indicating that the homopolymer has likely been removed during the sulfonation process.

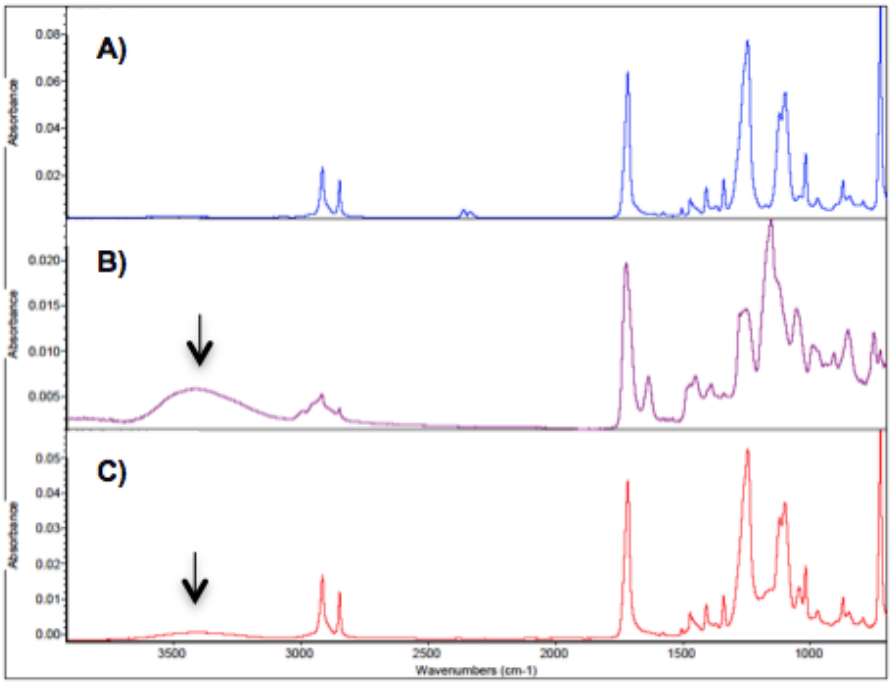

Figure 6.5. FTIR of the a) PET/PE Control B) 48% Grafting PErcentage and c) 12% WEight Gain sulfonated sample

The absorption band at 3400-3500 cm^{-1} is assigned to –OH stretching [14]. This large peak in spectrum B of the grafted PET/PE sample indicates that some epoxy rings may have opened during the grafting reactions. The large decrease in the size of the peak in spectrum C

of the sulfonated sample indicates that these –OH groups were reactive to the sulfonic acid groups during the functionalization reaction.

6.4.3 TOF-SIMS

An 80/20 PET/PE 16 segmented pie nonwoven was grafted and sulfonated. The grafted sample had a weight gain of 35%, while the final weight gain of the sulfonated sample was 19%. The distinguishing peaks of the sulfonated sample are identified in, Figure **6.6**.

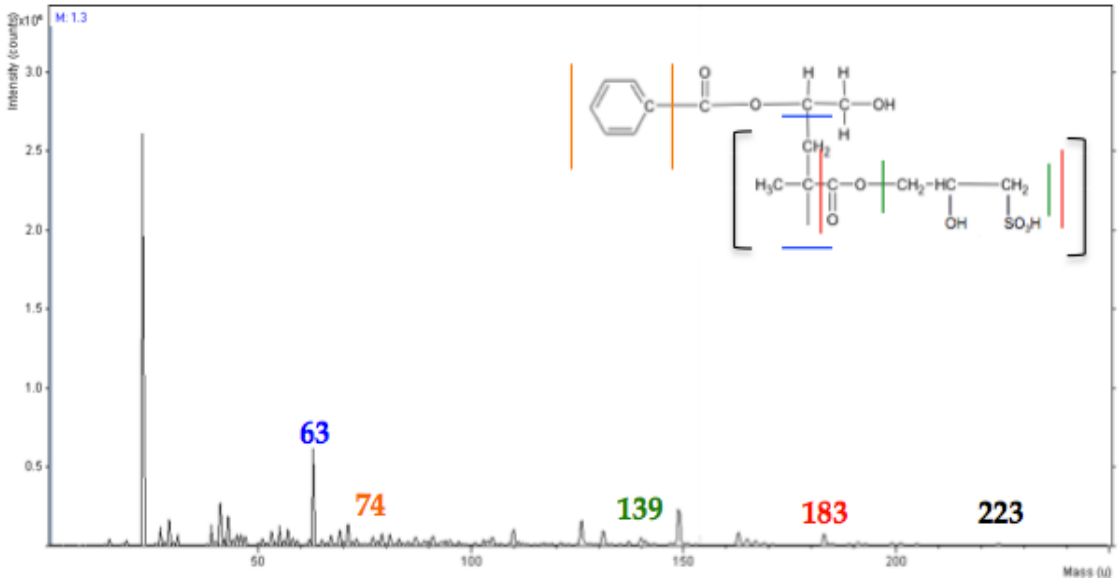

Figure 6.6. TOF-SIMS spectra of a functionalized pet/pe bicomponent sample with a final weight gain of 19%

The spectrum of the functionalized PET/PE bicomponent nonwoven contains distinctly different peaks than the grafted PET/PE sample. The peak at 63 is assigned to the GMA monomer graft chains. It is likely that the image associated with the 63 peak, and its

fragment segments, are due to the section of the chain that is grafting to the PET backbone. Peaks 139 and 183 are both fragments of the GMA monomer containing a sulfonic acid group. The peak at 223 represents the entire GMA monomer with a functional sulfonic acid group. The peak at 74 had been previously assigned to the aromatic ring of the PET repeat unit. The peaks at 74 and 193 both have very low intensity, indicating that the surface of the fibers is dominated by the grafted GMA and functional groups. This can be confirmed by investigating the surface images of the functionalized sample.

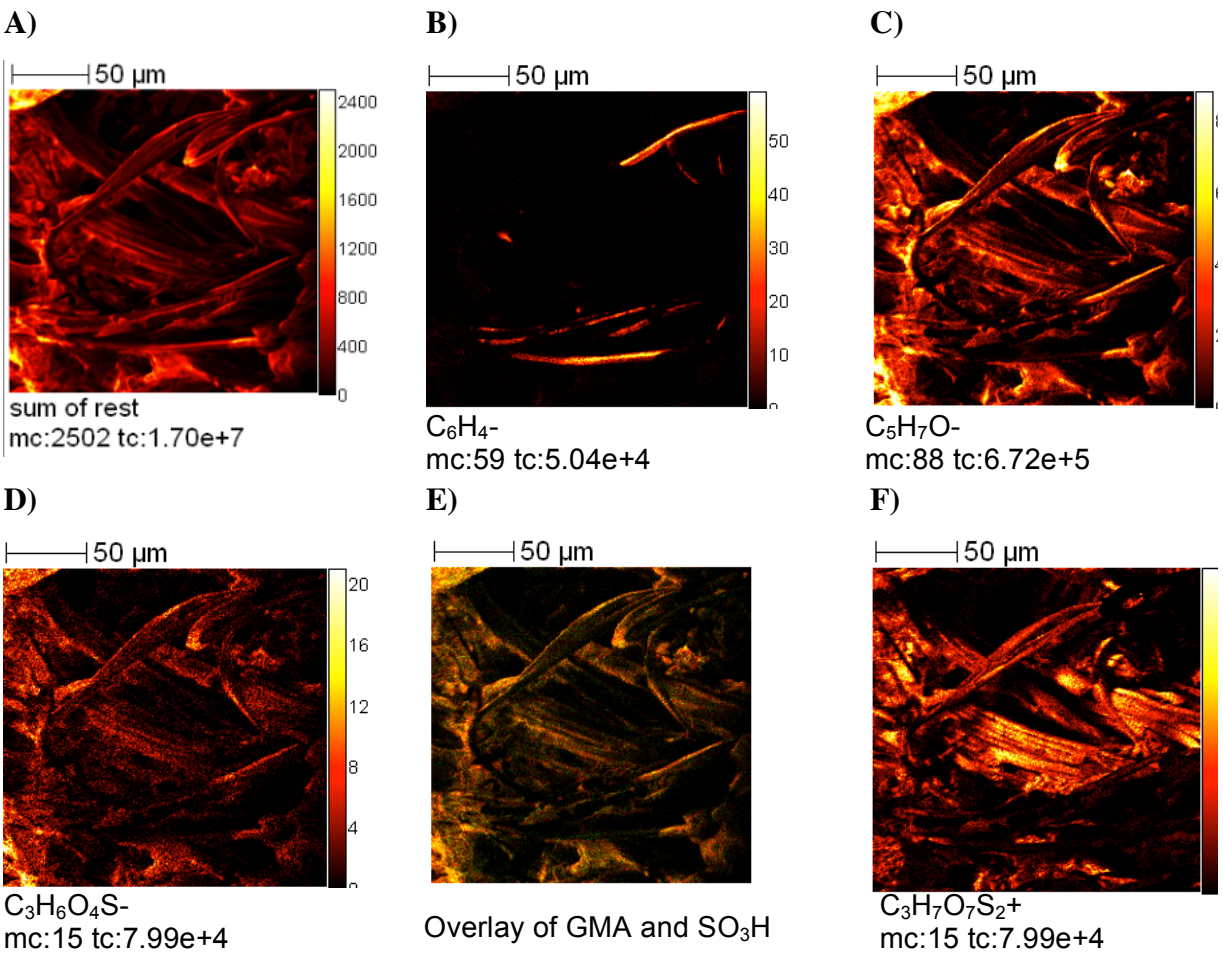

Figure 6.7. TOF-SIMS surface images of PET/PE sulfonated sample with 19% Weight gain A) Total Ion Image B) aromatic ring of PET C) GMA backbone D) GMA with Sulfonic Acid E) GMA backbone overlain on Sulfonic Acid and F) GMA repeat unit with two sulfonic Acid groups

The TOF-SIMS surface images of the 19% weight gain sulfonated sample are shown in Figure 6.7. The total ion image, Figure 6.7 A, clearly shows the fibers on the surface of the sample. Image B represents the aromatic benzene ring of PET, the unique marker used to identify the PET fibers. This appears to be the negative image of Image C, the GMA backbone indicating that uniform grafting has occurred along the surface of the PET fiber.

Image D shows the grafted GMA chains with the sulfonic acid groups attached to the epoxy ring.

Image E shows the overlain images of the GMA backbone and the GMA monomer with the sulfonic acid functional group attached. The red areas are just the GMA backbone, the green areas are only sulfonic acid groups, and the yellow areas are where the GMA and sulfonic acid monomers are both present. It is evident that the grafted GMA areas also contain sulfonic acid functional groups, indicating that conversion of the epoxy groups to functional groups has occurred. Image F represents a mass of 269. This is equivalent to the total weight of a GMA monomer with two sulfonic acid groups. The ion count of this image is quite high, suggesting that many of the GMA monomer epoxy rings have converted to two sulfonic acid groups, resulting in twice the functionalization per epoxy ring.

6.5 Total Ion Exchange Capacity Via Titration

The sulfonated samples were back titrated to calculate the ion exchange capacity of the functionalized samples. The samples in the proton form were equilibrated in sodium hydroxide, NaOH. The concentration of the NaOH was calculated by back titrating with hydrochloric acid, HCl, and the concentration was used to calculate the concentration of SO_3 groups per gram of material. The SO_3 group density was compared to the grafting percentage, Figure 6.8.

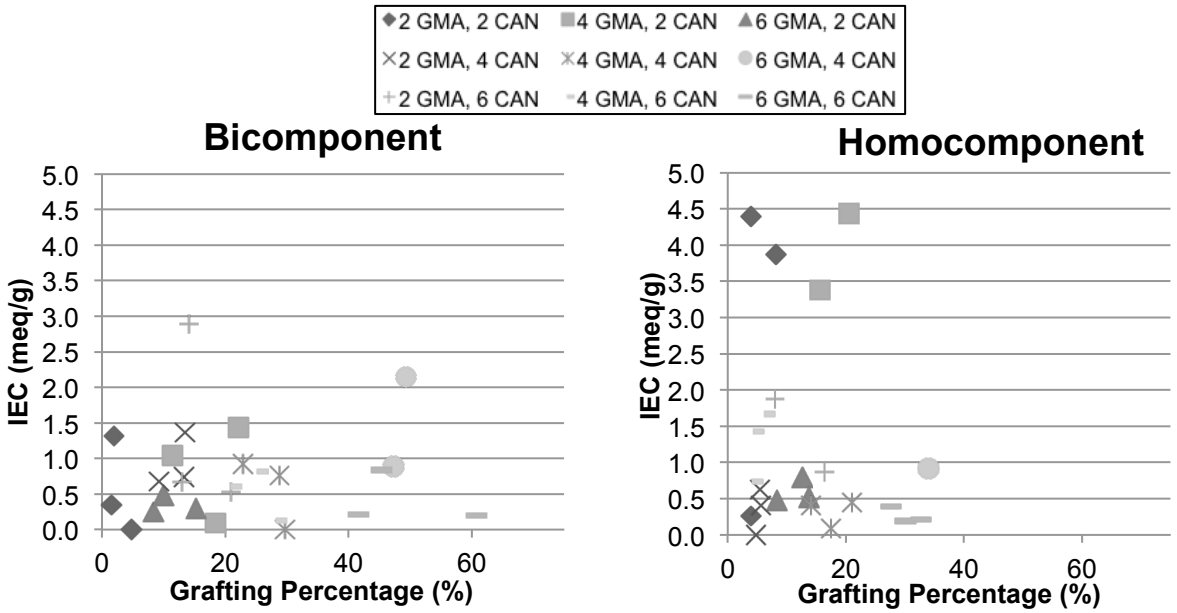

Figure 6.8. Ion exchange capacity of the A) Bicomponent and b) Homocomponent nonwovens at varying Grafting concentrations

The sulfonate group density of the bicomponent and homocomponent nonwovens is between 0.2- 4.5 meq/g. This range of capacities is comparable to commercially available ion exchange resins. There is not a strong relationship between the grafting percentage and the resulting ion exchange capacity; high grafting percentages do not result in high functionalization. This indicates that the high grafting percentages of the bicomponent nonwovens are likely the result of homopolymer that is trapped in the intricate web structure after grafting.

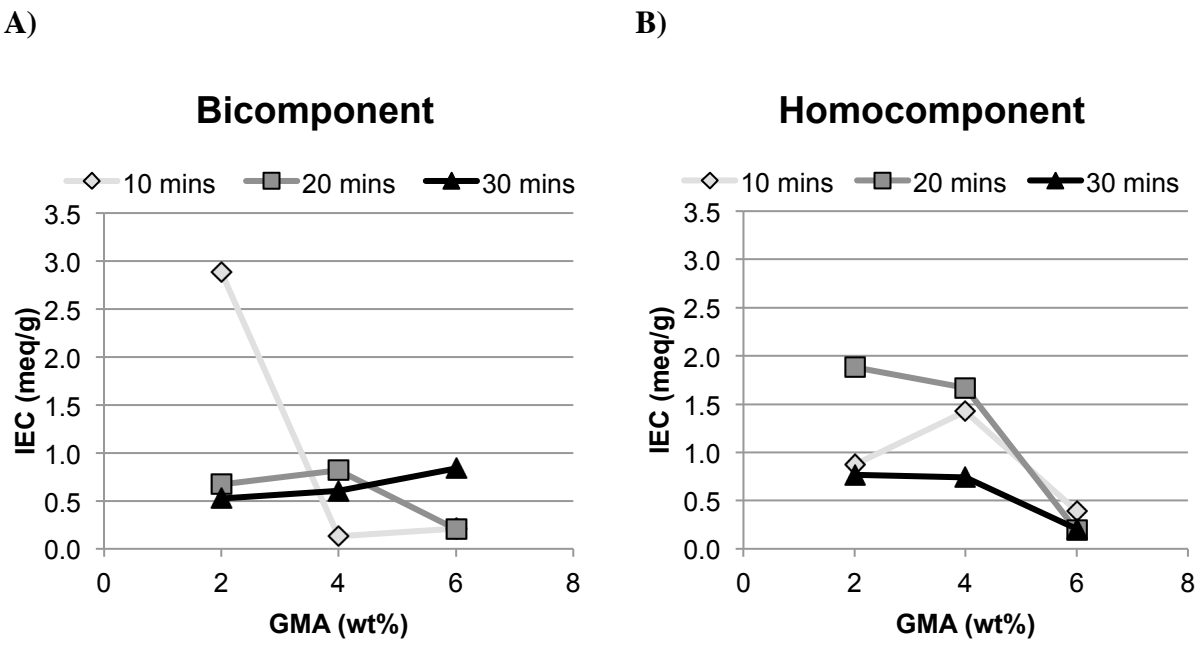

Figure 6.9. Effect of gMA concentration on IEC of A) Bicomponent and B) Homocomponent nonwovens at varying grafting times and 6 mm CAN

At high initiator concentration there is no significant difference between the bicomponent and homocomponent nonwovens. This was consistent at most of the grafting conditions except for the lowest monomer and initiator concentrations, Figure 6.10.

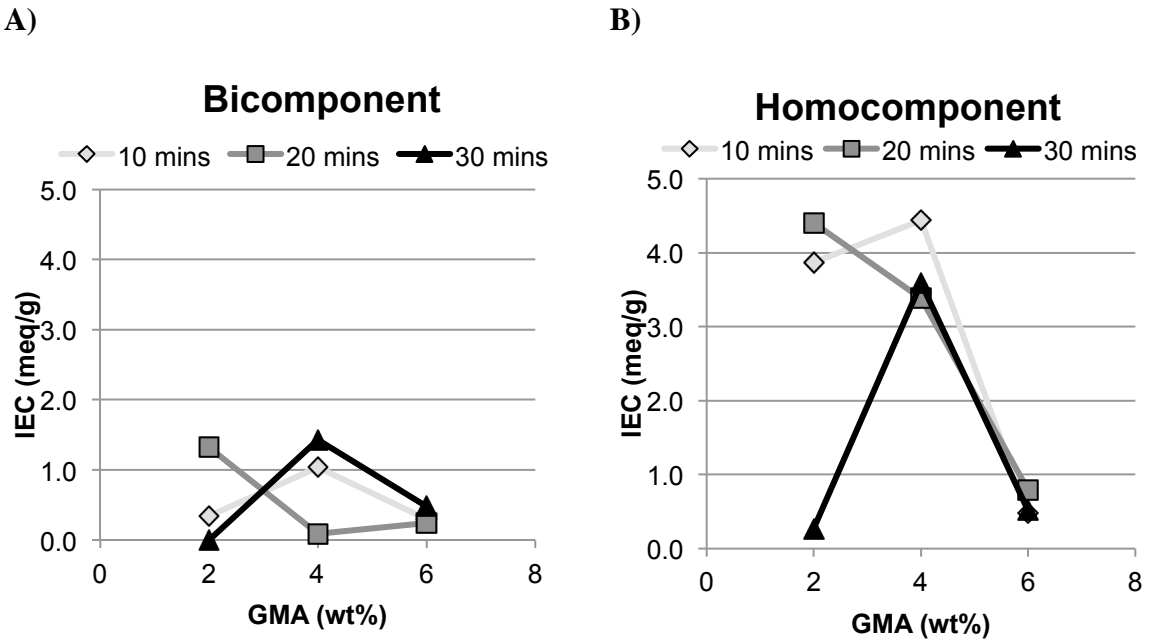

Figure 6.10. Effect of GMA monomer on the ion exchange capacity of the A) Bicomponent and B) Homocomponent nonwovens at initiator Concetration of 2 mM

At low initiator concentrations, both the homocomponent and bicomponent nonwovens reach a maximum capacity at 4 wt% GMA. There is a large decrease in the capacity of the samples at high monomer concentrations. The homocomponent nonwoven has a significantly higher sulfonate group density than the bicomponent samples at low monomer and initiator concentrations. These high capacities are also achieved at low grafting times of 10 and 20 minutes. Longer grafting times of 30 minutes are most likely leading to high homopolymer formation that does not allow for functionalization. It is possible to achieve high sulfonate group densities by grafting the homocomponent nonwoven with low initiator concentrations.

The discrepancy in capacities between the two materials is most likely due to morphological differences and not the different amount of PET fiber present. The capacities

can also be evaluated based on the amount of PET fiber, rather than the weight of the total sample, Figure 6.11.

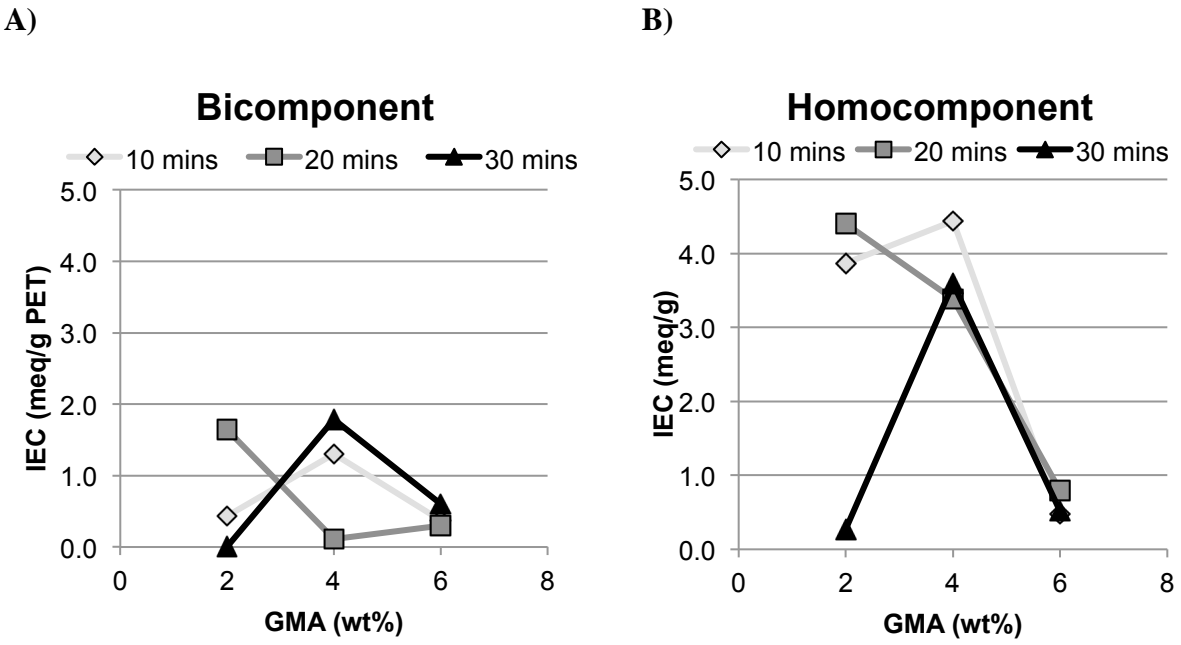

Figure 6.11. Effect of GMA monomer on ion exchange capacity in terms of weight oF PET in the A) Bicomponent and B) Homocomponent samples with 2 mm CAN

In the case of the bicomponent nonwoven, 20% of this material is PE fiber which is most likely not taking part in the functionalization reaction. There is only a 20% increase in the capacities of the bicomponent samples when the capacity is calculated based on the weight of the PET fibers in the structure. The homocomponent nonwoven still has a much higher capacity than the bicomponent nonwoven, indicating the difference is due to the web structure. Upon fracturing of the PET/PE bicomponent nonwoven, a large degree of web consolidation occurs, decreasing the porosity of the materials. The homocomponent web

maintains a much more open structure. The high porosity of the nonwoven allows the grafting solution to flow through the sample and does not restrict functionalization to the surface of the material.

6.6 Conclusion

PET/PE bicomponent and PET homocomponent nonwovens were grafted with Glycidyl methacrylate monomers followed by sulfonation to attached sulfonate functional groups. Grafting and functionalization were confirmed using FTIR, while the uniformity was evaluated with TOF-SIMS. The sulfonate group density was calculated via back titration.

Successful grafting of the GMA monomers on the PET fibers was confirmed using FTIR. It was also found that the epoxy rings of the GMA monomers were converted to sulfonate function groups, indicating that the fibers had been functionalized. Using TOF-SIMS it was evident that uniform grafting had occurred on the surface of the PET fibers, while the PE fibers of the bicomponent nonwoven were left ungrafted. High grafting percentages, up to 60% weight gain of the bicomponent nonwoven, were achieved. However, after doing back titration to calculate the sulfonate group density it was found that high grafting percentages did not result in high densities of sulfonate groups. At low initiator concentration and after 10 minutes of grafting time, the homocomponent samples reached up to 4.5 meq/g sulfonate group density.

The majority of the bicomponent and homocomponent samples reached a maximum equilibrium of about 1.5 meq/g. The leveling off of the sulfonate group density at these values indicates that the functionalization may be occurring primarily on the surface of the samples. The range of sulfonic acid group densities is comparable to the typical ion exchange capacities of commercially available ion exchange resins, making these materials possible competitors in the ion exchange field.

6.7 References

[1] N. Somanathan, B. Balasubramaniam, and V. Subramaniam, "Grafting of Polyester Fibers," *J. Macromol. Sci. Part*, vol. 32, no. 5, pp. 1025–1036, May 1995.

[2] J. Song, Y. Jin, G. Fu, A. He, and W. Fu, "A facile approach toward surface sulfonation of natural cotton fibers through epoxy reaction," *J. Appl. Polym. Sci.*, vol. 124, no. 2, pp. 1744–1750, Apr. 2012.

[3] K. C. Gupta and K. Khandekar, "Graft copolymerization of acrylamide onto cellulose in presence of comonomer using ceric ammonium nitrate as initiator," *J. Appl. Polym. Sci.*, vol. 101, no. 4, pp. 2546–2558, Aug. 2006.

[4] D. J. McDowall, B. S. Gupta, and V. T. Stannett, "Grafting of vinyl monomers to cellulose by ceric ion initiation," *Prog. Polym. Sci.*, vol. 10, no. 1, pp. 1–50, Jan. 1984.

[5] I. Casinos, "Mechanisms for the radical graft polymerization of vinyl and/or acrylic monomers on cellulose," *Polymer*, vol. 35, no. 3, pp. 606–615, Feb. 1994.

[6] N. Chansook and S. Kiatkamjornwong, "Ce(IV)-initiated graft polymerization of acrylic acid onto poly(ethylene terephthalate) fiber," *J. Appl. Polym. Sci.*, vol. 89, pp. 1952–1958, Aug. 2003.

[7] G. Odian and J. H. T. Kho, "Ceric Ion Initiated Graft Polymerization onto Poly(vinyl Alcohol)," *J. Macromol. Sci. Part - Chem.*, vol. 4, no. 2, pp. 317–330, Mar. 1970.

[8] A. Wachinski, *Ion exchange treatment for water*. Denver CO: American Water Works Association, 2006.

[9] F. Ku?era and J. Jan?  ?, "Homogeneous and heterogeneous sulfonation of polymers: A review," *Polym. Eng. Sci.*, vol. 38, no. 5, pp. 783–792, May 1998.

[10] F. G. Helfferich, *Ion exchange*. New York: Dover Publications, 1995.

[11] K. Saito, M. Ito, H. Yamagishi, S. Furusaki, T. Sugo, and J. Okamoto, "Novel hollow fiber membrane for the removal of metal ion during permeation: preparation by radiation-induced cografting of a crosslinking agent with reactive monomer," *Ind. Eng. Chem. Res.*, vol. 28, no. 12, pp. 1808–1812, Dec. 1989.

[12] K. Saito, K. Saito, K. Sugita, M. Tamada, and T. Sugo, "Cation-Exchange Porous Hollow-Fiber Membranes Prepared by Radiation-Induced Cografting of GMA and EDMA Which Improved Pure Water Permeability and Sodium Ion Adsorptivity," *Ind. Eng. Chem. Res.*, vol. 41, no. 23, pp. 5686–5691, Nov. 2002.

[13] N. Kwak, T. Hwang, S. Kim, Y. Yang, and K. Kang, "Synthesis of sulfonated PET-g-GMA fine ion-exchange fibers for water treatment by photopolymerization and their adsorption properties for metal ions," *Polym. Korea*, vol. 28, no. 5, pp. 397–403, Sep. 2004.

[14] Y. V. Bondar, H. J. Kim, and Y. J. Lim, "Sulfonation of (glycidyl methacrylate) chains grafted onto nonwoven polypropylene fabric," *J. Appl. Polym. Sci.*, vol. 104, no. 5, pp. 3256–3260, Jun. 2007.

[15] M. Kim, "Radiation-induced graft polymerization and sulfonation of glycidyl methacrylate on to porous hollow-fiber membranes with different pore sizes," *Radiat. Phys. Chem.*, vol. 57, no. 2, pp. 167–172, Feb. 2000.

[16] T. Kim and J. Kim, "Preparation and characterization of poly(3,4-ethylenedioxythiophene) (PEDOT) using partially sulfonated poly(styrene-butadiene-styrene) triblock copolymer as a polyelectrolyte," *Curr. Appl. Phys.*, vol. 9, no. 1, pp. 120–125, Jan. 2009.

[17] S. Li and J. Wei, "Evaluation of the influence of homopolymerization on the removal of water-insoluble organics by grafted polypropylene fibers," *Mar. Pollut. Bull.*, vol. 64, no. 6, pp. 1172–1176, Jun. 2012.

[18] D. M. Pinkerton and R. H. Stacewicz, "γ-Radiation-induced grafting of methyl methacrylate to polypropylene: The effects of water and mineral acid," *J. Polym. Sci. Polym. Lett. Ed.*, vol. 14, no. 5, pp. 287–291, May 1976.

[19] D19 Committee, "Test Method for Column Capacity of Particulate Mixed Bed IonExchange Materials," ASTM International, 2007.

[20] S. W. Lee, Y. Bondar, and D. H. Han, "Synthesis of a cation-exchange fabric with sulfonate groups by radiation-induced graft copolymerization from binary monomer mixtures," *React. Funct. Polym.*, vol. 68, no. 2, pp. 474–482, Feb. 2008.

[21] I. Kaur, R. Kumar, and N. Sharma, "A comparative study on the graft copolymerization of acrylic acid onto rayon fibre by a ceric ion redox system and a γ-radiation method," *Carbohydr. Res.*, vol. 345, no. 15, pp. 2164–2173, Oct. 2010.

[22] K. C. Gupta and K. Khandekar, "Ceric(IV) ion-induced graft copolymerization of acrylamide and ethyl acrylate onto cellulose," *Polym. Int.*, vol. 55, no. 2, pp. 139–150, Feb. 2006.

[23] L. Yu, S. Zhang, W. Liu, X. Zhu, X. Chen, and X. Chen, "Improving the flame retardancy of PET fabric by photo-induced grafting," *Polym. Degrad. Stab.*, vol. 95, no. 9, pp. 1934–1942, Sep. 2010.

Chapter 7

7 Sorption Properties of Functionalized PET/PE Bicomponent Nonwovens

Abstract

Cation exchange nonwovens based on PET/PE bicomponent and PET homocomponent nonwovens were produced via grafting of epoxy containing glycidyl methacrylate monomers followed by sulfonation. The effect of the grafting conditions (monomer concentration, initiator concentration, time of the reaction) on the grafting percentage and removal capacity of copper ions was studied. It was found that low GMA monomer concentrations and low reaction times (<30 mins) are necessary for achieving grafting percentages around 12%, maximizing the removal capacity of the functionalized nonwovens. Ion exchange capacities of 13 meq/g were achieved for both the homocomponent and bicomponent nonwovens. The sorption data of both materials fit the Langmuir model well indicating that monolayer sorption can be assumed. The data fit very well with pseudo second order models indicating the rate controlling mechanism is the ionic reaction of copper ions with sulfonate functional groups. Higher reaction rates and capacities were found with the bicomponent nonwoven compared to the homocomponent, indicating surface area has a significant impact on the effectiveness of the filtration media.

7.1 Introduction

Ion exchange resins have been used for many years as a method of removing heavy metals from water, recovering materials from waste water, and removing harmful gases from the air[1], [2], [3], [4]. Although these resins are highly selective in deionizing heavy metals and also have a high packing density, they still have many disadvantages. In order for the ions to be removed, they must interact with the functional groups on the surface of the resin. Therefore, the pores must be small enough to ensure there is adequate interaction between

the functional groups and the metal ions. A balance between the pore size and the pressure drop is necessary to maintain an efficient operating resistance. The high pressure necessary for resin operation can also destroy the structure of the beads[5].

The balance between the surface area and the operating resistance is the major drawback to using traditional ion exchange resins. With a need to increase the surface area and therefore the ion exchange capacity, while maintaining a low operating resistance, ion exchange fibers are being considered a reasonable alternative. Some research has been done on ion exchange fibers but there is still a need to improve their stability and capacity, as well as find a low cost alternative to the expensive base materials currently used [6], [7], [8], [9]. However, ion exchange fibers have not been able to replace the use of ion exchange resins in industry due to their low ion exchange capacity and high cost of production. A nonwoven material made from a low cost polymer and functionalized using cost effective methods would address this issue. The other limitation of the current ion exchange fibers is the low surface area due to the large fiber diameter. A bicomponent nonwoven material composed of cost effective microfibers, such as PET, would greatly increase the surface area of the base material compared to the current ion exchange fibrous materials.

Polyethylene terephthalate, PET, is one of the most widely used and readily available materials used in a multitude of applications. However, due to its hydrophobicity and lack of functional groups it is difficult to dye and can not be used for absorption applications[10]. Surface modification of polyethylene terephthalate (PET) is difficult due to its highly ordered structure and lack of reactive groups[10]. Achieving an efficient, cost effective method of surface modification of PET would have a profound impact on the functional fiber industry and provide a low cost base material for ion exchange filters.

Ceric salts have been extensively studied as a method for initiating the grafting of vinyl monomers on cellulose [11], [12], [13], [14]. However, few studies have been done to investigate its effectiveness of grafting onto PET fibers [15]. The suggested reaction scheme for the interaction between cerium ammonium nitrate and PET to initiate grafting of GMA is seen in . Cerium ions act as strong oxidizers when in acidic solution. An electron transfer of a

hydrogen atom occurs from the PET backbone to Ce(IV) to produce Ce(III). This hydrogen abstraction creates a radical on the PET which becomes the grafting site of the GMA monomer [16].

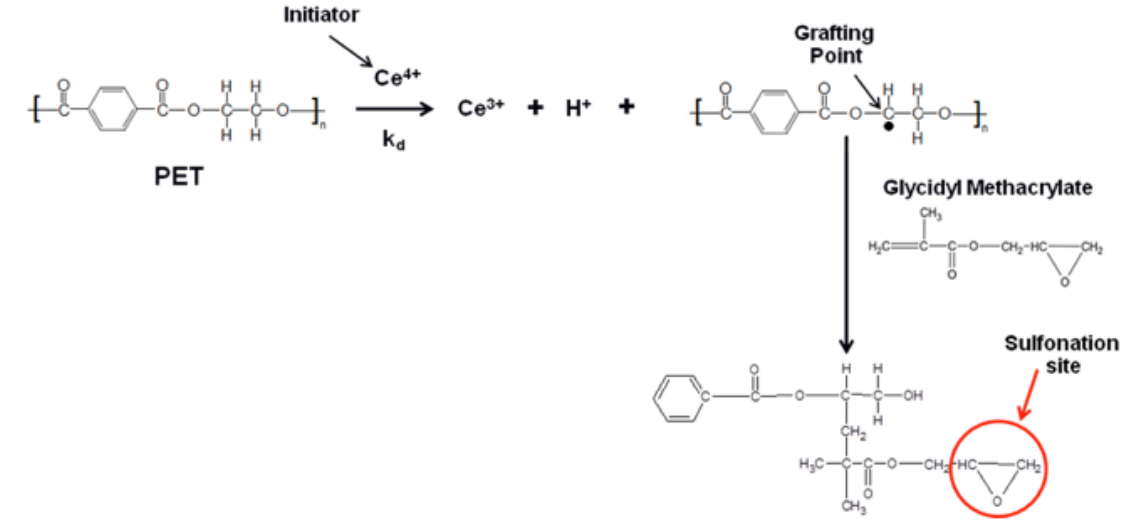

Figure 7.1. Suggested reactions scheme of the GMA grafting on PET initiated with cerium ion

The GMA grafted PET fibers are functionalized via sulfonation reactions. This is a process by which sulfonate, $-SO_3^-$, groups are attached to the epoxy groups of the GMA through a substitution reaction, producing strongly cationic exchange fibers. Strong acid cations can dissociate in both alkaline and acidic solutions, making them very versatile in the solutions in which they can be used and typically have a higher ion exchange capacity then weak acid cation exchange materials. Therefore, strong acid cation exchangers are the most widely used in industry [17].

Compounds such as sulfuric acid, sodium sulfite, sulfates, and variations of complexes have been used as the sulfonating agents[18]. Currently there are no known continuous

functionalization processes. Therefore, all chemical processes are done in batch type operations in a reaction kettle with the sulfonating agents and materials[19].

Sulfonation substitution reactions of GMA epoxy groups have been extensively studied [20], [21], [22], [23], [24], [25]. The suggested reaction between the GMA grafted PET fibers and sodium sulfite is seen in Figure **7.2**.

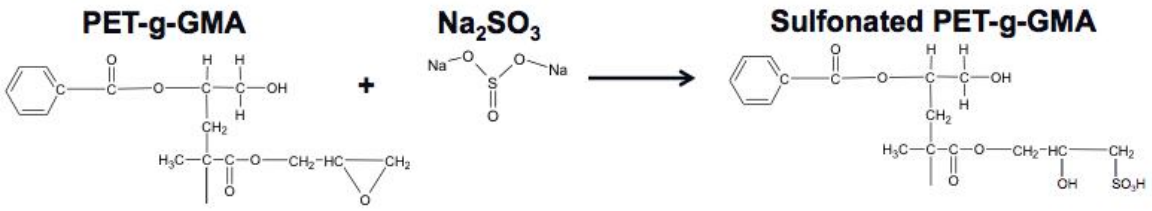

Figure 7.2. Suggested reaction scheme for sulfonation of GMA grafted PET with sodium sulfite as the sufonating agent

In the present study strong cation exchange nonwoven materials have been produced via grafting of glycidyl methacrylate monomers followed by subsequent sulfonation of the grafted monomers. The maximum capacity and removal rate of copper ions from solution are studied.

7.2 Experimental Procedure

7.2.1 Materials

For all of the following experiments, nonwovens composed of 80/20 PET/PE 16 segmented pie bicomponent fibers and a PET homocomponent were used, Table 7.1. These materials were made in the Pilot Plant of the Nonwoven's Institute. The PET/PE bicomponent fiber was fractured in the Jet Dyeing Machine for 120 minutes to achieve 100% fracture of the bicomponent fibers. The materials had a basis weight of 100 grams/meter^2 and were passed through the hydroentangling machine for one pass at 750 psi.

Table 7.1. Characteristics of nonwoven used for the experiments

Polymer	Ratio	Segments	Basis Weight (gsm)	Hydros	Fractured Time (mins)
PET	Homocomponent	1	100	1 (750 psi)	0
PET/PE	80/20	16	100	1 (750 psi)	90

For all of the grafting procedures, hydroquinone was removed from Glycidyl Methacrylate, GMA, prior to all experiments using an inhibitor remover column obtained from Sigma Aldrich. All other chemicals are used as received.

Table 7.2. List of the chemicals and solutions used for all grafting procedures

Solution	Acronym	Company	Purpose
Ceric Salt Grafting Solution			
Glycidyl Methacrylate	GMA	Sigma Aldrich	Epoxy containing monomer
Ceric Ammonium Nitrate	CAN	Fisher Scientific	Grafting Initiator
Nitric Acid	NHO_3	Fisher Scientific	Grafting Acid
Methanol	CH_3OH	Sigma Aldrich	Washing Solvent
Sulfonation Reaction Solution			
Sodium Sulfite (anhydrous)	Na_2SO_3	Fisher Scientific	Sulfonation
Isopropyl Alcohol	IPA	Sigma Aldrich	Sulfonation Solvent
Protonation Solution			
Sulfuric Acid	H_2SO_4	Sigma Aldrich	Protonation

7.2.2 Grafting of PET Fibers

The nonwoven samples were cut into 8x8 inch samples, washed in acetone for 24 hours, and dried completely before weighing. The grafting initiator, CAN, was dissolved in 100 mL of Nitric Acid, HNO_3. Distilled water was added to a 500 mL round bottom flask to bring the total solution volume to 400 mL and flushed with nitrogen for 5 minutes. The CAN/HNO_3 solution, sample, and stirring rod were then added to the flask. The flask was lowered into a mineral oil bath at 60 ºC and the solution was flushed with nitrogen for 15 minutes. The GMA monomer was then added to the flask to begin the reaction. Reaction times ranged from 10-30 minutes. The concentrations of GMA and CAN are found in Table 7.3

Table 7.3. Concentrations of Grafting solutions

GMA Concentration (wt%)			CAN Concentration		
2	4	6	2	4	6

After the specified reaction time the PET-g-GMA samples are washed in methanol on a mechanical shaker at 60 ºC for 4 hours, then washed for 3 hours in methanol with a probe sonicator. The samples were rinsed in DI water and dried until a constant weight was achieved.

7.2.3 Functionalization of PET Fiber Via Sulfonation

The grafted PET and PET/PE nonwovens (PET-g-GMA) were sulfonated at 70 ºC on a mechanical shaker in a 10/15/75 weight percent solution of Sodium Sulfite/ Isopropyl Alcohol/ Distilled Water for 4 hours. The samples were repeatedly washed in DI Water at 70 ºC on a mechanical shaker until the conductivity of the wash water reached that of DI water and dried completely at 80 ºC.

The sulfonated samples were then protonated (put in the hydrogen form) in 400 mL of 0.5 M H_2SO_4 on a mechanical shaker at 70 ºC for 2 hours. The samples are removed, rinsed in cold DI water until neutral pH, and dried at 80 ºC until a constant weight is achieved.

Several analytical techniques were used to monitor the reactions. No analytical technique is perfect and all are used together to get an overall idea of the effects of the grafting and functionalization.

7.2.3.1 Grafting Percentage

The grafting efficiency of the monomer on the fibrous substrates is reported as a function of the weight increase of the sample, Equation 7.1:

$$GP(\%) = \frac{W_g - W}{W} \times 100\% \qquad \textbf{(7.1)}$$

where W is the weight of the sample before grafting and W_g is the weight after grafting.

The major problem experienced with graft polymerization reactions is in the formation of homopolymer that adheres to the grafting substrate. This homopolymer is a product of the monomers reacting with each other rather than the grafting substrate[26], [27]. Therefore, the grafting percentage value includes grafting monomer as well as any remaining homopolymer.

7.2.3.2 TOF-SIMS

The TOF-SIMS analysis was done in the Analytical Instrumentation Facility at NCSU with an ion TOF-SIMS 5 machine. 124 scans was done for each sample at a resolution of 50 nm.

7.2.4 Metal Uptake Experiments

7.2.4.1 Adsorption Isotherm

The isothermal adsorption behavior is evaluated based on the maximum copper removal at varying copper concentrations. 100 ml solutions of copper nitrate trihydrate were prepared at 75, 125, 175, 225, 325, 375 mg/l. The concentration of copper ions (g/L), $C_{Cu^{2+}}$, was is calculated based on the ratio of copper ions in a copper nitrate trihydrate molecule, molecular weight of copper (63.54 g/mol) in copper nitrate trihydrate (241.6 g/mol),

$$C_{Cu^{2+}} = C_{CuNO_3} \mathrm{g} \frac{MW_{Cu^{2+}}}{MW_{CuNO_3}} \qquad \textbf{(7.2)}$$

where C_{CuNO_3} is the concentration of copper nitrate trihydrate (g/L), $MW_{Cu^{2+}}$ is the molecular weight of copper (63.54 g/mol), and MW_{CuNO_3} is the molecular weight of copper nitrate trihydrate (241.6 g/mol).

The samples were agitated in the copper solutions on a mechanical shaker at 60 ˚C at 200 rpm. After 24 hours, 2 ml aliquots were removed from each solution and diluted with 50 μl of 35 wt% nitric acid and HPLC water in a 50 ml volumetric flask. The concentration of copper ion in the solutions was calculated using Flame Atomic Absorption (FAA) in the

Analytical Technique Laboratory at North Carolina State University. The removal capacity of the materials, q_e (mg/g), was defined as

$$q_e = \frac{(C_0 - C_e)V}{W_s} \quad \textbf{(7.3)}$$

where C_0 and C_e are the concentrations (mg/L) of the initial and equilibrium copper solutions respectively, V is the volume (L), and W_s is the weight of the sulfonated sample in the proton form.

7.2.4.2 Kinetic Study

The kinetic ion exchange behavior is evaluated based on the removal of copper ions from solution over 24 hours. 100 ml of copper solutions are prepared at 75 mg/L in HPLC grade water based on the concentration of copper in the copper nitrate trihydrate molecule. Samples were placed in the solution in a 250 ml flat bottom boiling flask on a mechanical shaker at 60 ˚C and mixed under agitation at 200 rpm. 2 ml aliquots of solution were removed after 5, 10, 15, 30, 60, and 1,440 minutes, added to 50 μl of 35 wt% nitric acid and diluted to 50 mL with HPLC grade water in a volumetric flask. The concentration of copper ion in the solutions was calculated using Perkin Elmer Flame Flame Atomic Absorption (FAA) in the Analytical Technique Laboratory at North Carolina State University. A calibration curve with an R^2 value of .9999 was prepared with a standard copper solution.

7.3 Analytical Techniques

Several analytical techniques were used to monitor the reactions. No analytical technique is perfect and all are used together to get an overall idea of the effects of the grafting and functionalization.

7.3.1 Grafting Percentage

The grafting efficiency of the monomer on the fibrous substrates is reported as a function of the weight increase of the sample, Equation 7.4:

$$GP(\%) = \frac{W_g - W}{W} \times 100\% \quad \textbf{(7.4)}$$

where W is the weight of the sample before grafting and W_g is the weight after grafting.

The major problem experienced with graft polymerization reactions is in the formation of homopolymer that adheres to the grafting substrate. This homopolymer is a product of the monomers reacting with each other rather than the grafting substrate[26], [27]. Therefore, the grafting percentage value includes grafting monomer as well as any remaining homopolymer.

7.3.2 Flame Atomic Absorption

The copper concentrations were quantified using a Perkin Elmer Flame AA 300 available in the Analytical Services Laboratory at the College of Textiles at NC State University. Three readings were done for each solution. A calibration curve with an R^2 value of .9999 was prepared with a standard copper solution.

7.3.3 TOF-SIMS

The TOF-SIMS analysis was done in the Analytical Instrumentation Facility at NCSU with an ion TOF-SIMS 5 machine. 124 scans was done for each sample at a resolution of 50 nm.

7.4 Results and discussions

7.4.1 Effect of Grafting Conditions on Ion Exchange Capacity

The homocomponent and bicomponent samples were grafted via ceric salt initiation with varying monomer and initiator concentrations and at varying times. The grafted (PET/PE)-g-GMA samples were sulfonated for 4 hours in a 10/15/75 Sodium Sulfite/IPA/H_2O solution to attach sulfonate functional groups to the grafted monomers. The sulfonated samples were then put in the proton form by equilibration in a Sulfuric Acid solution for 2 hours. The effect of the GMA monomer concentration, CAN initiator concentration, grafting reaction time, and the grafting percentage on the ion exchange capacity of the nonwoven materials was investigated.

7.4.1.1 Effect of GMA Concentration

The effect of GMA monomer concentration on the grafting percentage and removal capacity of copper ions was investigated, Figure **7.3**.

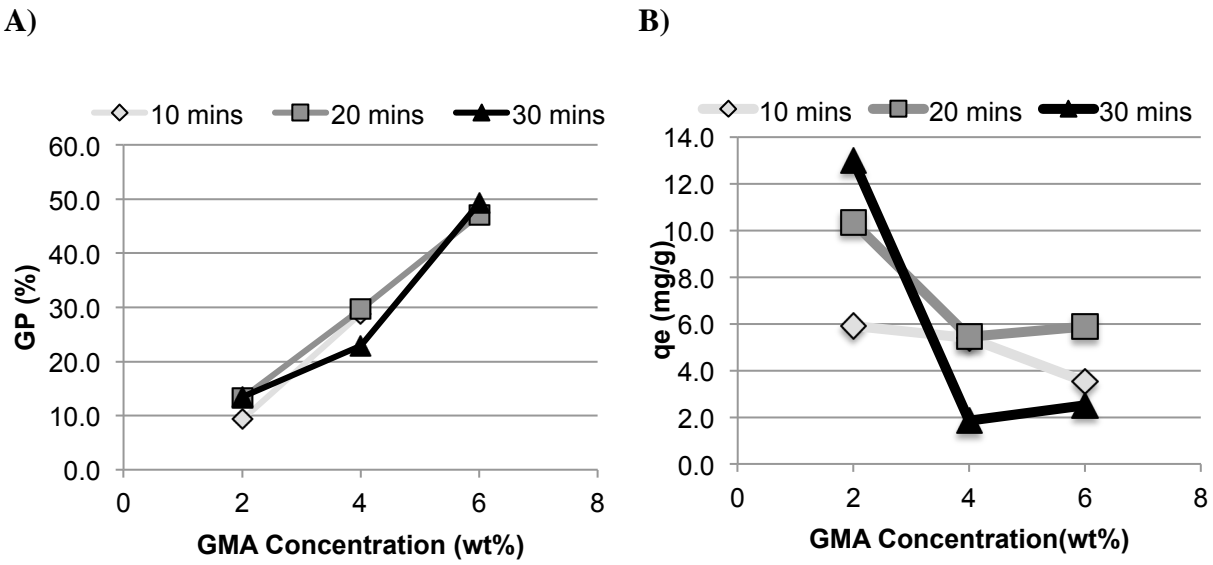

Figure 7.3. Effect of glycidyl methacrylate concentration on the A) Grafting PErcentage and B) Ion Exchange capacity of bicomponent samples grafted at increasing reaction time and 4 mM CAN concentration

There is a significant increase in the grafting percentage with an increase in the GMA grafting monomer concentration, Figure **7.3**A. However, the GMA concentration has a negative effect on the removal capacity of the samples, Figure **7.3**B. At high monomer concentrations there is more monomer present in the bulk solution. The formation of homopolymer of the grafting monomer is a competing reaction with the PET radical sites, a well known occurrence with both physical and chemical grafting procedures [26], [27]. This homopolymer should be washed off with the sonication following grafting. However, the

nonwoven structure is very intricate and it is highly likely that the homopolymer is trapped in the structure and obstructing the access to functional groups.

This behavior is evident in Figure **7.3** when considering the resulting ion exchange capacity of the material. A high GMA concentration of 6 wt% has a high grafting percentage of 50%, but a low copper ion removal capacity of 2 meq/g. At low initiator concentrations, 2 mM CAN, low GMA concentrations of 2 wt% result in very high removal capacities of about 13 meq/g. Achieving high ion exchange capacities at low GMA concentrations is quite advantageous for the industrial scale up of this process as the monomer is the greatest cost in this process. It was found that minimal amount were necessary to reach ion exchange capacities that far exceeded most commercially available resins.

7.4.1.2 Effect of CAN Concentration

The effect of the ceric ammonium nitrate (CAN) initiator concentration on the grafting percentage and the ion exchange capacity was investigated, Figure **7.4**.

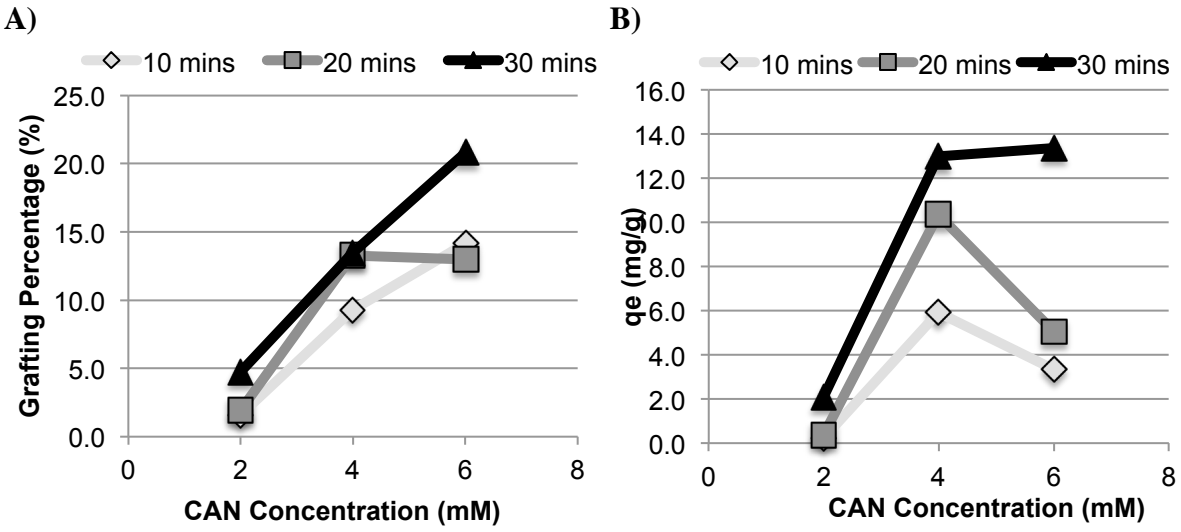

Figure 7.4. Effect of Ceric ammonium Nitrate Concentration on the ion exchange capacity of bicomponent samples grafted at increasing reaction time and 2 wt% GMA

At a low monomer concentration, it is evident that increasing the initiator concentration increases the grafting percentage, Figure **7.4**A. However, similar to the effects of monomer concentration the high grafting percentages did not result in high capacities, Figure **7.4**B. There is a large increase in the capacities of the bicomponent material from 2 mM to 4 mM, but a decrease in the capacity occurs when the initiator concentration is increased to 6 mM. It is likely that a high level of CAN initiator in the bulk solution causes a large amount of homopolymer to form in the solution and adhere to the surface of the nonwoven. This homopolymer is difficult to remove and leads to higher grafting percentages. However, the homopolymer does not aid in removing copper ions from solution. Therefore at this monomer concentration, high initiator concentrations are not necessary for producing materials with high capacities.

7.4.1.3 Effect of Reaction Time

The grafting reaction time plays an important role in the procedure and possible scale up of the functionalization process. The effect of the time of the grafting reaction on the grafting percentage and ion exchange capacity are investigated, Figure 7.5. Effect of grafting reaction time on the A) Grafting PErcentage and B) Ion exchange capacity of bicomponent samples grafting with 4 wt% GMA and 6 mM CAN

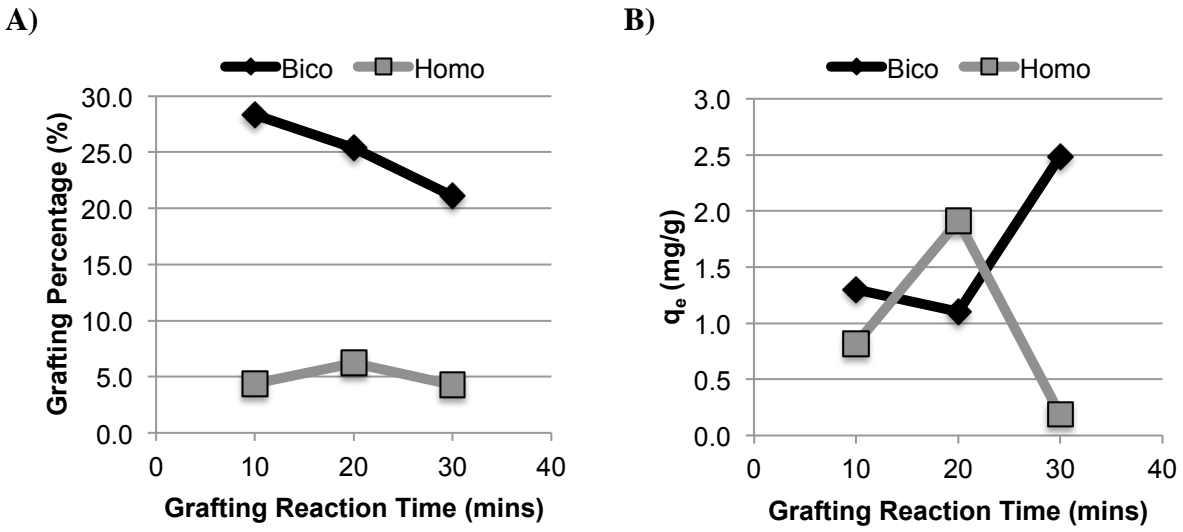

Figure 7.5. Effect of grafting reaction time on the A) Grafting PErcentage and B) Ion exchange capacity of bicomponent samples grafting with 4 wt% GMA and 6 mM CAN

Under the same grafting conditions, the bicomponent nonwovens have a much higher grafting percentage than the homocomponent nonwoven at all grafting times, especially 10 minutes. Upon fracturing of the fibers of the bicomponent samples, web consolidation occurs, decreasing the size of the pores compared with the homocomponent samples. This also provides high surface area of the PET fibers to increase the amount of functionalization and further increase the ion exchange capacity. This behavior is evident in Figure **7.5**, where the bicomponent nonwoven has a higher removal capacity than the homocomponent nonwoven at both high and low grafting times. The decrease in the grafting percentage at long grafting times of both materials is evidence that the higher grafting times result in a larger amount of homopolymer that is then removed after grafting. Despite this decrease in the grafting percentage of the bicomponent nonwoven, more functionalization is still occurring and a high removal capacity (2.5 mg/g) of the bicomponent nonwoven is achieved.

7.4.1.4 Effect of Grafting Percentage

The grafting percentage is the increase in the weight of the sample from the original sample to the grafted sample. This is often the first piece of information that is reported when performing such grafting procedures as a way of monitoring the extent of grafting [23], [28].

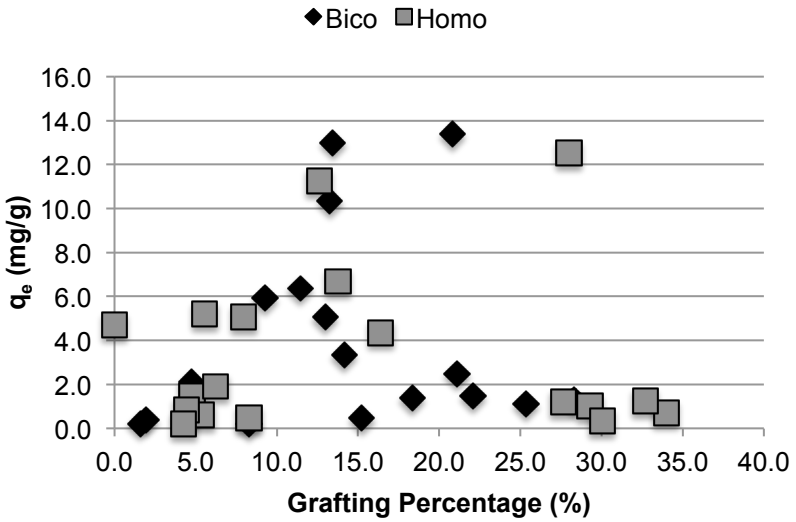

Figure 7.6. Relationship between Grafting Percentage and resulting ion exchange capacity of the Bicomponent and homocomponent samples

Looking at the full sample set of materials that were grafted at varying grafting conditions, it is evident that high grafting percentages do not lead to high ion exchange capacities. Although high removal capacities of more than 13 meq/g were achieved at grafting percentages of 20 and 30%, the bulk of the homocomponent and bicomponent samples reach a maximum capacity of about 11 meq/g at 12 GP%. After 12 GP% there is a large decrease in the removal capacity of the materials. This grafting percentage is on the low end of the grafting percentages that were achieved. This indicates that the high grafting percentages are likely due to GMA homopolymer that has formed during grafting and is

stuck in the intricate structure of the nonwoven materials. Because the pore structure of the nonwonven materials is so tortuous, it is difficult to fully remove the homopolymer even with excessive washing of the samples after grafting. This homopolymer is obstructing the access to the functional groups and results in low ion exchange capacities. Under these grafting conditions and with these materials, the target grafting percentage is around 12%, much lower than what is typically reported.

7.4.2 Effect of Ion Exchange Conditions of Removal of Copper Ions

The experimental conditions of the ion exchange procedure, such as the concentration of the copper solution and the contact time, have a significant impact on the removal efficiency of the copper ions from solution. Understanding the effects of these conditions can improve the efficiency of the filtration media.

7.4.2.1 Effect of Initial Concentration

The removal efficiency of the functionalized bicomponent and homocomponent nonwovens were tested at varying copper concentrations, from 20-125 mg/l, Figure **7.7**. These concentrations are based on the concentration of copper ions in solution, not the copper nitrate trihydrate concentration.

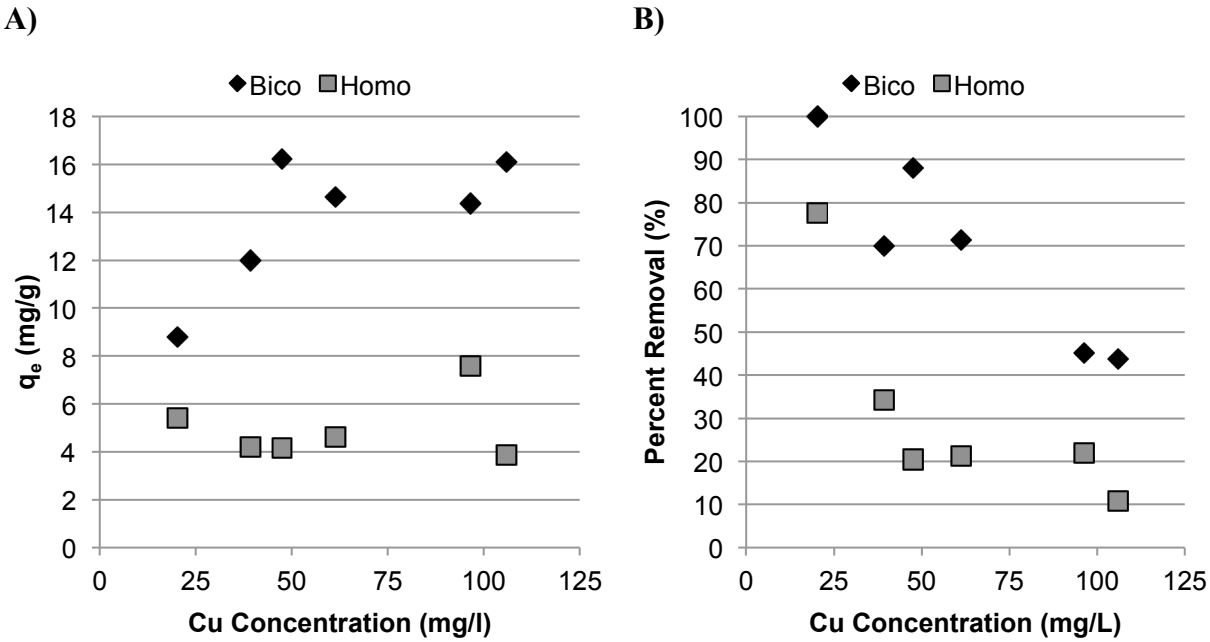

Figure 7.7. Effect of the initial concentration of Copper Ions on A) the removal capacity of the materials and b) the percent removal of copper ions of a bicomponent and homocomponent sample grafted with 4 wt% GMA, 4 mm CAN, and 20 mins reaction time

The removal efficiency of the copper ions from solution, over the range of 20-125 mg/l, is dependent on the concentration of the copper ions and the type of material, when tested at a natural pH of 6.2 and 24 hour contact time. The removal capacity of the materials increases to about 75 mg/l where it appears to level off, Figure **7.7**A, or drop off in the case of the homocomponent nonwoven. The bicomponent sample, with a grafting percentage of 29.6%, has a higher removal capacity than the homocomponent nonwoven, with a grafting percentage of 20.9%, at all copper concentrations. The percent removal of the functionalized materials decreases from 100% to 40% and10% for the bicomponent and homocomponent nonwovens, respectively, when the copper ion concentration is increased to 125 mg/l. The web structure of the functionalized material has a great effect on the removal of copper ions. The bicomponent nonwoven has a higher grafting percentage than the homocomponent nonwoven and a 25% higher removal capacity than the homocomponent nonwoven at nearly

every copper concentration. The increase in removal capacity of the bicomponent nonwoven is not proportional to the increase in grafting percentage compared to the homocomponent nonwoven. This can be explained by the greater surface area available on the bicomponent nonwoven on the outer surface of the sample that increases the accessibility of the functional groups.

The samples were washed in 100 ml of HPLC water on a mechanical shaker for 3 days to wash off any copper ions that might be physically removed by the web structure. When the washing solutions were tested with FAA, no copper ions were found in the solution, indicating the copper ions are likely attached by an ionic bond that has formed with the sulfonate functional group.

7.4.2.2 Effect of Contact Time

In order to evaluate the rate of removal of the copper ions from solution, batch experiments were performed in which samples were in contact with copper nitrate solutions and aliquots were removed at increasing times, over a 24 hour period. The homocomponent and bicomponent samples that were functionalized under the same conditions were compared.

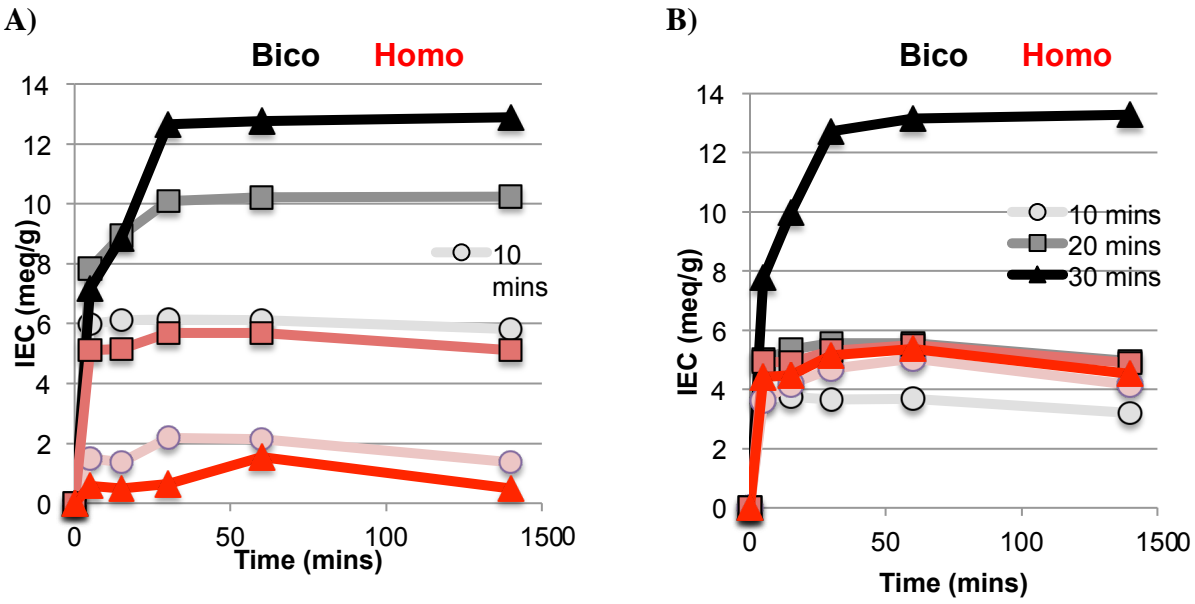

Figure 7.8. Removal efficiency of functionalized samples grafted with A) 2 wt% gMa and 4 mmol CAN and B) 2 wt% GMA and 6 mmol CAN at increasing reaction time

For both the homocomponent and bicomponent samples, the reaction between the sulfonate functional groups and copper ions occurs very rapidly, during the first 5-15 minutes of exposure. This is due to the large amount of surface area that is available at the beginning of the reaction. The bicomponent has a larger surface area than the homocomponent providing greater accessibility to the functional groups and thus a higher rate of removal. The samples reach equilibrium after 30 minutes of contact time. Many of the samples experienced a slight decrease in the capacity when the reaction was extended to 24 hours. This is likely do to a release of some ions that are trapped in the web structure after the initial interaction.

At the lower monomer concentration, the bicomponent nonwovens have about twice the copper removal efficiency as the homocomponent nonwovens, consistent with the higher grafting percentages these materials also experience. After 5 minutes of contact time, the

bicomponent nonwonvens that were grafted for 30 minutes at low monomer concentrations had a removal capacity of 8 meq/g of sample. This is highly comparable, if not greater, then the capacity of most commercially available ion exchange resins.

7.4.3 Equilibrium Study

The experimental conditions of the ion exchange procedure, such as the concentration of the copper solution and the contact time, have a significant impact on the removal efficiency of the copper ions from solution. Understanding the effects of these conditions can improve the efficiency of the filtration media. Mathematical models, known as adsorption isotherms, are used to describe the distribution of the adsorbate, the metal ions, between the liquid and the adsorbent material, the functionalized nonwoven. Adsorption isotherms, typically Langmuir and Freundlich, are defined by a set of assumptions that are based on characteristics of the surface of the material, the interaction between the ions in solution and the interaction between the ions and the material. The isotherms relate the amount of metal ions removed per unit mass of material, q_e, to the concentration of ions at equilibrium, C_e.

7.4.3.1 Effect of Initial Concentration

The removal efficiency of the functionalized bicomponent and homocomponent nonwovens were tested at varying copper concentrations, from 20-125 mg/l, Figure **7.9**. These concentrations are based on the concentration of copper ions in solution, not the copper nitrate trihydrate concentration.

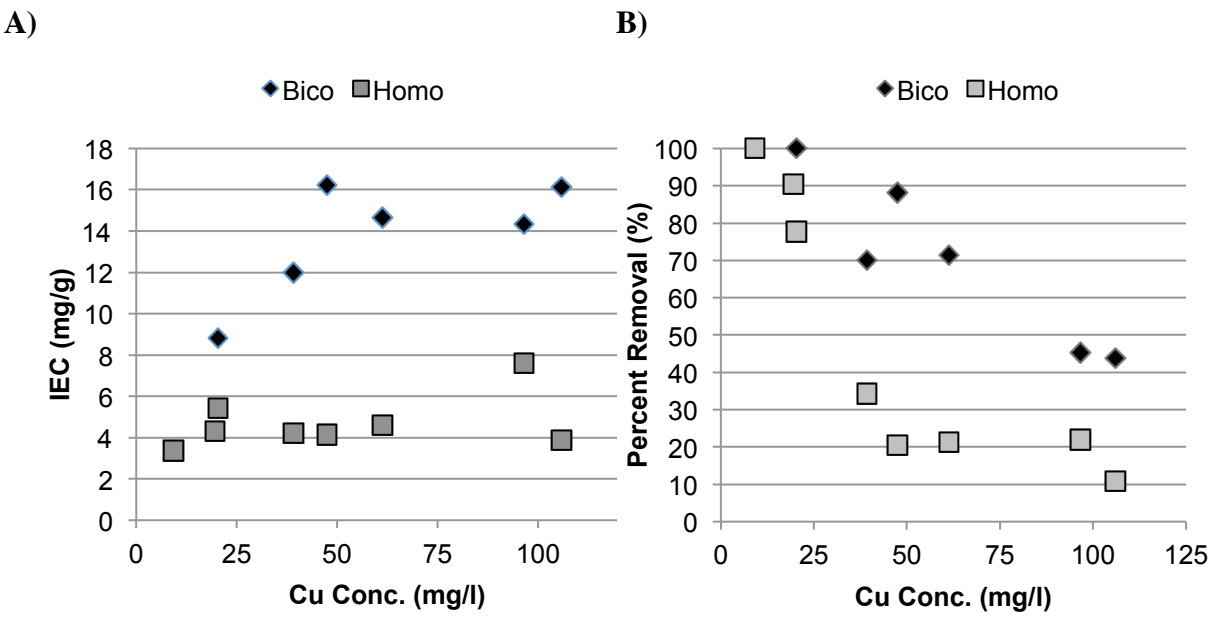

Figure 7.9. Effect of the initial concentration of Copper Ions on A) the removal capacity of the materials and b) the percent removal of copper ions of a bicomponent and homocomponent sample grafted with 4 wt% GMA, 4 mm CAN, and 20 mins reaction time

The removal efficiency of the copper ions from solution, over the range of 20-125 mg/l, is dependent on the concentration of the copper ions and the type of material, when tested at a natural pH of 6.2 and 24 hour contact time. The removal capacity of the materials increases to about 75 mg/l where it appears to level off, Figure **7.7**A, or drop off in the case of the homocomponent nonwoven. The bicomponent sample, with a grafting percentage of 29.6%, has a higher removal capacity than the homocomponent nonwoven, with a grafting percentage of 20.9%, at all copper concentrations. The percent removal of the functionalized materials decreases from 100% to 40% and10% for the bicomponent and homocomponent nonwovens, respectively, when the copper ion concentration is increased to 125 mg/l. The web structure of the functionalized material has a great effect on the removal of copper ions. The bicomponent nonwoven has a higher grafting percentage than the homocomponent nonwoven and a 25% higher removal capacity than the homocomponent nonwoven at nearly

every copper concentration. The increase in removal capacity of the bicomponent nonwoven is not proportional to the increase in grafting percentage compared to the homocomponent nonwoven. This can be explained by the greater surface area available on the bicomponent nonwoven on the outer surface of the sample that increases the accessibility of the functional groups.

The samples were washed in 100 ml of HPLC water on a mechanical shaker for 3 days to wash off any copper ions that might be physically removed by the web structure. When the washing solutions were tested with FAA, no copper ions were found in the solution, indicating the copper ions are likely attached by an ionic bond that has formed with the sulfonate functional group.

7.4.3.2 The Langmuir Isotherm

The Langmuir model assumes that the adsorbent has a homogenous surface with monolayer adsorption, where each functional group reacts with one ion. It also assumes that there is no interaction between the adsorbate ions that are attached to the surface [29][28]. The Langmuir model is written as:

$$q_e = \frac{q_m K_L C_e}{1 + K_L C_e} \qquad \textbf{(7.5)}$$

Equation **(7.5)** can be expressed in its linear form as

$$\frac{C_e}{q_e} = \frac{1}{q_m K_L} + \frac{C_e}{q_m} \qquad \textbf{(7.6)}$$

Where q_e, is the amount of adsorbed ions per unit mass (mg/g), C_e is the concentration of metal ions in solution at equilibrium (mg/L), q_m is the Langmuir constant describing the maximum number of metal ions per unit mass that can be removed after complete coverage (mg/g), and K_L is the Langmuir constant describing the energy of adsorption of the metal ions (L/mg). The plot of specific adsorption (C_e/q_e) versus the equilibrium concentration (C_e), Figure **7.10**, is used to calculate q_m and K_L.

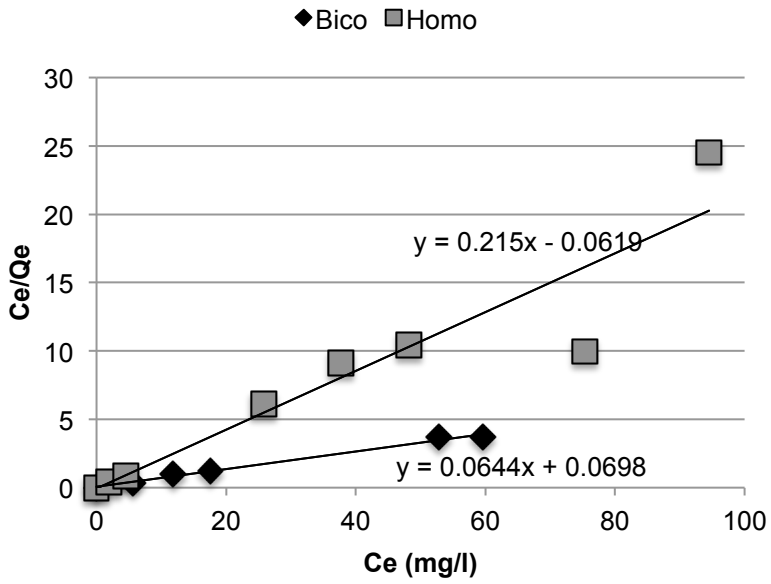

Figure 7.10. Langmuir Adsorption Isotherm of the Homocomponent and Bicomponent samples, grafting percentage of 20% and 29%, respectively

The slope and intercept of the regression line fit to the data of the bicomponent and homocomponent nonwovens are used to find the Langmuir constants q_m and K_L, Table **7.4**.

Table 7.4. Linear Langmuir Constants

Web Structure	q_m (mg/g)	K_L (L/mg)	R^2
Bicomponent	15.528	0.923	0.991
Homocomponent	4.65123	-3.473	0.87414

The Langmuir isotherm estimates the maximum adsorption capacity of the materials when complete monolayer coverage occurs. This value, q_m, is much higher for the bicomponent nonwoven than the homocomponent nonwoven. This can be explained by the

higher surface area available on the surface of the bicomponent nonwoven compared to the homocomponent. The bicomponent nonwoven has 4.5 times the surface area as the homocomponent nonwoven, about 80% of which is the PET surface (20% is the PE surface). Therefore, the bicomponent nonwoven has about 3.5 times the graftable surface area. This is consistent with the difference in q_m values of the two materials, indicating the high surface area of the bicomponent nonwoven is being utilized and yields high ion exchange materials.

The energy of adsorption of the bicomponent nonwoven, K_L, is also much higher than the homocomponent nonwoven, indicating a strong affinity between the copper ions and sulfonate functional groups. The negative K_L value of the homocomponent nonwoven indicates the the affinity between the copper ions and functional groups can be assumed to be undetectable. The R^2 values of the bicomponent and homocomponent nonwovens are 0.991 and 0.87414, respectively, indicating that the data fits the Langmuir model well.

The Separation Factor, S_F, is a dimensionless constant derived from the Langmuir isotherm constants that are used to describe the favorability of the reactions between the coppers ions with the functional groups on the nonwoven surface [30][29]. The Separation Factor is described as

$$S_F = \frac{1}{(1 + K_L C_0)} \qquad \textbf{(7.6)}$$

where K_L is the Langmuir isotherm constant (L/mg) and C_0 is the initial copper ion concentration (mg/L). The S_F values for the bicomponent and homocomponent nonwovens at 20 g/L and 105 g/L, the lowest and highest copper ion concentrations respectively, are seen in Table **7.5**

Table 7.5. S_F values of bicomponent and homocomponent nonwovens at 20 g/L and 105 g/l

Web Structure	Initial Concentration	
	20 g/L	105 g/L
Bicomponent	0.051	0.009
Homocomponent	-0.014	0.011

Separation values between 0 and 1, $0< S_F <1$, indicate favorable adsorption of the copper ions and that Langmuir is a favorable model for the adsorption behavior of the material [31][30]. The bicomponent values for both high and low initial copper concentrations are lower than the homocomponent nonwoven indicating that this adsorption is more favorable [32][31], while the higher initial copper concentrations are more favorable than the lower initial concentrations.

7.4.3.3 The Freundlich Isotherm

The Freundlich Isotherm is a commonly used model that defines the adsorption of adsorbates to the heterogeneous surface of the adsorbent, assuming that different sites with varying energies are present on the surface [31][30].

The Freundlich model is written as

$$q_e = K_f C_e^{1/n} \quad \textbf{(7.7)}$$

The logarithmic form of Equation 7.8:

$$\ln q_e = \frac{1}{n} C_e + \ln K_f \quad \textbf{(7.8)}$$

where q_e is the amount of copper removed per unit mass of sample (mg/g), K_f is the Freundlich constant related to the adsorption capacity, n is the Freundlich constant related to the adsorption intensity, and C_e is the concentration of the solution at equilibrium. The

natural log plot of lnq_e versus lnK_f is plotted for the bicomponent and homocomponent nonwovens and used to calculate the Freundlich isotherm constants.

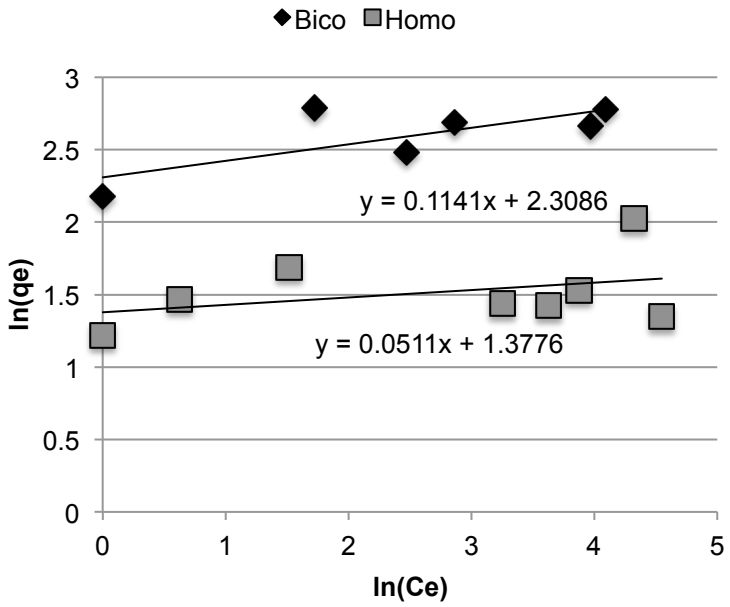

Figure 7.11. Freundlich isotherm of the natural log plots of the bicomponent and homocomponent nonwovens

The intercept and slope of the regression lines of the bicomponent and homocomponent plots are used to solve for the Freundlich isotherm constants, n and K_f, Table 7.6.

Table 7.6. Freundlich Constants for Bicomponent and Homocomponent Nonwovens

Web Structure	n	K_f (mg/g)	R^2
Bicomponent	8.764	10.060	0.558
Homocomponent	19.569	3.965	0.134

The n value describes the separation ability of the copper ions from solution. A value less than 10 indicates favorable adsorption and easy separation of the ions from solution[31][30]. The bicomponent nonwoven had favorable adsorption of the metal ions, while the homocomponent does not. K_f is an approximation of the maximum adsorption capacity of the materials. The value for the homocomponent sample is comparable to the q_m value obtained from the Langmuir constant, however, the bicomponent value is much lower. The R^2 value is very low for both the the homocomponent and bicomponent nonwoven, indicating that the data is not a good fit for the Freundlich model. The Langmuir model is a much stronger fit for these materials indicating that a homogenous monolayer surface is a better approximation that a heterogeneous surface. This indicates that much of the functionalization is occurring primarily on the surface of the samples.

7.4.4 Kinetic Study

It is of interest to understand the time dependent behavior of the copper ion removal process. The rate controlling mechanism of the chemical reactions, the reaction between the copper ions and functional groups on the surface of the nonwovens, are defined using pseudo first and second order models.

7.4.4.1 Effect of Contact Time

In order to evaluate the rate of removal of the copper ions from solution, batch experiments were performed in which samples were in contact with copper nitrate solutions and aliquots were removed at increasing times, over a 24 hour period. The homocomponent and bicomponent samples that were functionalized under the same conditions were compared.

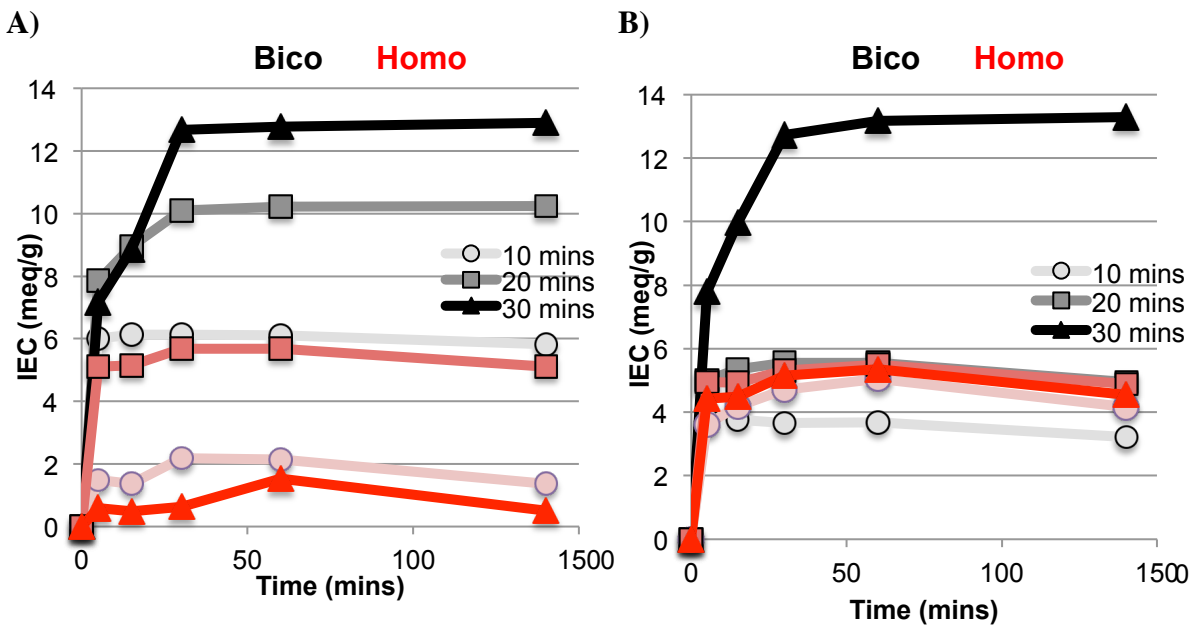

Figure 7.12. Removal efficiency of functionalized samples grafted with A) 2 wt% gMa and 4 mmol CAN and B) 2 wt% GMA and 6 mmol CAN at increasing reaction time

For both the homocomponent and bicomponent samples, the reaction between the sulfonate functional groups and copper ions occurs very rapidly, during the first 5-15 minutes of exposure. This is due to the large amount of surface area that is available at the beginning of the reaction. The bicomponent has a larger surface area than the homocomponent providing greater accessibility to the functional groups and thus a higher rate of removal. The samples reach equilibrium after 30 minutes of contact time. Many of the samples experienced a slight decrease in the capacity when the reaction was extended to 24 hours. This is likely do to a release of some ions that are trapped in the web structure after the initial interaction.

At the lower monomer concentration, the bicomponent nonwovens have about twice the copper removal efficiency as the homocomponent nonwovens, consistent with the higher grafting percentages these materials also experience. After 5 minutes of contact time, the bicomponent nonwonvens that were grafted for 30 minutes at low monomer concentrations

had a removal capacity of 8 meq/g of sample. This is highly comparable, if not greater, then the capacity of most commercially available ion exchange resins [33], [34], [35].

7.4.4.2 Kinetic Models

7.4.4.2.1 Pseudo First Order Model

The pseudo first order equation is defined as

$$\frac{dq_t}{dt} = k_1(q_e - q_t) \qquad \textbf{(7.9)}$$

Equation 7.9 can be integrated based on the boundary conditions *t=0* to *t=t* and *qt=0* and *qt=qt*, to have the integrate form

$$\ln(q_e - q_t) = \ln q_e - k_1 t \qquad \textbf{(7.10)}$$

where qt is the amount of copper adsorbed per unit of material (mg/g) at time *t*, k_1 is the pseudo first order rate constant (L/min) and *t* is the contact time. A plot of $\ln(q_e\text{-}q_t)$ against *t* gives a regression line where the slope is the adsorption rate constant, k_1.

7.4.4.2.2 Pseudo Second Order Model

The pseudo second order equation is defined as

$$\frac{dq_t}{dt} = k_2(q_e - q_t)^2 \qquad \textbf{(7.11)}$$

Equation (2.9) can be integrated to the linear form on the boundary conditions *t=0* to *t=t* and *qt=0* and *qt=qt* and expressed as

$$\frac{t}{q_t} = \frac{1}{h} + \frac{1}{q_e}t \qquad \textbf{(7.12)}$$

The initial adsorption rate, h (mg/g•min) as t➔0 is defined as

$$h = k_2 q_e^2 \qquad \textbf{(7.13)}$$

where k_t is the pseudo second order rate constant (g/mg•min) and q_e is the theoretical maximum absorption (mg/g). A regression plot of t/q_t against t give the value of q_e as the slope and *h* as the intercept.

The pseudo first and second order rates of the bicomponent and homocomponent nonwovens with similar maximum adsorption capacities, 12.9 and 12.5 meq/g respectively, were compared, Figure **7.13**.

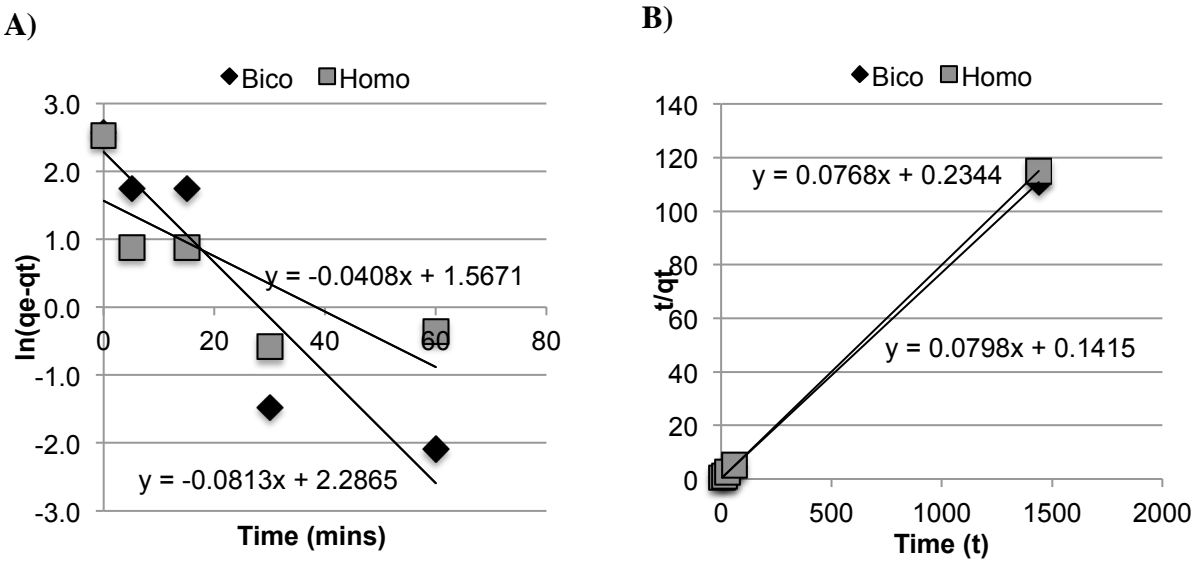

Figure 7.13. A) Pseudo first order reaction and B) Pseudo Second Order REaction for copper ions adsorpbed onto bicomponent (13.4 GP%) And homocomponent (28 GP%) Nonwovens at initial concentration of 75 g/L

The pseudo first and second order rate plots of the bicomponent and homocomponent nonwovens are shown. These plots were used to calculate the adsorption rate constants, k_1 and k_2, as well as the theoretical adsorption capacities, $q_{e,th}$, Table 7.7.

Table 7.7. Constants for the first and second order kinetic models

		Pseudo First Order			Pseudo Second Order			
Web Structure	q_{exp}	k_1	$q_{e,th}$	R^2	k_2	$q_{e,th}$	h	R^2
Bicomponent	12.99	0.0813	9.8404	0.857	0.0251	13.02	4.266	0.99998
Homocomponent	12.52	0.0408	4.7927	0.628	0.045	12.531	7.067	1

The high R^2 values of the pseudo second order model indicate the data fits the model very well and explains the adsorption behavior. Essentially all of the variance in the data can be explained by the pseudo second order model, indicated by the R^2>.99, indicating this is an excellent fit for the data. The pseudo second order model is based on the assumption that chemical adsorption is the rate limiting step in the ion exchange process and that the metal ions form bonds (ionic bonds in the case of copper and sulfonic acid) with the surface functional groups. These bonds are formed to maximize the coordination number of the ions with the surface of the material [32][31].

The low rate constants, k_2 of, of both the pseudo first and second order model indicate that the removal of copper ions by the bicomponent and homocomponent nonwovens is a favorable reaction. The theoretical adsorption capacities calculated with the pseudo second order model agree almost perfectly with the experimental adsorption capacities, proving that this is a good model to be used to predict the behavior of the functionalized materials. The extremely high adsorption rates, h, of both materials indicates the reaction is very favorable and occurs at a very rapid rate, the bicomponent having a higher rate than the homocomponent.

7.4.5 Removal Behavior of Nonwovens

The mechanism of removal of the copper ions from solution by the functionalized nonwovens was investigated by doing TOF-SIMS surface analysis, Figure 7.14

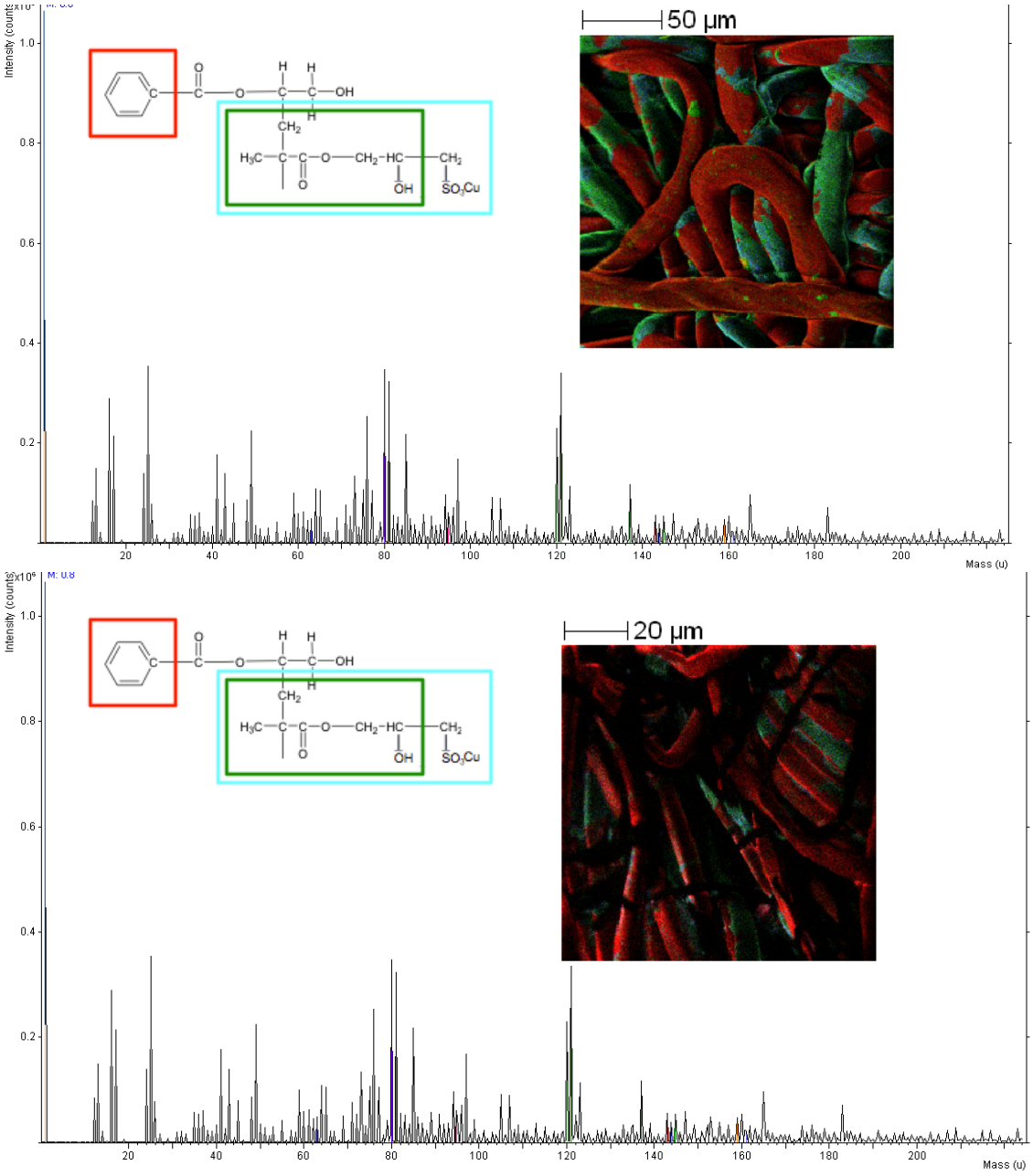

Figure 7.15. TOF SIMS graph and image of A) homocomponent nonwoven (5.061 mg/g) and B) functionalized Bicomponent Nonwoven (13.3 mg/g) after copper ion removal

The red areas of the TOF SIMS image represent ungrafted PET fibers, while the green areas are sulfonated GMA monomers attached to the PET fibers, and the aqua regions are the attached functional groups containing a copper ion. Copper ions were only found attached to sulfonate functional groups. No copper ions were detected on the surface of the PET fibers, indicating that no surface adsorption has occurred and the removal mechanism is primarily the ion exchange of the copper ions with sulfonate functional groups.

7.5 Conclusion

Strong cation exchange bicomponent and homocomponent nonwovens were developed that efficiently removed copper ions from solution. PET/PE bicomponent and PET homocomponent nonwovens were grafted with glycidyl methacrylate monomers followed by sulfonation to attach sulfonate functional groups and form strong cation exchange nonwoven materials. It was found that the target grafting percentage to maximize the ion exchange capacity of both materials is 12%. This reasonable grafting percentage is easily achieved with low GMA monomer concentrations and low grafting times of <30 minutes. Under these conditions, ion exchange capacities of 13 mg/g were achieved for the bicomponent nonwovens.

Through an equilibrium study, it was found that the removal capacity of copper ions by the homocomponent and bicomponent nonwovens is dependent on the concentration of copper ions. The removal capacity increases with increases copper concentration for both materials, reaching a maximum of 16 mg/g and 8 mg/g for the bicomponent and homocomponent nonwovens, respectively. Upon investigating the rate of removal of ions at an initial concentration of 75 mg/l, it was found that both materials reached equilibrium after 30 minutes of contact time and a significant number of ions were removed after just 5 minutes of contact time.

Langmuir and Freundlich adsorption models were used to investigate the sorption behavior of the materials. Both materials fit the Langmuir model much better than the Fruendlich, indicating that monolayer sorption can be assumed. The Langmuir model also

confirmed fast adsorption rates of both materials and predicted a much higher maximum adsorption for the bicomponent nonwoven than homocomponent, of 15 mg/g. The maximum absorption predicted with the Langmuir model was consistent with the difference in PET surface area of the two materials, indicating that the high surface area of the bicomponent nonwoven is utilized in the functionalization reaction. The separation factors at both high and low copper concentrations were low indicating that the removal of ions from solution is favorable.

The kinetic behavior of the materials was investigated with pseudo first and second order models. The data of both materials fit the pseudo second order model very well, indicating that the rate limiting step is the chemical adsorption of the copper ions. The rate constants of the pseudo second order model also confirmed the rate of adsorption of copper ions on the sample surface occurs very rapidly, more rapid for the bicomponent than homocomponent nonwovens. This is explained by the high surface area of the bicomponent nonwovens which provides high accessibility of functional groups. TOF-SIMS surface analysis confirmed that no copper ions were adsorbed onto the PET fibers and the primarily mechanism of copper removal was through ion exchange with the sulfonate functional groups.

The grafting and functionalization procedure defined in this study successfully produce materials with a high ion exchange capacity. The high removal capacity and rate of the functionalized bicomponent nonwovens make these materials a viable replacement for current commercially available ion exchange materials.

7.6 Reference

[1] C. Gerente, V. Lee, K. Lee, and C. Lee, "Application of Chitosan for the Removal of Metals From Wastewaters by Adsorption—Mechanisms and Models Review," *Crit. Rev. Environ. Sci. Technol.*, vol. 37, no. 1, pp. 41–127, Jan. 2007.

[2] M. P. Jones, B. L. Webb, D. A. Cook, and V. D. Jolley, "Comparing Nutrient Availability in Low-Fertility Soils using Ion Exchange Resin Capsules," *Commun. Soil Sci. Plant Anal.*, vol. 43, no. 1–2, pp. 368–376, Jan. 2012.

[3] Y. Bai and B. Bartkiewicz, "Removal of Cadmium from Wastewater Using Ion Exchange Resin Amberjet 1200H Columns," *Pol. J. Environ. Stud.*, vol. 18, no. 6, pp. 1191–1195, 2009.

[4] K. Fujiwara, "Separation functional fibers by radiation induced graft polymerization and application," *Nucl. Instruments Methods Phys. Res. Sect. B Beam Interactions Mater. Atoms*, vol. 265, no. 1, pp. 150–155, Dec. 2007.

[5] J. Economy, L. Dominguez, and C. L. Mangun, "Polymeric Ion-Exchange Fibers," *Ind. Eng. Chem. Res.*, vol. 41, no. 25, pp. 6436–6442, Dec. 2002.

[6] A. Zagorodni, *Ion exchange materials : properties and applications*. Amsterdam ;;London: Elsevier, 2007.

[7] V. S. Soldatov, A. A. Shunkevich, I. S. Elinson, J. Johann, and H. Iraushek, "Chemically active textile materials as efficient means for water purification," *Desalination*, vol. 124, no. 1–3, pp. 181–192, Nov. 1999.

[8] V. Soldatov, A. Shunkevich, and G. Sergeev, "Synthesis, structure and properties of new fibrous ion exchangers ☆ ," *React. Polym. Ion Exch. Sorbents*, vol. 7, no. 2–3, pp. 159–172, Jan. 1988.

[9] G. Medyak, A. Shunkevich, A. Polikarpov, and V. Soldatov, "Features of Preparation and Properties of FIBAN K-4 Fibrous Sorbents," *Russ. J. Appl. Chem.*, vol. 74, no. 10, pp. 1658–1663, Feb. 2001.

[10] N. Somanathan, B. Balasubramaniam, and V. Subramaniam, "Grafting of Polyester Fibers," *J. Macromol. Sci. Part*, vol. 32, no. 5, pp. 1025–1036, May 1995.

[11] J. Song, Y. Jin, G. Fu, A. He, and W. Fu, "A facile approach toward surface sulfonation of natural cotton fibers through epoxy reaction," *J. Appl. Polym. Sci.*, vol. 124, no. 2, pp. 1744–1750, Apr. 2012.

[12] K. C. Gupta and K. Khandekar, "Graft copolymerization of acrylamide onto cellulose in presence of comonomer using ceric ammonium nitrate as initiator," *J. Appl. Polym. Sci.*, vol. 101, no. 4, pp. 2546–2558, Aug. 2006.

[13] D. J. McDowall, B. S. Gupta, and V. T. Stannett, "Grafting of vinyl monomers to cellulose by ceric ion initiation," *Prog. Polym. Sci.*, vol. 10, no. 1, pp. 1–50, Jan. 1984.

[14] I. Casinos, "Mechanisms for the radical graft polymerization of vinyl and/or acrylic monomers on cellulose," *Polymer*, vol. 35, no. 3, pp. 606–615, Feb. 1994.

[15] N. Chansook and S. Kiatkamjornwong, "Ce(IV)-initiated graft polymerization of acrylic acid onto poly(ethylene terephthalate) fiber," *J. Appl. Polym. Sci.*, vol. 89, pp. 1952–1958, Aug. 2003.

[16] G. Odian and J. H. T. Kho, "Ceric Ion Initiated Graft Polymerization onto Poly(vinyl Alcohol)," *J. Macromol. Sci. Part - Chem.*, vol. 4, no. 2, pp. 317–330, Mar. 1970.

[17] A. Wachinski, *Ion exchange treatment for water*. Denver CO: American Water Works Association, 2006.

[18] F. Ku?era and J. Jan?  ?, "Homogeneous and heterogeneous sulfonation of polymers: A review," *Polym. Eng. Sci.*, vol. 38, no. 5, pp. 783–792, May 1998.

[19] F. G. Helfferich, *Ion exchange*. New York: Dover Publications, 1995.

[20] K. Saito, M. Ito, H. Yamagishi, S. Furusaki, T. Sugo, and J. Okamoto, "Novel hollow fiber membrane for the removal of metal ion during permeation: preparation by

radiation-induced cografting of a crosslinking agent with reactive monomer," *Ind. Eng. Chem. Res.*, vol. 28, no. 12, pp. 1808–1812, Dec. 1989.

[21] K. Saito, K. Saito, K. Sugita, M. Tamada, and T. Sugo, "Cation-Exchange Porous Hollow-Fiber Membranes Prepared by Radiation-Induced Cografting of GMA and EDMA Which Improved Pure Water Permeability and Sodium Ion Adsorptivity," *Ind. Eng. Chem. Res.*, vol. 41, no. 23, pp. 5686–5691, Nov. 2002.

[22] N. Kwak, T. Hwang, S. Kim, Y. Yang, and K. Kang, "Synthesis of sulfonated PET-g-GMA fine ion-exchange fibers for water treatment by photopolymerization and their adsorption properties for metal ions," *Polym. Korea*, vol. 28, no. 5, pp. 397–403, Sep. 2004.

[23] Y. V. Bondar, H. J. Kim, and Y. J. Lim, "Sulfonation of (glycidyl methacrylate) chains grafted onto nonwoven polypropylene fabric," *J. Appl. Polym. Sci.*, vol. 104, no. 5, pp. 3256–3260, Jun. 2007.

[24] M. Kim, "Radiation-induced graft polymerization and sulfonation of glycidyl methacrylate on to porous hollow-fiber membranes with different pore sizes," *Radiat. Phys. Chem.*, vol. 57, no. 2, pp. 167–172, Feb. 2000.

[25] T. Kim and J. Kim, "Preparation and characterization of poly(3,4-ethylenedioxythiophene) (PEDOT) using partially sulfonated poly(styrene-butadiene-styrene) triblock copolymer as a polyelectrolyte," *Curr. Appl. Phys.*, vol. 9, no. 1, pp. 120–125, Jan. 2009.

[26] S. Li and J. Wei, "Evaluation of the influence of homopolymerization on the removal of water-insoluble organics by grafted polypropylene fibers," *Mar. Pollut. Bull.*, vol. 64, no. 6, pp. 1172–1176, Jun. 2012.

[27] D. M. Pinkerton and R. H. Stacewicz, "γ-Radiation-induced grafting of methyl methacrylate to polypropylene: The effects of water and mineral acid," *J. Polym. Sci. Polym. Lett. Ed.*, vol. 14, no. 5, pp. 287–291, May 1976.

[28] K. Fujiwara, T. Masubuchi, K. Miyata, M. Shiozawa, T. Takato, and H. Harakawa, "Metal oxides immobilized fabrics by radiation induced graft polymerization," *Radiat. Phys. Chem.*, vol. 79, no. 3, pp. 238–240, Mar. 2010.

[29] R. I. Masel, *Principles of adsorption and reaction on solid surfaces*. New York: Wiley, 1996.

[30] S. Shahmohammadi-Kalalagh, H. Babazadeh, A. Nazemi, and M. Manshouri, "Isotherm and Kinetic Studies on Adsorption of Pb, Zn, and Cu by Kaolinite," *Casp. J. Environ. Sci.*, vol. 9, no. 2, pp. 243–255.

[31] D. A.O, "Langmuir, Freundlich, Temkin and Dubinin–Radushkevich Isotherms Studies of Equilibrium Sorption of Zn 2+ Unto Phosphoric Acid Modified Rice Husk," *Iosr J. Appl. Chem.*, vol. 3, no. 1, pp. 38–45, 2012.

[32] K. Sinthil and K. K, "EQUILIBRIUM AND KINETIC STUDY OF ADSORPTION OF NICKEL FROM AQUEOUS SOLUTION ONTO BAEL TREE LEAF POWDER," *J. Eng. Sci. Technol.*, vol. 4, no. 4, pp. 351–363, 2006.

[33] The Dow Chemical Company, "AMBERJET™ 1200 H," *Dow - Products and Services*,2011.[Online].Available: http://www.dow.com/products/product_detail.page?product=1120843&application=1120783. [Accessed: 18-Jul-2011].

[34] The Dow Chemical Company, "AMBERLYST™," *Dow - Products and Services*, 2011. [Online]. Available: http://www.amberlyst.com/sac.htm. [Accessed: 18-Jul-2011].

[35] The Dow Chemical Company, "Dowex," *Strong Acid Cation Exchange Resins*, 2013.[Online].Available: http://msdssearch.dow.com/PublishedLiteratureDOWCOM/dh_0202/0901b80380202d8f.pdf?filepath=liquidseps/pdfs/noreg/177-01728.pdf&fromPage=GetDoc. [Accessed: 02-May-2013].

Chapter 8

8 Conclusions and Recommendations

8.1 Conclusions

For this project ion exchange nonwovens were developed by functionalizing high surface area bicomponent nonwovens. The specific objectives were to: (1) establish the parameters necessary to maximize the fracturing of bicomponent fibers, (2) investigate the formation of ion exchange fibers by functionalizing base polymeric fibers, and (3) establish the relationship between the web and sorption properties of the ion exchange substrates.

These objectives were achieved through a two-step process. First, the high surface area substrates were developed by fracturing PET/PE segmented pie bicomponent nonwovens using a Mathis JFO Jet Dyeing Machine to achieve complete fracturing. Next, the conditions for grafting glycidyl methacrylate (GMA) monomers onto the PET homocomponent and 80/20 PET/PE 16 segmented pie nonwovens were investigated. This intermediate step was necessary to provide a site on the PET backbone that would accept functional groups. Grafting via UV initiation was attempted but resulted in large homopolymer formation. Ceric salt, specifically ceric ammonium nitrate (CAN), redox initiation proved to be a controllable process and was used to graft the GMA monomers. The grafted nonwovens were then sulfonated to create functional ion exchange fibers. Evaluation of the ion exchange properties of the resultant fibers through copper ion removal equilibrium and kinetic experiments revealed that the bicomponent nonwoven had a higher maximum capacity and rate of removal of copper ions than the homocomponent fiber.

Experimentation revealed the GMA monomer, CAN initiator, and the web structure to significantly affect grafting percentage. At low monomer and initiator concentrations, time was not a factor in grafting reactions and the two materials were comparable. However, with an increase in either the monomer or the initiator concentration, the bicomponent nonwoven significantly increased in grafting percentage over the homocomponent nonwoven. The

grafted samples were then sulfonated in an excess of sodium sulfite. FTIR and TOF-SIMS confirmed the presence of epoxy groups after grafting and sulfonic acid groups after sulfonation. Uniform grafting was observed, with large conversions of the epoxy group to sulfonic acid functional groups evident.

High grafting percentages did not have an effect on sulfonate group densities, tested using back titration, or copper removal. The sulfonate group densities for both the homocomponent and bicomponent under most grafting conditions were in the range of 0.2-1.5 meq/g, comparable to most commercially available ion exchange resins. However, at low monomer and initiator concentrations (2 wt% GMA and 2 mM CAN) the homocomponent nonwoven had larger sulfonate group densities, up to 4.5 meq/g.

Ion exchange capacities were evaluated through copper ion removal experiments. An equilibrium study found the removal capacity of copper ions by the homocomponent and bicomponent nonwovens to be dependent on the concentration of copper ions. Removal capacity increased as the copper concentration increased for both materials, reaching a maximum of 16 mg/g and 8 mg/g for the bicomponent and homocomponent nonwovens (respectively), with an equilibrium concentration of about 75 mg/l of copper. Upon investigation of the rate of removal of ions with an initial concentration of 75 mg/l, both materials were found to reach equilibrium after 30 minutes of contact time, with a significant number of ions removed after just 5 minutes of contact time. The equilibrium data fit the Langmuir model well, confirming that monolayer adsorption is likely occurring on a homogeneous surface. The Langmuir model predicted a much higher maximum adsorption for the bicomponent nonwoven than homocomponent (i.e., 15 mg/g compared to 4.65 mg/g). The difference in maximum capacities is consistent with the differences between PET surface area of the two materials, confirming that the high surface area of the bicomponent nonwoven is utilized in the functionalization reaction and has a significant effect on the removal of copper ions.

The target grafting percentage to maximize the ion exchange capacity of both materials is about 12%, this occurs at the lower end of the grafting percentages achieved throughout

the experiments. It is possible that the high grafting percentages are the result of large amounts of homopolymer produced during grafting that is not washed out after grafting. The bicomponent nonwoven has a lower permeability and higher solidity than the homocomponent, likely making it more difficult for the homopolymer to be removed during washing. The higher surface area of the bicomponent fiber leads to a high degree of functionalization with these functional groups quite accessible to copper ions in the copper removal experiments. It is still unknown why the titrated capacities of the homocomponent nonwoven were higher than the bicomponent, while the copper removal capacity was much lower.

The grafting and functionalization procedure defined in this study successfully produced materials with a high ion exchange capacity. The high surface area of the bicomponent nonwoven had a significant effect on the degree of functionalization, leading to a high removal capacity and rate of removal of copper ions. The results indicate that these materials are a viable replacement for current commercially available ion exchange materials.

8.2 Recommendations

The results of this research suggest that the high surface area functionalized bicomponent nonwoven has the potential to be a competitive ion exchange material in the industry and should be studied further.

8.2.1 Kinetic Experiments

Future research should further examine the kinetic behavior of the functionalized nonwovens. The experimental factors of the ion exchange environment could lead to more information on the ideal operating conditions for these materials. Factors such as pH, temperature, and agitation speed of the ion exchange experiments should be investigated, as these could have a significant impact on the ion exchange properties.

The materials developed through this research have proved to successfully remove high capacities of copper ions in a batch type experiment. As these materials are an improvement on the commercially available ion exchange resins, it is of interest to examine the removal

behavior in a column type set up. Although it is unlikely that fibrous ion exchange materials would be used in the same set up as the bead structures, this would provide a side by side comparison of the two technologies.

Copper is a relatively easy material to work with and an abundance of literature has been published on the behavior of copper ions, making it a favorable ion to be used for these initial experiments. Now that the initial groundwork for achieving high capacity functionalized nonwovens has been established, it would be of interest to investigate the removal of other metals ions that may be of more interest on an industrial level, such as arsenic or cadmium.

8.2.2 Scale up of the Functionalization Process

Most functionalization techniques are feasible in a laboratory environment but are difficult to scale up to a commercial level. The FIBAN group, producing some of the few commercially available ion exchange fibrous materials, functionalizes the PP fibers in a batch process with gamma radiation. The lack of a continuous process makes these materials very costly and time consuming to produce. The functionalization process developed in this research does not require the use of any harmful radiation to initiate the grafting, allowing for the potential for a roll to roll functionalization process, 1.

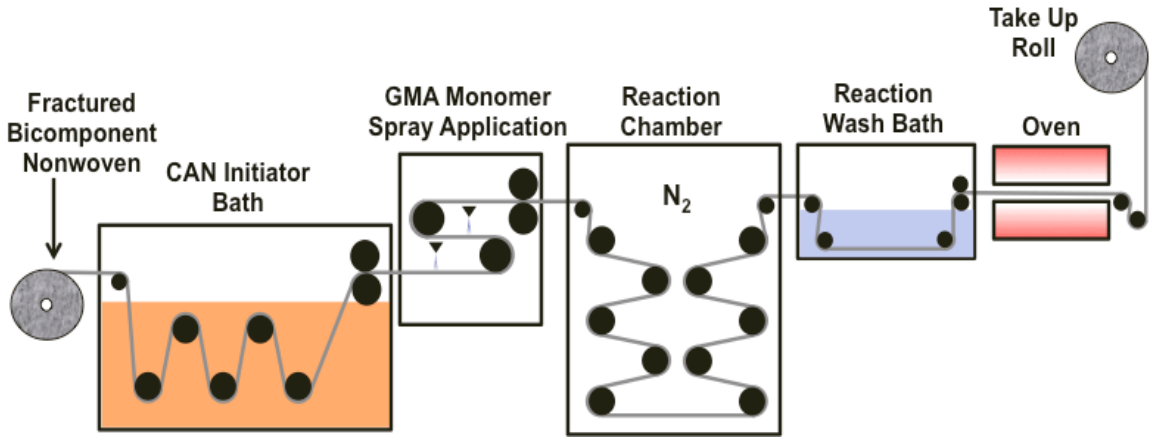

Figure 8.1. Potential roll to roll scale up

It is suggested that the high surface area fractured bicomponent nonwoven would be fed into a ceric ammonium initiator bath for an optimum amount of time. The fabric would leave the CAN chamber, the excess initiator solution rolled out, and fed into a chamber where GMA monomer would be sprayed on either side of the material. The excess monomer would be removed and the material would go through the reaction chamber where it be given enough time for the reaction to proceed. After the grafting reaction, the material would go through a reaction wash bath, possibly with agitation, to remove the remaining homopolymer. Finally, the grafted material would be dried and rolled on the take up roll. Not only is this process feasible, it would likely reduce the amount of homopolymer formed during the reaction because the reaction does not occur in a bulk solution.

APPENDICES

Appendix 1

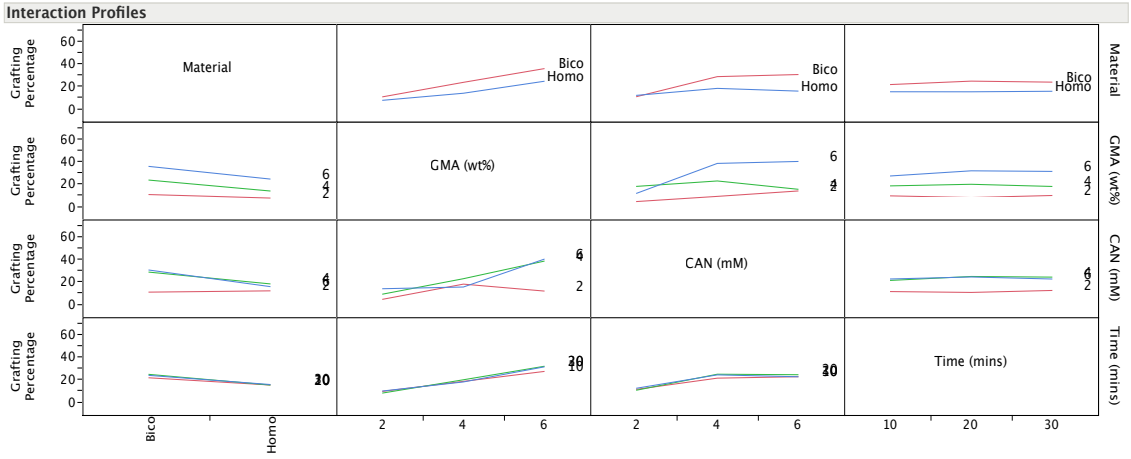
Interaction Profiles
Grafting Percentage
Material
GMA (wt%)
CAN (mM)
Time (mins)
Bico
Homo
2
4
6
10
20
30